

A policy-oriented vehicle simulation approach for estimating the CO2 emissions from Hybrid Light Duty Vehicles

*Original*

A policy-oriented vehicle simulation approach for estimating the CO2 emissions from Hybrid Light Duty Vehicles / Cubito, Claudio. - (2017). [10.6092/polito/porto/2675285]

*Availability:*

This version is available at: 11583/2675285 since: 2017-06-28T11:31:57Z

*Publisher:*

Politecnico di Torino

*Published*

DOI:10.6092/polito/porto/2675285

*Terms of use:*

Altro tipo di accesso

This article is made available under terms and conditions as specified in the corresponding bibliographic description in the repository

*Publisher copyright*

(Article begins on next page)



**ScuDo**  
Scuola di Dottorato ~ Doctoral School  
WHAT YOU ARE, TAKES YOU FAR

Doctoral Dissertation  
Doctoral Program in Energy Engineering (29<sup>th</sup> Cycle)

# **A policy-oriented vehicle simulation approach for estimating the CO<sub>2</sub> emissions from Hybrid Light Duty Vehicles**

By

**Claudio Cubito**

\*\*\*\*\*

**Supervisor:**

Prof. Federico Millo

**Doctoral Examination Committee:**

Prof. Zissis Samaras, Aristotle University

Prof. Giorgio Rizzoni, Ohio State University

Prof. Angelo Onorati, Politecnico di Milano

Prof. Michael Bargende, Universität Stuttgart

Prof. Ezio Spessa, Politecnico di Torino

Politecnico di Torino  
2017

## **Declaration**

I hereby declare that, the contents and organization of this dissertation constitute my own original work and does not compromise in any way the rights of third parties, including those relating to the security of personal data.

Claudio Cubito

2017

\* This dissertation is presented in partial fulfillment of the requirements for **Ph.D. degree** in the Graduate School of Politecnico di Torino (ScuDo).





*Dedicata a mia madre e mia nonna*



*Le grandi imprese sono il frutto della Follia che gli Dei concessero agli  
uomini, e così pure è opera della Follia l'amore che un essere umano nutre per un  
altro essere umano*

Platone, Fedro



## **Acknowledgment**

This research work was carried out with the closed collaboration between Politecnico di Torino and the European Commission - Joint Research Centre. The author would like to thank Prof. Federico Millo (Politecnico di Torino), Biagio Ciuffo and Simone Serra (Joint Research Centre) for their support and assistance with this project. Special thanks also go to my colleagues Giulio Boccardo, Sabino Caputo, Mohsen Mirzaeian, Andrea Piano, Mahsa Rafigh, Luciano Rolando, Daniele Porcu and Alessandro Zanelli for their advice and counsel. The author would also thank the VELA staff of Joint Research Centre, in particular Marcos Garcia Otura and Germana Trentadue for their technical support during the test campaign.



## **Abstract**

Pollutants emissions and fuel economy tests for passenger cars differ from region to region of the world, since different driving condition and vehicle fleet characterize different geographical areas. In particular, the European type approval procedure for passenger cars uses as reference cycle the New European Driving Cycle (NEDC), which is nowadays not representative of real driving conditions. Therefore, the European Commission has planned to introduce the Worldwide Harmonized Light Duty Test Procedure (WLTP) from September 2017. As a consequence, the CO<sub>2</sub> emissions target should be adapted, since the current 2020 goals are based on NEDC assessment.

The European Commission and the Joint Research Centre (JRC) are therefore developing a simulation tool called CO2MPAS (CO<sub>2</sub> Module for Passenger and commercial vehicles Simulation) for the correlation of CO<sub>2</sub> emissions from WLTP to NEDC, which will be used for the type approval of European passenger cars from 2017, avoiding expensive duplicate test campaigns for car manufactures. However, the implementation of CO2MPAS has so far involved solely conventional light duty vehicles.

Within this context, a research project has been carried out in closed collaboration between Politecnico di Torino and JRC for the development of CO2MPAS for Hybrid Electric Vehicles (HEVs) and Plug-In Hybrid Electric Vehicles (PHEVs). The correlation model is based on a unique simplified physical approach, which should be able to detect the powertrain behavior along the NEDC cycle from the physical measurements along the new driving cycle, estimating with a good accuracy the CO<sub>2</sub> emissions (within  $\pm 3$  g/km).





# Contents

1. Introduction.....	1
1.1 European Legislation Framework .....	1
1.2 Impact of actual technologies on CO <sub>2</sub> reduction: A real case study .....	7
1.3 CO <sub>2</sub> MPAS.....	16
2. Experimental campaign on hybrid vehicles.....	18
2.1 Introduction .....	18
2.2 Case study.....	18
2.2.1 The Yaris Hybrid .....	19
2.2.2 The Golf GTE PHEV .....	22
2.3 The experimental set-up .....	24
2.4 Test procedure .....	29
2.4.1 HEVs protocol .....	31
2.4.2 PHEVs protocol .....	33
2.5 Energy management analysis .....	36
2.5.1 Yaris Hybrid: EMS analysis .....	37
2.5.2 Golf GTE: EMS analysis .....	51
2.6 CO <sub>2</sub> emissions.....	65
2.6.1 Yaris Hybrid: K-Factor and CO <sub>2</sub> emissions .....	65
2.6.2 Golf GTE: electric range and CO <sub>2</sub> emissions .....	67
3. Hybrid Meta-Model .....	69
3.1 Introduction .....	69
3.2 The Meta-Model logic .....	71
3.2.1 HEV simulation logic .....	71
3.2.2 PHEV simulation logic .....	74
3.3 Energy Management System identification.....	77
3.3.1 Internal Combustion Engine operating strategy .....	78
3.3.2 Powertrain efficiency and regenerative braking .....	85
3.3.3 Power adsorption from auxiliary components .....	88

3.3.4 E-Boost and Smart Charge identification and modelling .....	89
3.3.5 Engine power evaluation .....	93
3.3.6 Engine coolant temperature modelling .....	94
3.3.7 Cold start modelling .....	95
3.3.8 Engine speed modelling .....	99
3.3.9 Battery parameters .....	100
3.3.10 CO <sub>2</sub> virtual maps .....	101
4. Meta-Model validation .....	104
4.1 Introduction .....	104
4.2 The Yaris Hybrid test case .....	104
4.2.1 High SOC case .....	105
4.2.2 Low SOC case .....	108
4.2.3 CO <sub>2</sub> Type approval value for the Yaris Hybrid .....	112
4.3 The Golf GTE test case .....	114
4.3.1 The charge depleting case .....	114
4.3.2 The charge sustaining case .....	118
4.3.3 CO <sub>2</sub> Type approval value for the Golf GTE .....	121
5. Conclusions .....	123
6. References .....	126

# List of Figures

Figure 1: Comparison of global CO <sub>2</sub> regulation for passenger cars in terms of NEDC gCO <sub>2</sub> /km [4].....	2
Figure 2: Vehicle speed profile of WLTC class 3.2 .....	4
Figure 3: Speed and acceleration distributions along the WLTC and NEDC cycles .....	5
Figure 4: Conventional powertrains - RLs for NEDC and WLTP procedures.....	9
Figure 5: Conventional powertrains - ICE operating points along the NEDC and WLTC TMH for vehicle 1 .....	11
Figure 6: Conventional powertrains - ICE operating points along the NEDC and WLTC TMH during for vehicle 2.....	11
Figure 7: Conventional powertrains - Energy delivered by the ICE for vehicle 1 and vehicle 2 along the NEDC and WLTC cycles during the “hot start” case .....	12
Figure 8: Conventional powertrains - CO <sub>2</sub> emissions as function of cycle energy demand.....	12
Figure 9: Conventional powertrains - ICE operating points along the WLTC cycle using the EU (cyan) and the TMH (red) RLs for vehicle 1 .....	13
Figure 10: Conventional powertrains - Energy delivered by the ICE for vehicle 1 along the WLTC cycles using EU RLs during the “hot start” case.....	13
Figure 11: Conventional powertrains - “Cold Start” share along the NEDC and WLTC cycles .....	14
Figure 12: Conventional powertrains - Effect of “Cold Start” on CO <sub>2</sub> emissions along the NEDC an WLTC cycles.....	15
Figure 13: Conventional powertrains - Coolant temperature profiles along the NEDC (left) and WLTC (right) for vehicle 2 .....	15
Figure 14: Conventional powertrains: effectiveness analysis of stop-start for vehicle 1(left) and vehicle 2 (right) along the NEDC and WLTC cycle.....	15
Figure 15: Yaris Hybrid - Schematic of the eCVT architecture [19] .....	19
Figure 16: Yaris Hybrid – EV mode.....	21
Figure 17: Yaris Hybrid – Smart Charge mode.....	21
Figure 18: Yaris Hybrid – E-Boost mode.....	22
Figure 19: Golf GTE – Schematic of the FAS architecture.....	23
Figure 20: Golf GTE – Hybrid menu [20].....	24

Figure 21: VELA 8 chassis dyno and emission system overview .....	25
Figure 22: Climatic chamber and chassis dynamometer at VELA 8 lab .....	25
Figure 23: Yaris Hybrid - Current measurement .....	28
Figure 24: Golf GTE – Current measurement .....	28
Figure 25: Yaris Hybrid – Detail of current clamp positioning.....	29
Figure 26: RLs for WLTP and NEDC procedures .....	30
Figure 27: Yaris Hybrid – Cycle energy demand along the WLTC (Left) and NEDC (Right).....	31
Figure 28: Golf GTE – Cycle energy demand along the WLTC (Left) and NEDC (Right).....	31
Figure 29: Example of battery indicator for Toyota Hybrids [23] .....	32
Figure 30: An example of SOC profile during the Condition A test [22] .....	34
Figure 31: Golf GTE - Speed steps used for the battery discharge .....	35
Figure 32: An example of SOC profile during the Condition B test [22] .....	35
Figure 33: Electric distance computation along the NEDC cycle according to [22] .....	36
Figure 34: Yaris Hybrid - On/Off and battery SOC for the “High SOC” case along the WLTC (Top) and NEDC (Bottom).....	38
Figure 35: Yaris Hybrid - On/Off and battery SOC for the “Low SOC” case along the WLTC (Top) and NEDC (Bottom).....	39
Figure 36: Yaris Hybrid - Engine coolant temperature profiles along the WLTC (Top) and NEDC (Bottom) for the “High SOC” case .....	40
Figure 37: Yaris Hybrid – ICE actuation as a function of battery SOC for the “High SOC” (Top) and for the “Low SOC” (Bottom) along the WLTC .....	41
Figure 38: Yaris Hybrid: ICE actuation as a function of battery SOC for the “High SOC” (Top) and for the “Low SOC” (Bottom) along the NEDC .....	42
Figure 39: Yaris Hybrid - ICE actuation as a function of vehicle speed for the “High SOC” (Top) and the “Low SOC” (Bottom) along the WLTC.....	43
Figure 40: Yaris Hybrid - ICE actuation as a function of vehicle speed for the “High SOC” (Top) and the “Low SOC” (Bottom) along the NEDC .....	44
Figure 41: Yaris Hybrid - ICE actuation as a function of the product between vehicle speed and acceleration for the “High SOC” (Top) and the “Low SOC” (Bottom) along the WLTC .....	45

Figure 42: Yaris Hybrid - ICE actuation as a function of the product between vehicle speed and acceleration for the “High SOC” (Top) and the “Low SOC” (Bottom) along the NEDC .....	46
Figure 43: Yaris Hybrid - Identification of the ICE operating conditions for the “High SOC” (Top) and the “Low SOC” (Bottom) as a function of battery SOC along the WLTC .....	47
Figure 44: Yaris Hybrid - Identification of the ICE operating conditions for the “High SOC” (Top) and the “Low SOC” (Bottom) as a function of battery SOC along the NEDC .....	48
Figure 45: Yaris Hybrid - Identification of the ICE operating conditions for the “High SOC” (Top) and the “Low SOC” (Bottom) as a function the product between vehicle speed and acceleration along the WLTC .....	49
Figure 46: Yaris Hybrid - Identification of the ICE operating conditions for the “High SOC” (Top) and the “Low SOC” (Bottom) as a function the product between vehicle speed and acceleration along the NEDC .....	50
Figure 47: Yaris Hybrid - Vehicle operating mode share along the WLTC cycle for the “High SOC” (Left) and the “Low SOC” (Right) .....	51
Figure 48: Yaris Hybrid - Vehicle operating mode share along the NEDC cycle for the “High SOC” (Left) and the “Low SOC” (Right) .....	51
Figure 49: Golf GTE - ICE On/Off and battery SOC for the ZEV mode along the WLTC (Top) and NEDC (Bottom) .....	52
Figure 50: Golf GTE - ICE actuation as a function of battery SOC for the E-Mode along the WLTC (Top) and NEDC (Bottom) .....	53
Figure 51: Golf GTE - ICE actuation as a function of vehicle speed for the E-Mode along the WLTC (Top) and NEDC (Bottom) .....	54
Figure 52: Golf GTE - ICE actuation as a function of vehicle speed for the E-Mode along the WLTC (Top) and NEDC (Bottom) .....	55
Figure 53: Golf GTE - Identification of the ICE operating conditions for the E-Mode along the WLTC (Top) and NEDC (Bottom) as a function of battery SOC .....	56
Figure 54: Golf GTE - Identification of the ICE operating conditions for the E-Mode along the WLTC (Top) and the NEDC (Bottom) as a function the product between vehicle speed and acceleration .....	57
Figure 55: Golf GTE - vehicle operating mode share for the E-Mode along the WLTC (Left) and NEDC (Right) .....	58
Figure 56: Golf GTE - ICE On/Off and battery SOC for the GTE mode along the WLTC (Top) and NEDC (Bottom) .....	59

Figure 57: Golf GTE - ICE actuation as a function of battery SOC and traction power for the GTE mode along the WLTC (Top) and NEDC (Bottom).....	60
Figure 58: Golf GTE - ICE actuation as a function of vehicle speed and traction power demand for the GTE mode along the WLTC (top) and NEDC (Bottom) ..	61
Figure 59: Golf GTE - ICE actuation as a function of the product between vehicle speed and acceleration and traction power demand for the GTE mode along the WLTC (Top) and NEDC (Bottom).....	62
Figure 60: Golf GTE - Identification of the ICE operating conditions in GTE mode as a function of battery SOC along the WLTC (Top) and NEDC (Bottom) .....	63
Figure 61: Golf GTE - Identification of the ICE operating conditions as a function of the product between vehicle speed and acceleration for the GTE mode along the WLTC (Top) and NEDC (Bottom).....	64
Figure 62: Golf GTE - Vehicle operating mode share for the GTE mode along the WLTC (Left) and NEDC (Right).....	65
Figure 63: Yaris Hybrid - CO <sub>2</sub> emissions for the “Low SOC” and “High SOC” cases .....	66
Figure 64: Yaris Hybrid - K-Factor correction .....	67
Figure 65: Golf GTE - CO <sub>2</sub> emissions along the NEDC and the WLTC combining the E-Mode with the GTE.....	68
Figure 66: Normal operating conditions of HEV/PHEV vehicles.....	70
Figure 67: Meta-Model flow chart - Detection of the ICE On/Off strategy for HEVs .....	72
Figure 68: Meta-Model flow chart - Detection of the “Cold Start” strategy and calibration of the engine speed and coolant temperature empirical relations for HEVs.....	73
Figure 69: Meta-Model flow chart - Simulation of NEDC cycle and TA CO <sub>2</sub> emissions computation for HEVs .....	74
Figure 70: Meta-Model flow chart - Detection of the ICE On/Off strategy for PHEVs .....	75
Figure 71: Meta-Model flow chart - Detection of the “Cold Start” strategy and calibration of the engine speed and coolant temperature empirical relations for PHEVs .....	76
Figure 72: Meta-Model flow chart - Detection of the “Cold Start” strategy and calibration of the engine speed and coolant temperature empirical relations for PHEVs .....	77
Figure 73: Vehicle operating area for the Yaris Hybrid .....	78

Figure 74: Definition of the minimum number of points per each SOC band depending on the battery initial energy level.....	79
Figure 75: Example of SOC band organization for an HEV with battery fully charged.....	80
Figure 76: Example of On/Off curves for a HEV with the battery fully charged at the beginning of the cycle.....	81
Figure 77: Example of On/Off curves for a HEV with the battery discharged at the beginning of the cycle.....	81
Figure 78: Example of SOC band organization for a PHEV in CD .....	83
Figure 79: Example of On/Off curves for a PHEV in CD .....	84
Figure 80: Example of On/Off curves for a PHEV in CS .....	85
Figure 81: Example of efficiency maps generated by the Meta-Model for a PHEV for the electric driving (Top) and the regenerative braking (Bottom) .....	87
Figure 82: Detection of the minimum power recovered during the regenerative braking event.....	88
Figure 83: Example of high voltage circuit for hybrid cars [25] .....	88
Figure 84: Example of detection of power adsorption from auxiliary components for two different test along the Low phase of WLTC cycle .....	89
Figure 85: Example of measurements organization in hybrid conditions for the E-Boost/Smart Charge detection .....	90
Figure 86: Depth of the sub-volume .....	91
Figure 87: Base of the sub-volume .....	91
Figure 88: Complete sub-volume .....	92
Figure 89: Example of the volume splitting for an HEV to identify the E-Boost/Smart Charge modes .....	92
Figure 90: Example of Smart Charge map for an HEV vehicle .....	93
Figure 91: Example of Electric Boost map for an HEV vehicle .....	93
Figure 92: Modelling of the hybrid powertrain .....	94
Figure 93: Temperature calibration range for a PHEV along the WLTC .....	95
Figure 94: Engine status, engine coolant temperature and battery SOC profiles along the WLTC Low phase for an HEV .....	96
Figure 95: Engine status, engine coolant temperature and battery SOC profiles along the WLTC Medium phase for an HEV .....	97
Figure 96: Engine speed profile along the WLTC Low phase for an HEV.....	97

Figure 97: Example of “Cold Start” area for an HEV vehicle.....	98
Figure 98: ICE power map during the “Cold Start” for an HEV vehicle .....	98
Figure 99: Engine speed calibration range for an HEV vehicle .....	99
Figure 100: Equivalent circuit model of the battery .....	100
Figure 101: Example of battery parameters optimization along the WLTC cycle for an HEV .....	101
Figure 102: “Cold Start” CO <sub>2</sub> emissions as function engine speed and torque for an HEV .....	102
Figure 103: “Hot Start” CO <sub>2</sub> emissions as function engine speed and torque for an HEV .....	102
Figure 104: Example of “Cold” map for an HEV .....	103
Figure 105: Example of “Hot” map for an HEV .....	103
Figure 106: Yaris Hybrid validation - Powertrain behavior along the ECE cycle for the High SOC case.....	105
Figure 107: Yaris Hybrid validation - Powertrain behavior along the EUDC cycle for the High SOC case .....	106
Figure 108: Yaris Hybrid validation - Coolant temperature profile along the NEDC cycle for the High SOC case.....	107
Figure 109: Yaris Hybrid validation - Engine speed profile along the NEDC cycle for the High SOC case .....	107
Figure 110: Yaris Hybrid validation - Instantaneous CO <sub>2</sub> emission profile along the NEDC cycle for the High SOC case.....	108
Figure 111: Yaris Hybrid validation - Cumulated CO <sub>2</sub> emissions along the NEDC cycle for the High SOC case.....	108
Figure 112: Yaris Hybrid validation - Powertrain behavior along the ECE cycle for the Low SOC case.....	109
Figure 113: Yaris Hybrid validation - HEV validation: powertrain behavior along the EUDC cycle for the Low SOC case.....	110
Figure 114: Yaris Hybrid validation - Coolant temperature profile along the NEDC cycle for the Low SOC case .....	110
Figure 115: Yaris Hybrid validation - Engine speed profile along the NEDC cycle for the Low SOC case.....	111
Figure 116: Yaris Hybrid validation - Instantaneous CO <sub>2</sub> emission profile along the NEDC cycle for the Low SOC case.....	111



Figure 117: Yaris Hybrid validation - Cumulated CO <sub>2</sub> emissions along the NEDC cycle for the Low SOC case .....	112
Figure 118: Yaris Hybrid validation – K-Factor .....	113
Figure 119: Yaris Hybrid validation - Comparison between the experimental and simulated CO <sub>2</sub> emissions along the NEDC.....	114
Figure 120: Golf GTE validation - Powertrain behavior along the first NEDC cycle during the CD test.....	115
Figure 121: Golf GTE validation - Powertrain behavior along the second NEDC cycle during the CD test.....	115
Figure 122: Golf GTE validation - Powertrain behavior along the third NEDC cycle during the CD test.....	116
Figure 123: Golf GTE validation - Powertrain behavior along the fourth NEDC cycle during the CD test.....	116
Figure 124: Golf GTE validation - Engine speed profile along the four NEDC cycle repetitions during the CD.....	117
Figure 125: Golf GTE validation - Instantaneous CO <sub>2</sub> emission profile along the four NEDC cycle during the CD test.....	117
Figure 126: Golf GTE validation - Powertrain behavior along the ECE cycle during the CS test.....	119
Figure 127: Golf GTE validation - Powertrain behavior along the EUDC cycle during the CS test.....	119
Figure 128: Golf GTE validation - Coolant temperature profile along the NEDC cycle during the CS test .....	120
Figure 129: Golf GTE validation - Engine speed profile along the four NEDC cycle repetitions during the CS test.....	120
Figure 130: Golf GTE validation - Instantaneous CO <sub>2</sub> emission profile along the four NEDC cycle during the CS test.....	121
Figure 131: Golf GTE validation - Cumulated CO <sub>2</sub> emissions along the NEDC cycle during the CS test .....	121
Figure 132: Golf GTE validation - Comparison between the experimental and simulated CO <sub>2</sub> emissions along the NEDC.....	122

# List of Equations

Equation 1: Computation of TML according to [9].....	5
Equation 2: Computation of TMH according to [9] .....	5
Equation 3: K-Factor definition.....	32
Equation 4: TA CO <sub>2</sub> for HEVs .....	33
Equation 5: Brake-off criterion.....	35
Equation 6: TA CO <sub>2</sub> emissions for PHEVs .....	36
Equation 7: Calculation of the minimum number of points per each SOC band ..	79
Equation 8: Calculation of the minimum number of points per each speed band ..	80
Equation 9: Calculation of the minimum number of points per each acceleration band.....	82
Equation 10: Calculation of battery power .....	85
Equation 11: Calculation of motive power .....	86
Equation 12: Calculation of the powertrain efficiencies during the electric drive ( $\eta_{EV}$ ) and the regenerative braking ( $\eta_{Reg}$ ) .....	86
Equation 13: Definition of the depth of the sub-volume .....	90
Equation 14: Definition of the width of the sub-volume .....	91
Equation 15: Definition of the height of the sub-volume .....	92
Equation 16: Output power from the gearbox .....	94
Equation 17: Correlation between the motive power and the gearbox output.....	94
Equation 18: Computation of the ICE power .....	94
Equation 19: Engine coolant temperature model.....	95
Equation 20: Battery power computation during the “Cold Start” .....	99
Equation 21: Modelling of engine speed during the “Cold Start” .....	99
Equation 22: Modelling of engine speed during the “Hot Start” .....	100
Equation 23: Ohm’s law .....	100
Equation 24: Error function .....	101
Equation 25: CO <sub>2</sub> emissions function during the “Cold Start” .....	102
Equation 26: CO <sub>2</sub> emissions function during the “Hot Start” .....	103

# List of Tables

Table 1: Summary of the characteristics of NEDC and WLTC class 3.2 .....	7
Table 2: Conventional powertrains - Vehicle characteristics .....	8
Table 3: Conventional powertrains - Vehicle test conditions .....	9
Table 4 Conventional powertrains - Energetic analysis and CO <sub>2</sub> emissions during the “Cold Start” .....	10
Table 5: Yaris Hybrid – Vehicle characteristics .....	20
Table 6: Golf GTE – Vehicle characteristics .....	23
Table 7: Current clamp characteristics .....	27
Table 8: Power analyzer characteristics .....	27
Table 9: Vehicle test conditions .....	30
Table 10: Driving mode selection [18] .....	33
Table 11: Yaris Hybrid - comparison between the K-Factors calculated along the NEDC and WLTC cycles .....	66
Table 12: Yaris Hybrid - CO <sub>2</sub> TA values .....	67
Table 13: Golf GTE - Values of the electric range for the NEDC and the WLTC .....	67
Table 14: Yaris Hybrid validation – Comparison between the experimental and simulated K-Factor .....	113
Table 15: Yaris Hybrid – Comparison between the experimental and simulated CO <sub>2</sub> TA values .....	114
Table 16: Golf GTE validation - Comparison between the experimental and simulated electric distance .....	118
Table 17: Golf GTE validation - Comparison between the experimental and simulated CO <sub>2</sub> TA values .....	122

# Acronyms

Four Wheels Driving	4WD
Automatic Transmission	AT
Charge Depleting	CD
Charge Sustaining	DOVC
CO <sub>2</sub> Module for Passenger and commercial vehicles Simulation	CO2MPAS
Compression Ignition	CI
Constant Volume Sampler	CVS
Critical Flow Venturi	CFV
Direct Current	DC
Dual Clutch Transmission	DCT
Electric Boost	E-Boost
Electric Continuous Variable Transmission	eCVT
Electric Vehicle	EV
Energy Management System	EMS
Engine Control Unit	ECU
Environment Protection Agency	EPA
European Automobile Manufacturers' Association	ACEA
European Union	EU
Extra Urban Driving Cycle	EUDC
Flywheel Alternator Starter	FAS
Global Technical Regulation	GTR
Green House Gas	GHG
Heating, Ventilating and Air Conditioning System	HVAC
Hybrid Electric Vehicle	HEV
Internal Combustion Engine	ICE
Joint Research Centre	JRC

Laboratory of Applied Thermodynamic	LAT
Mass Laden Vehicle	MVL
Mass of Optional Equipment	OM
Mass Running Order	MRO
Motor Generator	MG
New European Driving Cycle	NEDC
On Board Diagnostic	OBD
Open Circuit Voltage	OCV
Particulate Matter	PM
Particulate Number	PN
Plug-In Hybrid Electric Vehicle	PHEV
Power to Mass Ratio	PMR
Road Load	RL
Spark Ignition	SI
State Of Charge	SOC
Test Mass High	TMH
Test Mass Low	TML
Type Approval	TA
Urban Driving Cycle	UDC
Vehicle Emissions LAboratory	VELA
Wide Open Throttle	WOT
Worldwide harmonized Light duty Test Cycle	WLTC
Worldwide harmonized Light duty Test Procedure	WLTP



# Chapter 1

## Introduction

### 1.1 European Legislation Framework

Within the European Union (EU), the transport sector is responsible for 20% of Greenhouse Gas (GHG) emissions, making it the second largest emitting sector after the energy production. Within the transport sector, the 94% of GHG emissions come from the light-duty vehicles [1,2]. In 1998, the European Automobile Manufacturers' Association (ACEA) adopted the commitment to reduce average CO<sub>2</sub> emissions from new cars to 140 g/km by 2008 [3,4]. However, in 2009 the EU introduced mandatory CO<sub>2</sub> standards for new passenger cars, setting a 2015 target of 130 g/km for new vehicle fleet [5]. The aim of this regulation was to push carmakers to invest and develop new technologies to lower emissions from passenger cars, promoting at the same time the long-term competitiveness of the European industry [5]. In 2013, the European Parliament, based on two proposals made by the European Commission, voted on the 2020 CO<sub>2</sub> standards, setting a value of 95 g/km as new vehicle fleet limit, based on measurements along the New European Driving Cycle (NEDC) [6]. The European CO<sub>2</sub> target across the years is reported in Figure 1.

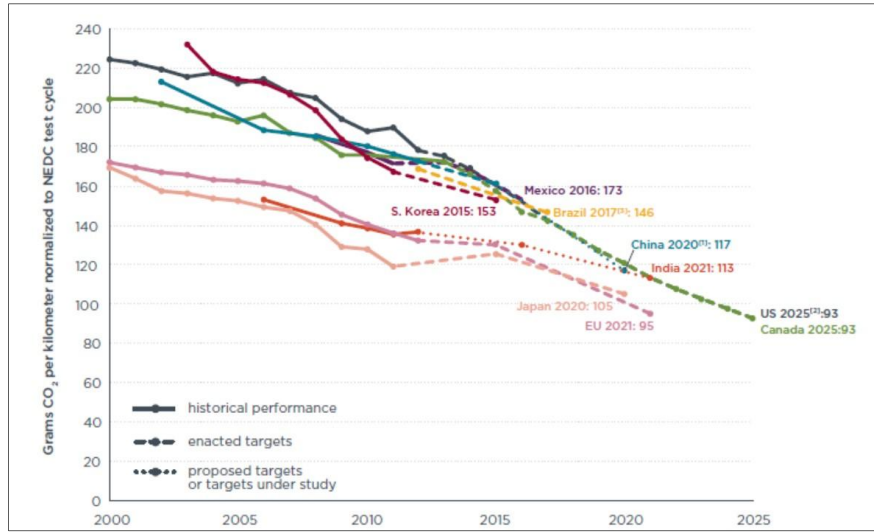


**Figure 1:** Comparison of global CO<sub>2</sub> regulation for passenger cars in terms of NEDC gCO<sub>2</sub>/km [6]

The introduction of mandatory targets contributed to a significant reduction of the average CO<sub>2</sub> emissions level, which dropped from 160 g/km in 2006 to 132 g/km in 2012 over the NEDC cycle, corresponding to a 17% reduction [6]. The 95 g/km target, which corresponds to 3.8 l/100 km of fuel consumption, requests an additional reduction of 27% for all manufacturers in the period 2015-2020.

However, several works [7,8] demonstrated a large discrepancy between the Type Approval (TA) and real life CO<sub>2</sub> emissions. In particular [8] analyses the data of 600.000 cars, considering Gasoline, Diesel and Hybrid vehicles, collected from 6 European countries and 11 different sources, showing an increasing divergence between TA and “real world” from 8% of 2001 to 37% of 2014 for conventional powertrains. While considering only Hybrid Electric Vehicles (HEVs), the deviation ranges from 39% of 2010 to 45% of 2014. Mock et al. in [8] identifies several reasons to explain the divergence between the TA and real life CO<sub>2</sub> emissions:

- **Driving cycle:** the NEDC is characterized by moderate transient and several steady state phases, which are not representative of real driving conditions;
- **Laboratory testing:** the NEDC, as other TA tests, takes place in a controlled laboratory environment on a chassis dynamometer, where temperature and humidity are under control. Moreover, the European TA procedure introduces several flexibilities in the test procedure, which are exploited by the car manufacturers, for example the neglecting of the battery State of Charge (SOC) variation along the cycle for conventional powertrains, special test driving techniques and the use of pre-series parts, which are not representative of production vehicles;



- **Road Load (RL) determination:** the TA procedure allows different flexibilities and tolerances to vehicle manufacturers during the RLs measurement on the test track such as the tire selection and preparation, the ambient test conditions and the pre-conditioning of the vehicle. Moreover, the NEDC procedure allows the use of the mass of the lightest vehicle model version for CO<sub>2</sub> compliance testing, which does not take into account the contribution of optional equipment on board;
- **Technology deployment:** different vehicle technologies are on average more effective during laboratory TA testing than under “real world” driving conditions. Different examples includes the stop-start, optimized control strategies for HEVs, automatic transmissions and engine downsizing;
- **Auxiliary loads:** auxiliary devices, such as the air conditioning and the infotainment, increase fuel consumption in real life. Nonetheless, these devices are switched off during the TA test, leading to unrealistically low CO<sub>2</sub> emissions values.

To reduce the gap between the TA test and the “real world” conditions, a technical group of the United Nations (U.N.) in 2007 decided to develop a worldwide-harmonized test procedure for light-duty vehicles, aiming to have a laboratory test representative of the average driving characteristics around the world and to make worldwide uniform the TA legislative contest. In particular, the second aspect is very important for the automotive industry, because if the test conditions were harmonized, it would be easier and cheaper to offer vehicles in different markets. The new test procedure is the Worldwide harmonized Light-duty Test Procedure (WLTP) and its reference driving cycle is the Worldwide harmonized Light-duty Test Cycle (WLTC). The development of the new test cycle was derived from real world driving data, collected from five different regions: EU, USA, India, Korea and Japan, over different road types (urban, rural, motorway) and driving conditions, covering a wide range of vehicles categories, engine capacities, Power to Mass Ratio (PMR) and manufacturers [9]. In 2010, the USA Environmental Protection Agency (EPA) decided to withdraw its participation to the development of WLTP, moving its resources to the preparation for the 2012-2016 and 2017-2025 GHG standards. Therefore, it was clear that the WLTP could not become a worldwide procedure as originally envisioned. Nevertheless, the working group decided to continue its work to finish the WLTP development by 2014, which was approved on March 2014 [10]. The application of WLTP in EU is planned by September 2017.

Figure 2 illustrates the complete WLTC driving cycle, which is composed by four different phases: Low, Medium, High and Extra-High, which are representative of urban, rural and highway driving conditions. Whereas this cycle will be adopted by different geographical areas, each market has the possibility to adapt it within certain framework settings. For example, Japan and India will not apply the high-speed phases of the WLTC, so that the overall test cycle will be different from EU, due to the different composition of the vehicle fleet [8].

Therefore, during the WLTC development it was necessary to adapt the test cycle to three vehicle classes: class 1, class 2 and class 3 characterized by different PMR categories. All vehicles with a PMR above 34 kW/ton belong to class 3, so they will use the complete WLTC cycle. Within class 3 there are two versions of the WLTC, which essentially differ by the maximum vehicle speed. The version 3.1 is applied to vehicles with a maximum speed below 120 km/h, while the version 3.2 above 120 km/h. The class 2 is applied to vehicles with a PMR between 22 kW/ton and 34 kW/ton. It has four phases as the class 3, but with lower accelerations and top speed in each phase. The WLTC class 1 was designed for lower powered vehicles with a PMR below 22 kW/ton and it has only the low and medium phases [9].

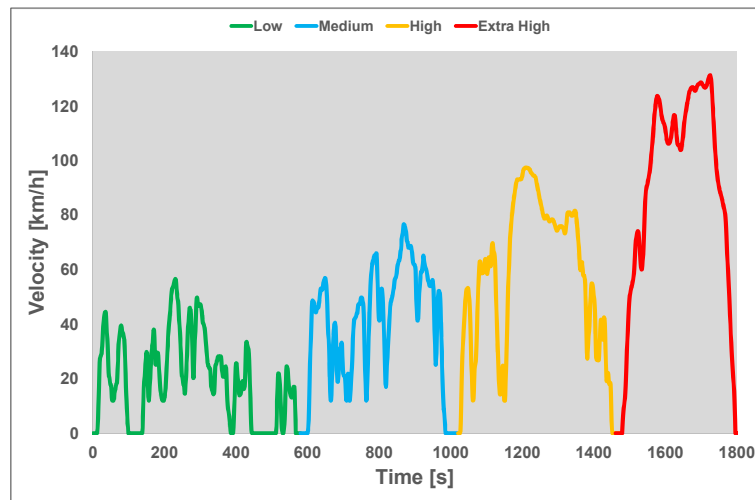


**Figure 2:** Vehicle speed profile of WLTC class 3.2

The WLTC class 3.2 is representative for the majority of the existing vehicles in Europe and it is more dynamic than the NEDC cycle, since it covers a wide range of engine operating conditions and it is more representative of real driving. It is characterized by higher speeds, steeper accelerations and less idling time compared to the NEDC, as shown in and in Figure 3 and in Table 1.

The mass and the RLs used during the TA procedure have an important role on pollutants and CO<sub>2</sub> emissions. The WLTP procedure to overcome some of the limitation of the actual TA procedure takes into account the weight of optional equipment and the vehicle payload when determining the mass of the vehicle. For practical reasons the United Nation Economic Commission for Europe (UNECE) decided to test only two vehicle versions:

- The first vehicle indicated as Test Mass Low (TML) requires the lowest amount of energy to drive the test cycle, which has no optional equipment, lowest rolling resistance and least aerodynamic drag;
- The second is characterized by the highest cycle energy demand of a vehicle model family indicated as Test Mass High (TMH), since it is equipped with

all the optional equipment, it has the highest rolling resistance and aerodynamic drag.

The TML and TMH are calculated according to the Global Technical Regulation (GTR) [11] as reported in Equation 1 and Equation 2:

$$TML = MRO + 25 + 0.15 \cdot MVL$$

**Equation 1:** Computation of TML according to [11]

$$TMH = MRO + OM + 25 + 0.15 \cdot MVL$$

**Equation 2:** Computation of TMH according to [11]

Where ***MRO*** is the Mass in Running Order, ***OM*** is the mass of optional equipment and ***MVL*** is the laden mass of the vehicle. The CO<sub>2</sub> emissions of all other vehicles in between TML and TMH are based on a regression line that connects the two tested model versions along the WLTC cycle.

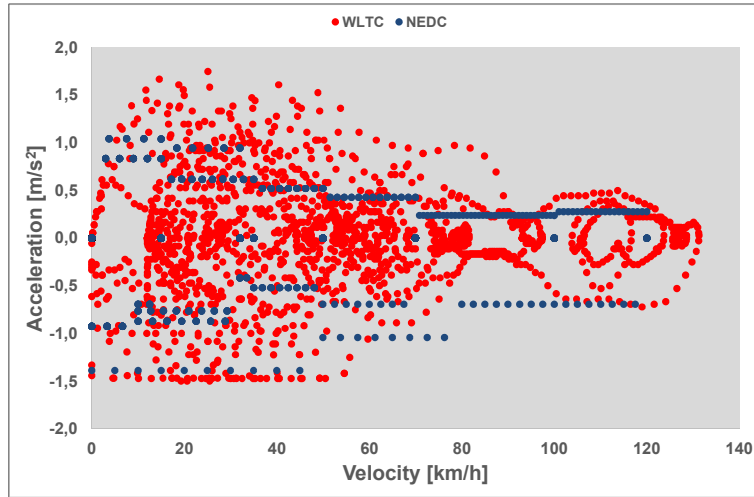


**Figure 3:** Speed and acceleration distributions along the WLTC and NEDC cycles

In addition to the different cycle characteristics and the test conditions, the WLTC differs from the NEDC for the following reasons [10,12,13]:

- The engine “Cold Start” increases CO<sub>2</sub> emissions due to higher mechanical friction and to the after-treatment warm-up. Since the WLTC is longer (1800 seconds and 23 km) than the NEDC (1180 seconds and 11 km), the impact of “Cold Start” on CO<sub>2</sub> emissions decreases;
- In WLTC the stop share corresponds to 12.6%, because there are less stop phases than in the NEDC (23.7% stop share), reducing the effectiveness of stop-start technology and consequently resulting in a lower CO<sub>2</sub> benefit;
- The WLTC cycle reaches higher speeds and it has stronger accelerations and thereby, on average, higher loads than the NEDC, leading the engine to

operate at higher efficiencies and consequently limiting the CO<sub>2</sub> emissions worsening;

- Along the NEDC cycle, vehicles equipped with manual transmissions have to follow a precise shift pattern defined as function of time. Instead, the WLTP adapts the gearshift strategy for manual transmissions to the individual characteristics of the vehicle, reducing the engine speed and resulting in an overall engine efficiency improvement.

Since the introduction of WLTP is planned for September 2017, the CO<sub>2</sub> emissions target should be adapted, because the current 2020 goals are based on NEDC assessment. The European Commission and the Joint Research Centre (JRC) are therefore developing a simulation tool called CO<sub>2</sub> Module for Passenger and commercial vehicles Simulation (CO2MPAS) for the correlation of CO<sub>2</sub> emissions from WLTP to NEDC, which will be used for the TA of European passenger cars from 2017, avoiding expensive duplicate test campaigns for car manufactures. However, the implementation of CO2MPAS has so far involved solely conventional light duty vehicles, while the impact of the new TA procedure on HEVs and Plug-In Hybrid Electric Vehicles (PHEVs) still has to be fully analyzed.

**Table 1:** Summary of the characteristics of NEDC and WLTC class 3.2

	Unit	NEDC	WLTC
<b>Start Condition</b>	kg	cold	cold
<b>Duration</b>	s	1180	1800
<b>Distance</b>	km	11.03	23.27
<b>Mean Velocity</b>	km/h	33.6	46.5
<b>Max Velocity</b>	km/h	120.0	131.3
<b>Mean Acceleration</b>	m/s <sup>2</sup>	0.59	0.41
<b>Max Acceleration</b>	m/s <sup>2</sup>	1.04	1.67
<b>Min Deceleration</b>	m/s <sup>2</sup>	-1.39	-1.50
<b>Mean Deceleration</b>	m/s <sup>2</sup>	-0.82	-0.45
<b>Stop Phases</b>	m/s <sup>2</sup>	14	9
<b>Shares</b>			
<b>Stop</b>		23.7%	12.6%
<b>Constant Driving</b>		40.3%	3.7%
<b>Acceleration</b>		20.9%	43.8%
<b>Deceleration</b>		15.1%	39.9%

## 1.2 Impact of actual technologies on CO<sub>2</sub> reduction: A real case study

The introduction of stringent limits on CO<sub>2</sub> emissions pushed car manufacturers to introduce different technical solutions to increase the overall powertrain efficiency along the NEDC cycle. The actual technology portfolio includes the stop-start, advanced cooling systems, engine downsizing and vehicle electrification [12,14]. This section analyses the impact of the WLTP procedure on CO<sub>2</sub> emissions for two different passenger cars, described in Table 2.

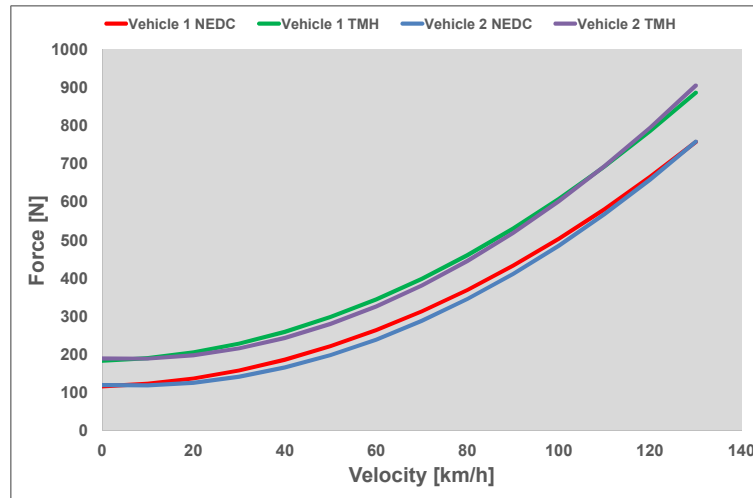
**Table 2:** Conventional powertrains - Vehicle characteristics

	<b>Vehicle 1 (SI)</b>	<b>Vehicle 2 (CI)</b>
<b>Curb Mass</b>	1260 kg	1400 kg
<b>Gross Mass</b>	1830 kg	2080 kg
<b>Engine</b>	4 in-line cylinder SI turbocharged 16V Euro5	4 in-line cylinder CI turbocharged 16V Euro5
<b>Displacement</b>	1400 cm <sup>3</sup>	1600 cm <sup>3</sup>
<b>Max Torque</b>	250 Nm @ 2500 rpm	320 Nm @ 2250 rpm
<b>Max Power</b>	160 HP @ 5500 rpm	135 HP @ 3500 rpm
<b>Gearbox</b>	Manual with 6 gears	Manual with 6 gears

The first one is a Euro 5 C-segment vehicle equipped with a turbocharged Spark Ignition (SI) engine of 1.4 l and a six gear manual transmission, while the second is a Euro 5 C-segment combined with a turbocharged Compression Ignition (CI) of 1.6 l and a six gear manual transmission. This analysis carried out in closed collaboration with the JRC is based both on experimental acquisitions and mathematical simulations, developed in GT-Suite environment [15,16] using a “quasi-static” approach, in which the Internal Combustion Engine (ICE), the transmission efficiency and the 12V battery are represented through performance maps, which have been experimentally measured under steady state operating conditions. Although this methodology neglects transient phenomena, such as the turbo lag, simulating the transient events as a sequence of steady state events, it has been proven to be suitable for the purpose of this work [17]. The experimental campaign, carried out on a vehicle chassis dyno, was performed along the NEDC and WLTC, considering different thermal status at the beginning of the cycle. In particular, in the “Hot Start” case the ICE coolant temperature is around 90°C, while in the “Cold Start” is around 23/25 °C. The two vehicles were tested along the WLTC cycle considering only the TMH case, because it represents the most severe condition according to the WLTP procedure. The mathematical models, developed and validated based on the experimental tests, were used to evaluate the weight on CO<sub>2</sub> emissions of test mass/RLs, of “Cold Start” and of stop-start along the NEDC and WLTC cycles. Vehicles test conditions for the two driving cycles are listed in Table 3, while the differences between the RLs are shown in Figure 4.

**Table 3:** Conventional powertrains - Vehicle test conditions

		Unit	NEDC	TMH
<b>Vehicle 1 (SI)</b>	<b>Test Mass</b>	kg	1360	1570
	<b>F<sub>0</sub></b>	N	116.8	183.7
	<b>F<sub>1</sub></b>	N/(km/h)	0.337	0.347
	<b>F<sub>2</sub></b>	N/(km/h) <sup>2</sup>	0.0353	0.0389
<b>Vehicle 2 (CI)</b>	<b>Test Mass</b>	kg	1500	1770
	<b>F<sub>0</sub></b>	N	120.3	190.1
	<b>F<sub>1</sub></b>	N/(km/h)	-0.518	-0.503
	<b>F<sub>2</sub></b>	N/(km/h) <sup>2</sup>	0.0417	0.0462

**Figure 4:** Conventional powertrains - RLs for NEDC and WLTP procedures

The increase of test mass/RLs and the higher dynamics of WLTC cycle compared to NEDC lead to an average increase of cycle energy demand of 45%, while the average CO<sub>2</sub> increase is limited to 20% as summarized in Table 4, taking into account also the effect of “Cold Start”. The average increase of ICE efficiency along the WLTC cycle limits the CO<sub>2</sub> penalty, as shown in Figure 5 and Figure 6. The red dots represent the engine operating points along the WLTC cycle in the TMH condition, the blue ones stand for the NEDC, the black continuous line represents the Wide Open Throttle (WOT) curve and finally the contour lines are

the isoefficiency curves of the ICE. Both engines along the NEDC cycle work with a Brake Mean Effective Pressure (BMEP) below 12 bar in the low efficiency area (Figure 5 and Figure 6 blue continuous line), with an average efficiency in the “hot start” case of 25% for the SI engine and of 27.5% for the CI. While on WLTC, the average efficiency, considering the same engine thermal status as before, increases because both engine operate in the medium-high load area (Figure 5 and Figure 6 red continuous line) and the majority of operating points are located between 1500 rpm to 2000 rpm, where the effect of engine friction is lower compared to high speed regions. The average efficiency of the SI engine is around 30%, while the CI is equal to 32%, showing an average increase of 5% respect to the NEDC cycle.

**Table 4** Conventional powertrains - Energetic analysis and CO<sub>2</sub> emissions during the “Cold Start”

		Unit	<i>NEDC</i>	<i>WLTC TMH</i>
<b>Vehicle 1 (SI)</b>	<b>Energy Demand</b>	Wh/km	<i>117</i>	<i>169</i>
	<b>CO<sub>2</sub> Emissions</b>	g/km	<i>149</i>	<i>164</i>
<b>Vehicle 2 (CI)</b>	<b>Energy Demand</b>	Wh/km	<i>143</i>	<i>176</i>
	<b>CO<sub>2</sub> Emissions</b>	g/km	<i>120</i>	<i>149</i>

The analysis of the engine operating points can also be carried out in a different way as shown in Figure 7, where the energy delivered by the engine is grouped in load bins. Along the NEDC cycle a significant fraction of energy is provided by the two powertrains under poor efficiency conditions, while along the WLTC cycle in the TMH case the center of gravity of the energy distribution is moved toward to the maximum efficiency area.

The growing of CO<sub>2</sub> emissions from NEDC to WLTP is mainly due to the test procedure rather than the new driving cycle. The effect of mass and RLs along the WLTC on CO<sub>2</sub> emissions was rated through the vehicle simulation, neglecting the effect of thermal transient. As shown in Figure 8, the two vehicles were simulated along the WLTC cycle using the mass and the RLs prescribed by the European TA procedure, indicated as EU. Vehicle 2 shows that the driving cycle is responsible only of 5% increase of CO<sub>2</sub> emissions, while the mass and RLs are responsible of 20%. Instead, vehicle 1 along the WLTC with the EU RLs shows a slight reduction of CO<sub>2</sub> emissions compared to NEDC (-1.5%). The main reason is due to the average increase of the engine efficiency combined with the less severe operating conditions of the ICE, as shown in Figure 9 and Figure 10, where the cyan points are the engine operating points along the WLTC using the EU RLs.



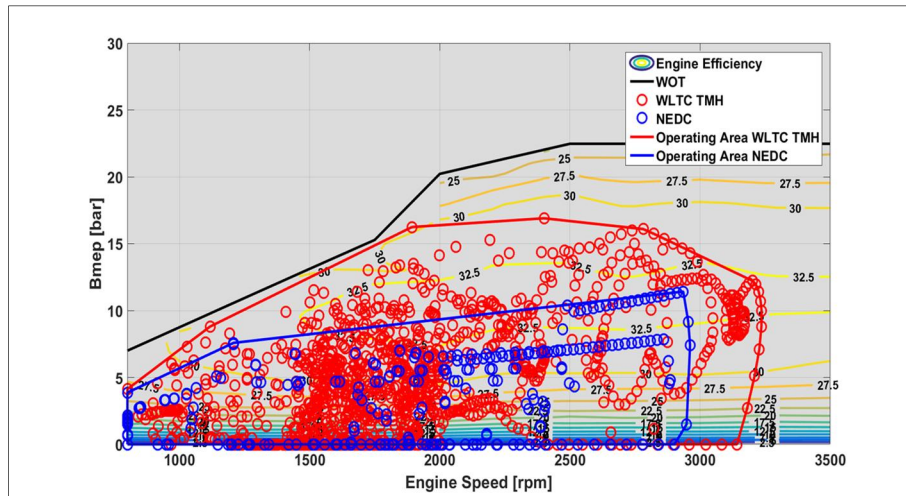


**Figure 5:** Conventional powertrains - ICE operating points along the NEDC and WLTC TMH for vehicle 1

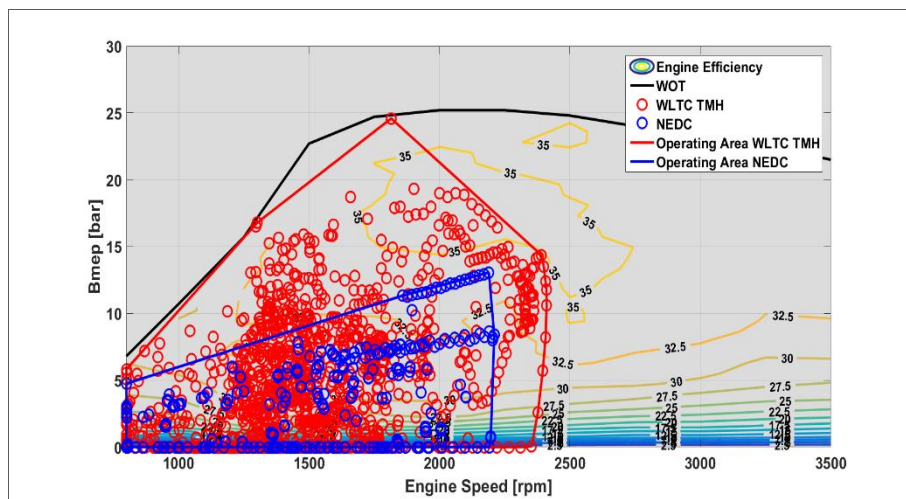


**Figure 6:** Conventional powertrains - ICE operating points along the NEDC and WLTC TMH for vehicle 2

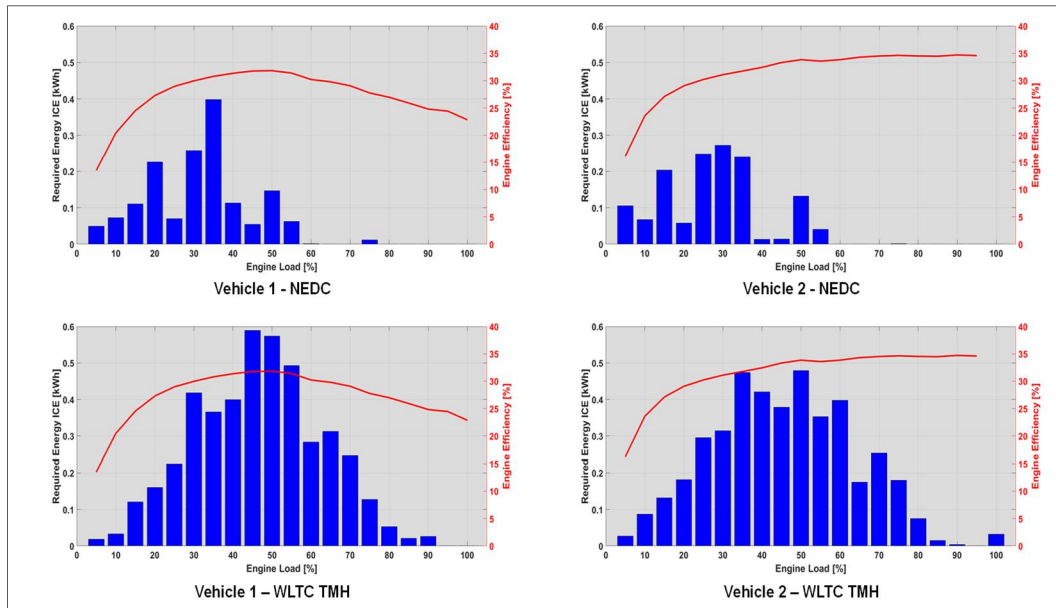


**Figure 7:** Conventional powertrains - Energy delivered by the ICE for vehicle 1 and vehicle 2 along the NEDC and WLTC cycles during the “hot start” case

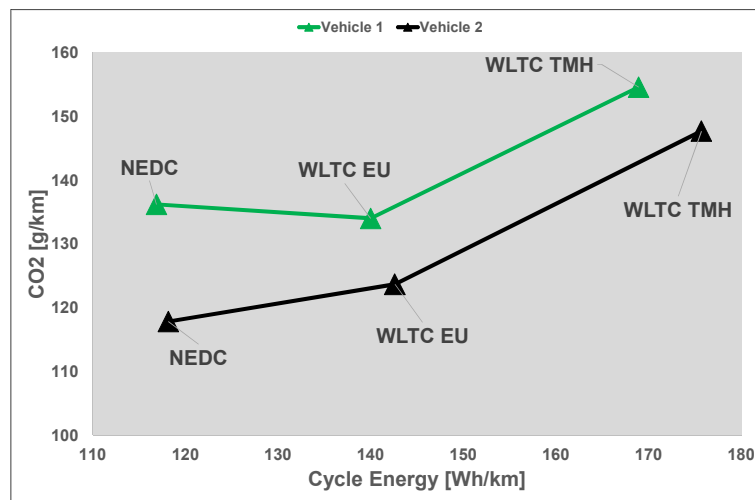


**Figure 8:** Conventional powertrains - CO<sub>2</sub> emissions as function of cycle energy demand

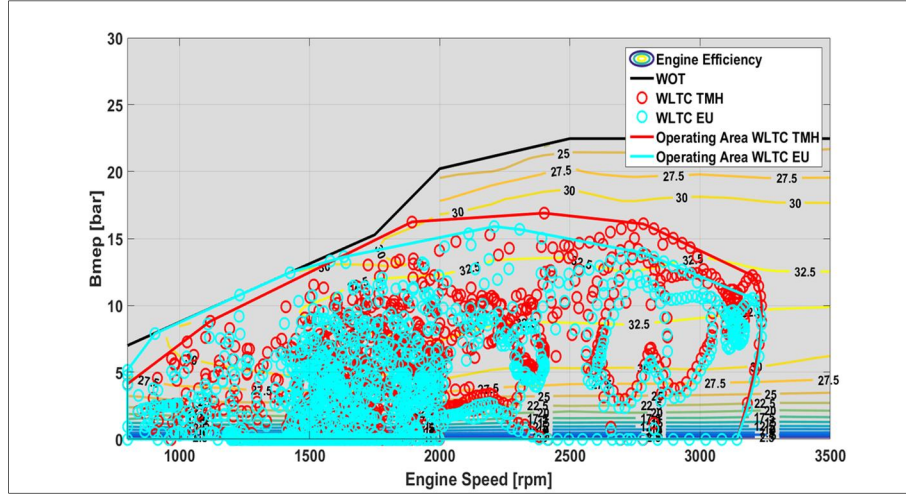


**Figure 9:** Conventional powertrains - ICE operating points along the WLTC cycle using the EU (cyan) and the TMH (red) RLs for vehicle 1

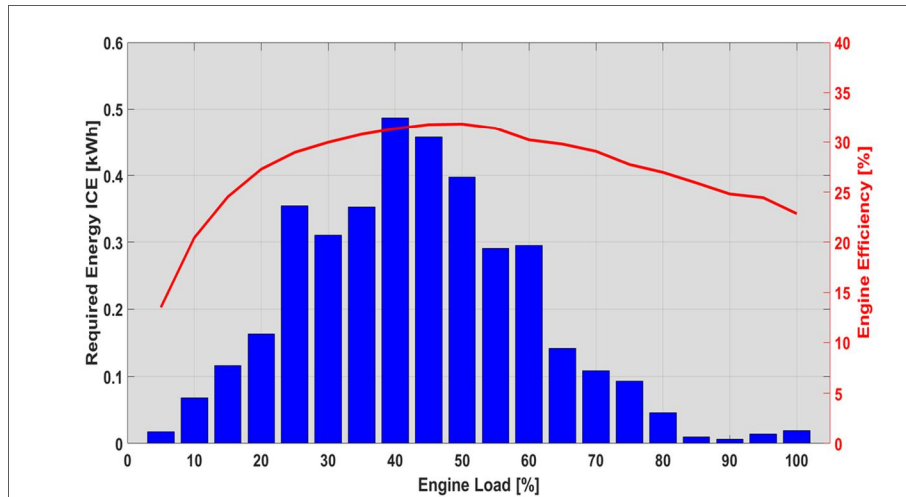


**Figure 10:** Conventional powertrains - Energy delivered by the ICE for vehicle 1 along the WLTC cycles using EU RLs during the “hot start” case

As mentioned in [10], the effect of “Cold Start” on CO<sub>2</sub> emissions is reduced from NEDC to WLTP. Along the NEDC, the “Cold Start” has a significant impact on CO<sub>2</sub> emissions, since the load demand to the ICE is very low, making the engine warm-up a complex problem. Therefore, the automotive industry adopted various technical solutions to speed-up the engine warm-up, such as the use of switchable pumps or thermal encapsulation [18,19]. This section analyses the share of “Cold Start” for both driving cycles and its effect on CO<sub>2</sub> emissions. Through the analysis of the coolant temperature measurements, it is possible to evaluate the share of the “Cold Start”, assuming for both vehicles as 70°C the reference temperature of the warm engine condition. The SI engine is characterized by higher operating

temperatures than the CI engine. Therefore, vehicle 1 has a shorter duration of the warm-up phase compared to vehicle 2 along the NEDC, corresponding respectively to 35% and 59% of the cycle. While on WLTC using the TMH, the warm-up share is around 21% of the cycle for vehicle 1 and 23% for vehicle 2, as summarized in Figure 11.

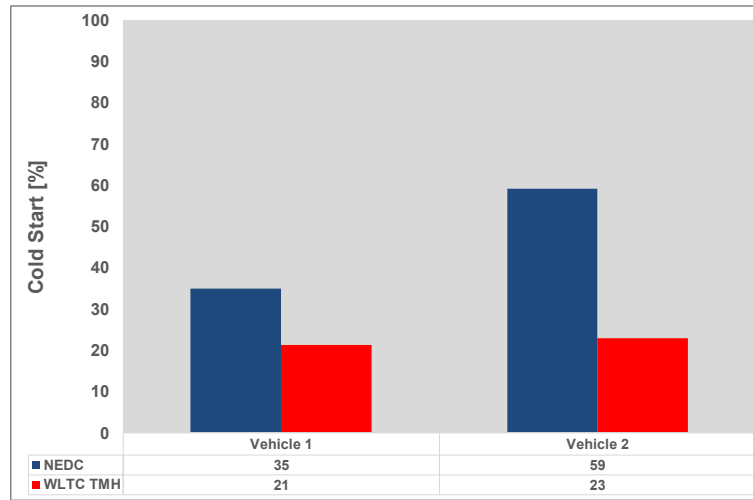


**Figure 11:** Conventional powertrains - “Cold Start” share along the NEDC and WLTC cycles

The duration of the “Cold Start” is reduced from NEDC to WLTC since the engine on average operates at higher loads, as highlighted in Figure 5 and Figure 6. Thus, the effect of thermal transient on CO<sub>2</sub> emissions will be limited as reported in Figure 12. In fact, the growing of CO<sub>2</sub> emissions on NEDC for vehicle 1 is around 9.5%, while on WLTC is 5%, which is almost half. For vehicle 2, the situation is slightly different, since on NEDC the increase is around 2.5%, while on WLTC is around 1%. The reduction of the negative effects for the CI engine on NEDC is due to the presence of a switchable pump to speed-up the warm-up by disabling the coolant circuit pump until a threshold temperature is reached, as evident from the temperature profiles reported in Figure 13.

An important device to reduce the CO<sub>2</sub> emissions is the stop-start, but, as highlighted by [10], its effectiveness is limited to the NEDC cycle, since as shown Table 1 the stop phases represents the 23.7% of the cycle while on WLTC only 12.6%. This part analyses the effectiveness of the stop-start device along the WLTC cycle using the mathematical model, without taking into account the effect of the thermal transient. As illustrated in Figure 14, the stop-start on vehicle 1 reduces the CO<sub>2</sub> emissions of 5% along the NEDC cycle, while on WLTC the decrease is limited only to 2%. Similarly, for vehicle 2 the reduction on NEDC is 4%, while on WLTC is still 2%. These results confirm the limited effectiveness of stop-start technology on WLTC, proving that the efficiency of such device is strictly related to the driving conditions.

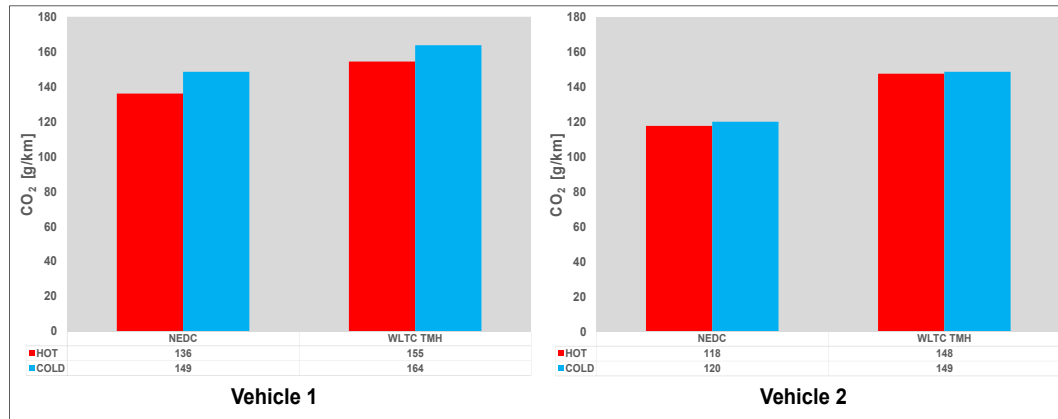


**Figure 12:** Conventional powertrains - Effect of "Cold Start" on CO<sub>2</sub> emissions along the NEDC and WLTC cycles

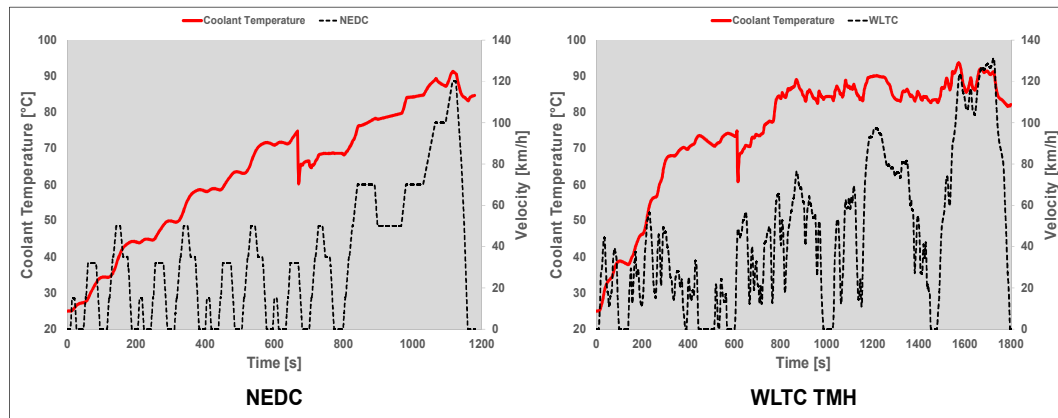


**Figure 13:** Conventional powertrains - Coolant temperature profiles along the NEDC (left) and WLTC (right) for vehicle 2

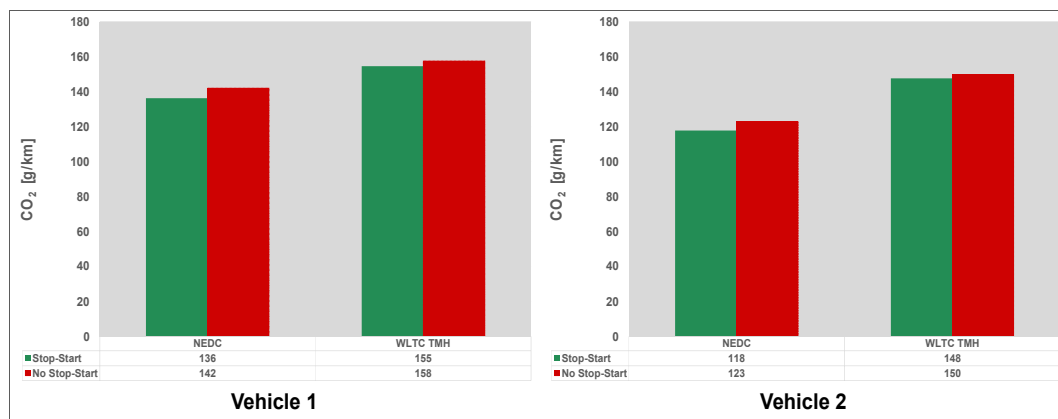


**Figure 14:** Conventional powertrains: effectiveness analysis of stop-start for vehicle 1 (left) and vehicle 2 (right) along the NEDC and WLTC cycle

### 1.3 CO2MPAS

The 2020 CO<sub>2</sub> emissions target for European fleet are set to 95 g/km on the current TA procedure. However, the EU planned to introduce by 1<sup>st</sup> September 2017 the new WLTP procedure, which will generate significant differences in the CO<sub>2</sub> levels respect to the measured emissions under the existing NEDC procedure, as demonstrated in 1.2. During the WLTP phase-in, from 2017 to 2020, it is important to monitor the compliance of sold vehicles with the specific emission targets using the NEDC based CO<sub>2</sub> values. With the aim to reduce the testing burden for both manufactures and TA authorities, the European Commission proposed the use of a simulation tool, which uses as input data the measurements derived from the WLTP TA test [20]. The correlation model is called CO2MPAS and it is developed by the JRC together with the support of Laboratory of Applied Thermodynamics (LAT) of the Aristotle University and of vehicle manufactures, which provided laboratory tests necessary for the development of the model and its validation [21]. The development of CO2MPAS involves solely the CO<sub>2</sub> emissions, because it is not necessary to set new limits for regulated pollutants such as NO<sub>x</sub>, CO, Particulate Matter (PM) and Particulate Number (PN).

CO2MPAS is a fully vehicle simulation model based on standard vehicle longitudinal dynamics and energy consumption simulation, which was designed according to the following requirements:

- Capture the effect of specific technologies developed for the fuel consumption reduction, when individually applied or in combination, at vehicle level under different operating conditions, using physical models and limiting the use of statistical factors, with an accuracy of 2-3% as compared to the measurements;
- Limit the number of inputs to the vehicle characteristics and measurements already available during the TA test [22].

To detect correctly the CO<sub>2</sub> emissions along the NEDC cycle, CO2MPAS should identify accurately the engine power, gear shifting in case of Automatic Transmissions (AT), the powertrain efficiencies and the engine thermal transient. The model was thoroughly validated with respect to real vehicle measurements [22] for conventional powertrains. The application of CO2MPAS during the TA is regulated by [20,23], which present the correct use and the controls made by European authorities to prevent possible fraud. In particular [20] highlights the possibility for European authorities to perform a series of random physical tests to prevent the exploitation of correlation model's tolerances to lower artificially the CO<sub>2</sub> emissions values used for target compliance purposes. In this case, the European Commission can apply a correction factor to increase the average specific emissions of a manufacturer.

Within this context, the research project, which is here reported, carried out in closed collaboration between Politecnico di Torino and JRC has the purpose to

extend predictive capabilities of CO2MPAS for HEVs and PHEVs. The goal is the development of a predictive model capable to simulate a wide range of hybrid architectures and technologies along the NEDC cycle, using a small amount of measurements available from the WLTP test, such as the battery current/voltage, the engine speed, the coolant temperature and the CO<sub>2</sub> emissions. The starting point was the analysis of the hybrid portfolio technologies and architectures available on the market, selecting the most representative vehicle models to set-up the experimental test campaign, described in Chapter 2, necessary for the development of the model and its validation.

The definition of a unique mathematical model able to predict the Energy Management System (EMS) behavior for different architectures and technological solutions represented the most difficult part of the project. The implemented methodology exploits a simplified approach, presented in Chapter 3, which analyses the experimental acquisitions to detect the main control parameters of a hybrid powertrain such as the ICE enabling, the actuation of Electric Boost (E-Boost) and Load Point Moving (or Smart Charge), the “Cold Start” strategies, etc.

Finally, the model validation, presented in Chapter 4, focuses on the correct detection of the engine enabling along the NEDC cycle, on the proper simulation of the parallel mode (E-Boost and Load Point Moving) and finally on the computation of CO<sub>2</sub> emissions according to the European regulation [24], trying to reach a target error of  $\pm 3$  g/km.

## Chapter 2

# Experimental campaign on hybrid vehicles

### 2.1 Introduction

This chapter will present the test campaign carried out at JRC VELA laboratory on HEVs and PHEVs, necessary for the development of the CO2MPAS. The main outcome is represented by the reverse engineering activity on two different passenger cars, characterized by different hybridization levels and architectures.

The purpose is the characterization of the EMS through a limited number of information derived from the experimental test carried out on the chassis dyno along the WLTC to build a model capable to predict the CO<sub>2</sub> emissions on the NEDC cycle. Therefore, the vehicles were tested on the two cycles applying the Regulation 83 [24], which is actually used for the TA procedure of European cars sold in Europe. The necessity to characterize the vehicle performance on NEDC is necessary not only to validate the code, but also to understand if the EMS strategies, which will be exploited on WLTC, will be comparable to those developed for the NEDC.

### 2.2 Case study

The development and validation of the correlation function or Meta-Model is based on the test activities carried out on two different hybrid passenger cars with different architecture and level of hybridization. Since the code should be able to simulate properly both HEVs and PHEVs, two different vehicles were considered:



- The Toyota Yaris Hybrid, which is an Euro 6 B-Segment HEV, is equipped with an Electric Continuous Variable Transmission (eCVT);
- The Volkswagen Golf GTE, which is a Euro 6 C-Segment PHEV, is combined with a Flywheel Alternator System (FAS) architecture.

### 2.2.1 The Yaris Hybrid

The Yaris hybrid is a complex hybrid equipped with an eCVT hybrid architecture, represented in Figure 15, combined with a SI engine. The main characteristics are listed in Table 5.

In the eCVT system the rotational shaft of the planetary gear carrier is directly linked to engine and it transmits the motive power to the outer ring gear and the inner sun gear via pinion gears. The ICE is a four-cylinder in-line Atkinson 1.5 l gasoline with a maximum power of 55 kW at 4800 rpm and a compression ratio of 13:1. The rotational shaft of the ring gear is directly linked to the 45 kW Motor Generator 2 (MG2) and it transmits the drive force to the wheels, while the rotational shaft of the sun gear is directly linked to the electric generator (MG1) [25]. The high voltage battery is a Nickel Metal Hydrate (NiMH) made by 120 cells connected in series.

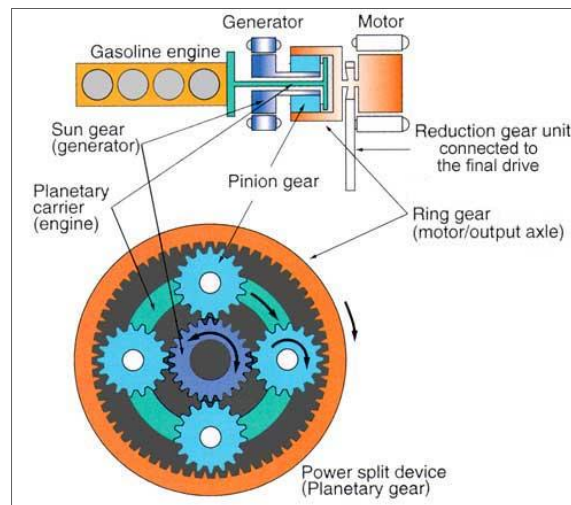


**Figure 15:** Yaris Hybrid - Schematic of the eCVT architecture [25]

**Table 5:** Yaris Hybrid – Vehicle characteristics

<b>Technical Data</b>	
<b>Curb Mass</b>	1120 kg
<b>Gross Mass</b>	1565 kg
<b>ICE</b>	Spark Ignition Atkinson Cycle Displacement: 1.5 l Rated power: 55 kW @ 4800 rpm Rated torque: 111 Nm @ 3600–4800 rpm
<b>MG2</b>	Maximum output power: 45 kW Maximum output torque: 169 Nm
<b>Battery</b>	Type: NiMH Capacity: 6.5 Ah Nominal voltage: 144 V Energy: 1 kWh

The Yaris Hybrid along a driving cycle can operate in two different operating modes depending on the battery energy level and on the driver's power demand:

1. ***Electric Vehicle (EV)***: when the ICE operates in an inefficient range, such as at low-medium speeds, the engine is turned off and the traction power is provided only by the MG2, as illustrated in Figure 16;

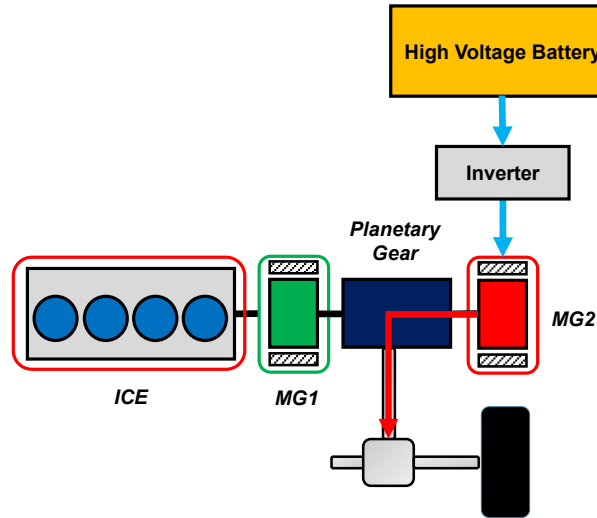


Figure 16: Yaris Hybrid – EV mode

2. **Parallel Hybrid:** the engine is enabled at medium-high speeds and it supports the vehicle driving, allowing the powertrain to operate in two different ways depending on battery SOC and on accelerator pedal:
  - a. **Smart Charge or Load Point Moving:** the ICE operating points are moved closed to the optimal efficiency area and the power exceeding the vehicle propulsion needs is used to recharge the battery through the generator MG1, as depicted in Figure 17 by the green line;

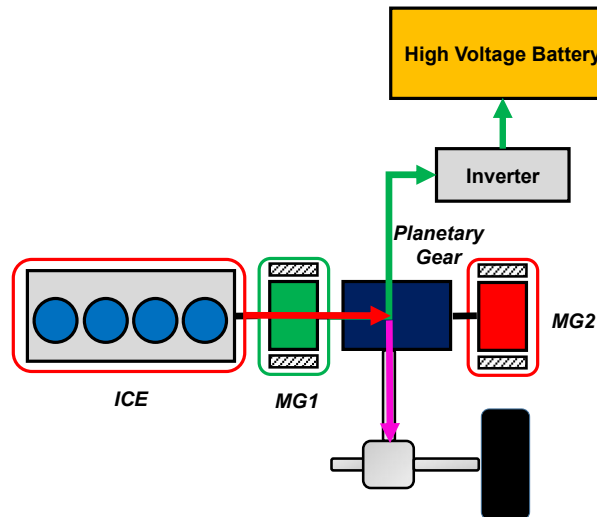


Figure 17: Yaris Hybrid – Smart Charge mode

- b. **Electric Boost (E-Boost):** the high voltage battery provides an extra power contribution to the MG2, represented by the magenta arrow, to

support the engine during sudden load demand, as illustrated in Figure 18.

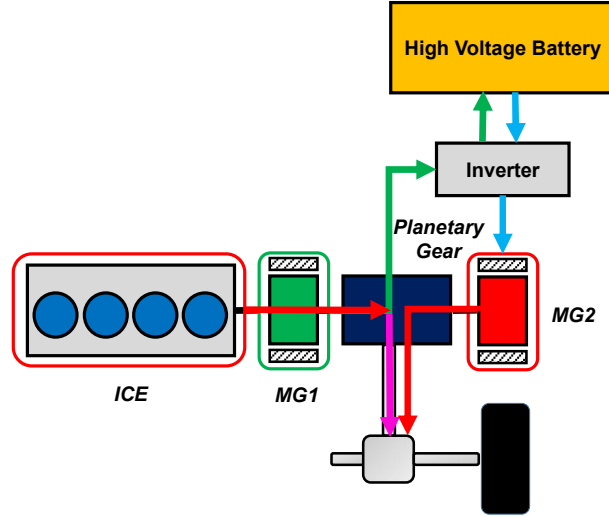


Figure 18: Yaris Hybrid – E-Boost mode

### 2.2.2 The Golf GTE PHEV

The Golf GTE is a parallel PHEV equipped with FAS hybrid architecture, combined with a SI engine and a six gear Dual Clutch Transmission (DCT). The main vehicle characteristics are listed in Table 6.

As depicted in Figure 19, the 75 KW electric machine (E-Motor), which is a permanent magnet synchronous motor, is located between the 1.4 l SI engine and the six-speed DCT. The ICE is a four-cylinder in-line turbocharged with a maximum power of 110 kW from 5000 to 6000 rpm and a rated torque of 250 Nm from 1600 to 3500 rpm. The high voltage battery is a Lithium Ion, made of 96 cells connected in series with a nominal energy of 9 kWh.

The FAS architecture allows the powertrain to operate in two different ways:

1. **EV**: the engine is shut down and all the power necessary to propel the vehicle is provided by the E-Motor. During the pure electric drive, the clutch is open to avoid power dissipation caused by the ICE dragging.
2. **Parallel**: the clutch is closed then the ICE is operative and it propels the vehicle.

As the Toyota Yaris Hybrid, the Golf GTE enables in Parallel mode the E-Boost or the Load Point Moving, depending on the accelerator pedal position and on the battery SOC. Conversely, both operating conditions are managed by the E-Motor.

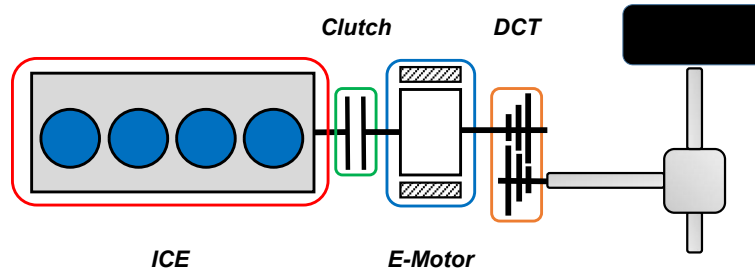


**Figure 19:** Golf GTE – Schematic of the FAS architecture

**Table 6:** Golf GTE – Vehicle characteristics

Technical Data	
<b>Curb Mass</b>	1524 kg
<b>Gross Mass</b>	2020 kg
<b>ICE</b>	Spark Ignition Turbocharged Displacement: 1.4 l Rated power: 110 kW @ 5000-6000 rpm Rated torque: 250 Nm @ 1600–3500 rpm
<b>E-Motor</b>	Maximum output power: 75 kW Maximum output torque: 330 Nm
<b>Battery</b>	Type: Lithium Ion Capacity: 25 Ah Nominal voltage: 345 V Energy: 8.5 kWh

This vehicle offers various operating modes selectable by the driver from the infotainment panel (shown in Figure 20), enabling the electric driving in different conditions:

1. **E-Mode:** it allows always the electric driving when the high voltage battery is sufficiently charged and the vehicle speed is below 130 km/h;

2. **Hybrid Auto Mode:** the vehicle can be driven electrically at low/medium speeds, depending on the charge level of the high voltage battery and the accelerator pedal;
3. **GTE:** this modality is suitable for a sport driving style by changing the engine and gearbox maps to make the car more responsive to accelerator pedal;
4. **Battery Hold Mode:** the vehicle is driven by the ICE and the high voltage battery is not used for the electric drive, keeping unchanged the electric range;
5. **Battery Charge Mode:** the ICE propels the vehicle and the E-Motor is used to charge the high voltage battery [26].

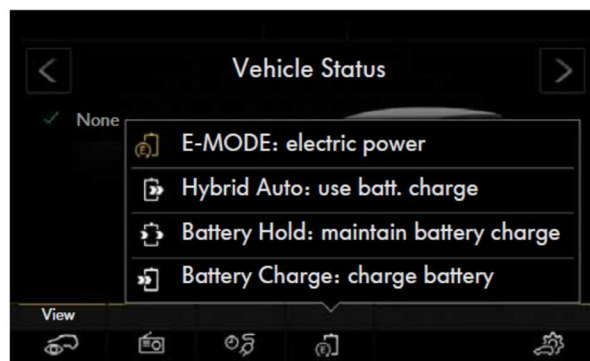
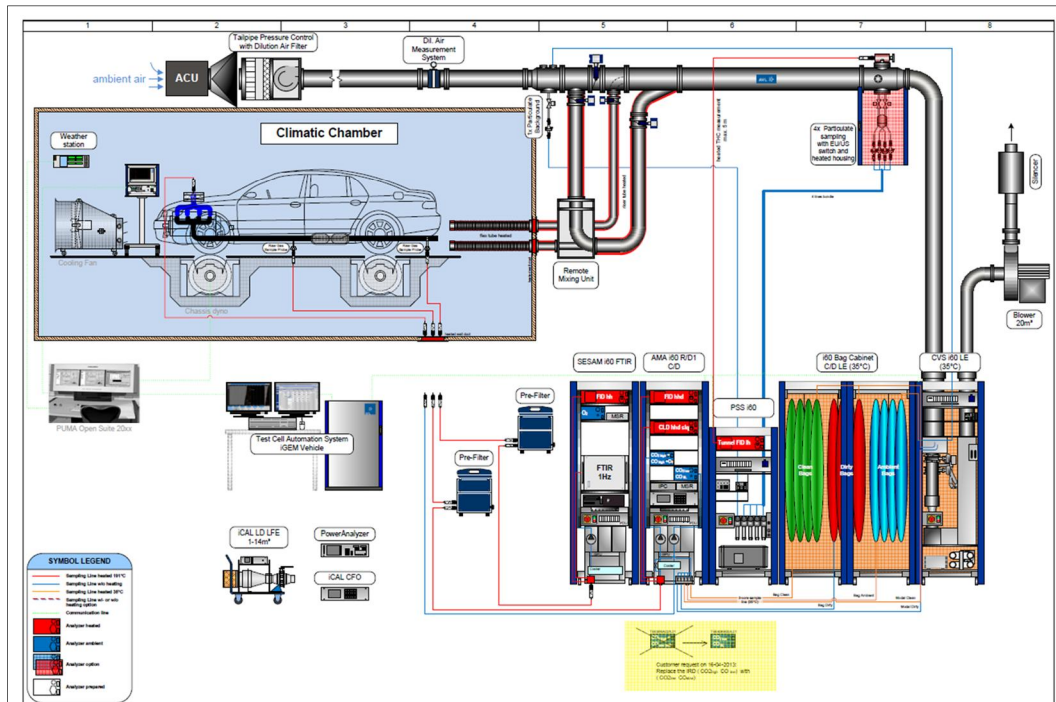


Figure 20: Golf GTE – Hybrid menu [26]

## 2.3 The experimental set-up

The measurements of gaseous emissions and of vehicle parameters representative of the EMS conduct were done on a chassis dynamometer, which simulates the resistive force through the installed rollers controlled by an electric machine. The test cell of the VELA lab, depicted in Figure 21 and Figure 22, is equipped with a four Wheel-Drive (4WD) chassis dynamometer, having two rollers benches with a diameter of 48 inches (1.219 m), allowing a maximum traction force of 3300 Nm and an inertia range between 454 to 2720 kg. The chassis dynamometer is installed in a climatic chamber, which has the capability to simulate several ambient conditions from -30 to 50 °C and a wide humidity range.



**Figure 21:** VELA 8 chassis dyno and emission system overview



**Figure 22:** Climatic chamber and chassis dynamometer at VELA 8 lab

The sampling of gaseous emissions is managed through a Critical Flow Venturi – Constant Volume Sampler (CFV – CVS), where the exhaust gasses are diluted with air to maintain a total constant flow rate under all driving conditions, allowing

a simple calculation of the mass-based emission in g/km. The dilution of exhaust gasses is necessary to avoid the condensation of water vapor, which could adulterate the measurements of particular pollutants such as the PM, and it inhibits the reaction between different chemical species. However, the use of dilution reduces the concentration of chemical species, requesting the adoption of more sensible and accurate measurement devices. The CVS dilution ratio is typically between 10 and 30, which compared to the dilution occurring in the ambient is very small, which is from 500 to 1000 [27].

The emissions bench produces two different measurements of pollutants: the bag and the modal. During the modal measurement, the sampling probe is located inside the dilution tunnel and it samples a quantity of exhaust gasses directly proportional to the diluted flux, which is analyzed second by second producing an emission profile along the cycle. Instead, the bag analysis collects the exhaust gasses inside a bag during the test, which will be analyzed at the end of the cycle. The bag measurement is more accurate than the modal for two different reasons:

- Before the measurements of pollutants concentrations inside the bag, the emission bench “sniffs” a small quantity of the gas to adjust the sensitivity of the instrument, than in modal this accuracy level is not possible due to the continuous measurements in a short amount of time;
- The exhaust gasses are well mixed with air inside the bags, so the measured concentration is representative of the flow.

The development of the Meta-Model requests the use of modal emissions to build the CO<sub>2</sub> virtual maps necessary to compute the emissions along the NEDC cycle, which will be illustrated in Chapter 3.

In addition to gaseous emissions, it is important to measure the parameters representative of the EMS conduct such as the engine speed, the coolant temperature, the current and the voltage from the high voltage battery. The ICE speed and the coolant temperature were acquired from the On Board Diagnosis (OBD), using a commercial tool available on the market. The measurements of current were done using a power analyzer, a Yokogawa WT1800, together with a current clamp, which characteristics are listed in Table 7 and Table 8.

Since the difficulties to have a direct access to the high voltage battery, the current measurements were done at the terminals of the inverter, through which the Direct Current (DC) flows, as shown in Figure 23 and Figure 24. For the Toyota Yaris it was difficult to clamp the current sensor to the high voltage cable due to the thickness of the insulation system. Therefore, the electric insulation was disassembled from the inverter and bridged to the inverter case to prevent possible ECU errors, as shown in Figure 25.



**Table 7:** Power analyzer characteristics

<b>YOKOGAWA WT1800</b>		
<b>Measurement Range</b>	Voltage	Peak value: 3000 V Continuous: 2000 V
	Current	Peak value: peak value of 150 A Continuous: peak value of 150 A
<b>Voltage/Current Accuracy</b>		$\pm 0.1\%$
<b>Power Accuracy</b>		$\pm 0.05\%$
<b>Input Impedance</b>		2 M $\Omega$
<b>Sampling Speed</b>		2 MS/s
<b>A/D Converter</b>		Resolution: 16 bits
		Conversion rate: 500 ns

**Table 8:** Current clamp characteristics

<b>HIOKI 3274</b>	
<b>Measurement Range</b>	Peak value: 300 Arms Continuous: 150 Arms
<b>Noise</b>	25 mArms
<b>Input Impedance</b>	1 m $\Omega$ @ 100 Hz
	10 $\Omega$ @ 100 MHz
<b>Power Supply Voltage</b>	12 V
<b>Operating Temperature and Humidity</b>	0-40 °C, 80% rh

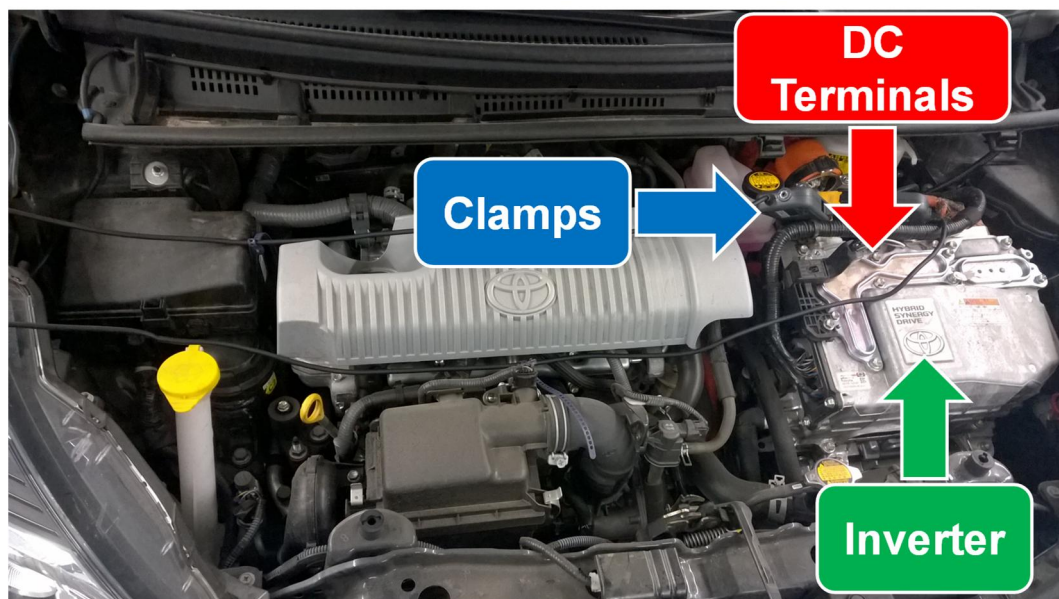


**Figure 23:** Yaris Hybrid - Current measurement

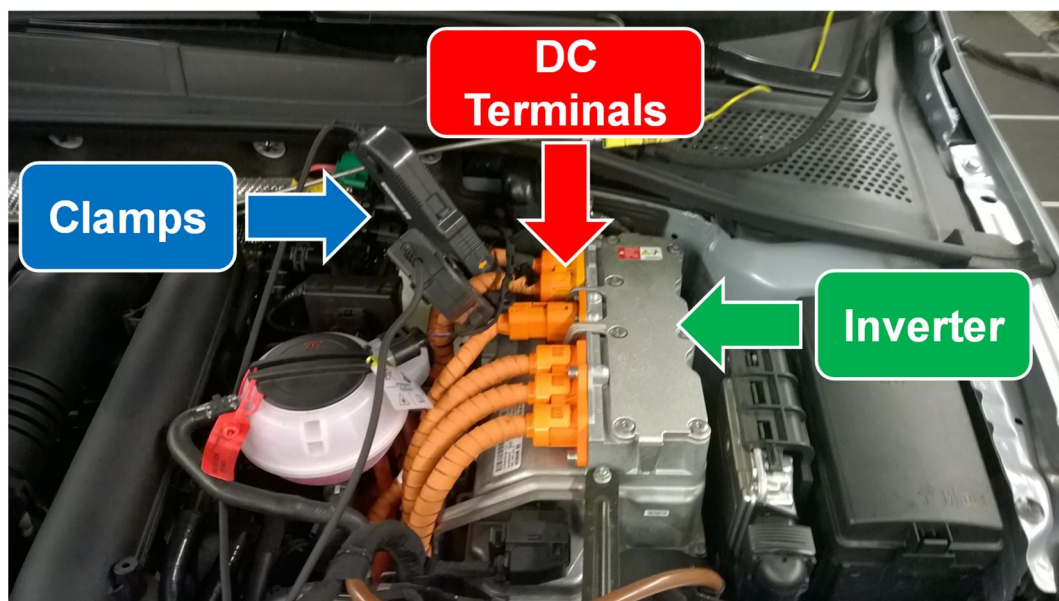


**Figure 24:** Golf GTE – Current measurement



**Figure 25:** Yaris Hybrid – Detail of current clamp positioning

The measurement of the battery voltage represents a critical issue for safety reason and for the difficulty to have a direct access to the terminals. In the Toyota Yaris the high voltage battery is placed behind the rear seats, permitting the direct connection from the terminals to the power analyzer. Conversely, for the Golf GTE this operation was not possible because the battery pack is placed on the car floor. Therefore, for the high voltage measurement was used a CAN scan tool specific for Volkswagen cars.

## 2.4 Test procedure

The test along the WLTC and NEDC cycles for the two hybrid vehicles were carried out according the Regulation 83 [24], which is actually used for TA procedure of European passenger cars. The decision to use the same procedure for both cycles lies on the equivalence between the UNECE GTR15 [11] and the actual one, which differ only for the test condition (mass and RLs) and the computation of TA CO<sub>2</sub> emissions. Moreover, the Meta-Model should compute the CO<sub>2</sub> emissions along the NEDC according the actual TA procedure.

The WLTC tests were carried out following the requirements of the WLTP procedure in terms of RLs and test mass, according to the UNECE GTR15 [11]. The RLs and test masses used for the two vehicles are reported in Table 9 and the impact of different RLs computation is reported in Figure 26.

As mentioned in Chapter 1, the switch from NEDC to WLTP will determine an average increase of about 45% of the energy demand for both test case, as shown

in Figure 27 and Figure 28, affecting the electric drive and consequently the CO<sub>2</sub> emissions.

**Table 9:** Vehicle test conditions

		Unit	NEDC	WLTP
<b>Yaris Hybrid</b>	Test Mass	kg	1130	1325
	F0	N	61	120.5
	F1	N/(km/h)	0.19	0.33
	F2	N/(km/h) <sup>2</sup>	0.0269	0.0302
<b>Golf GTE</b>	Test Mass	kg	1590	1710
	F0	N	125.3	187.9
	F1	N/(km/h)	0.080	0.082
	F2	N/(km/h) <sup>2</sup>	0.0513	0.0551

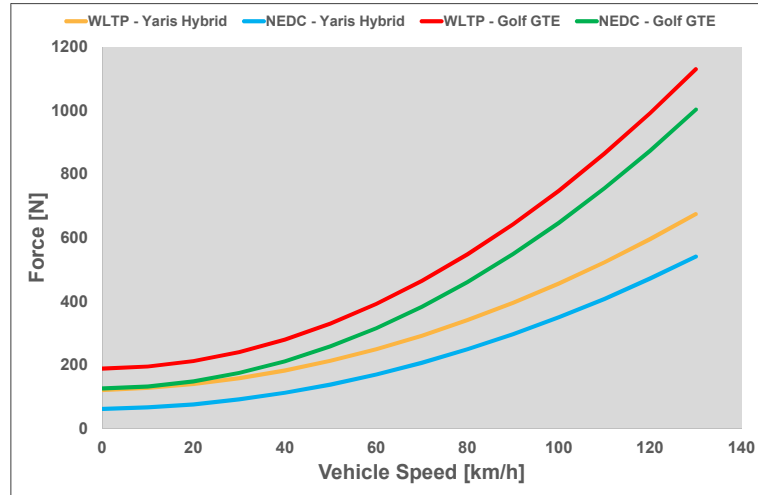


**Figure 26:** RLs for WLTP and NEDC procedures

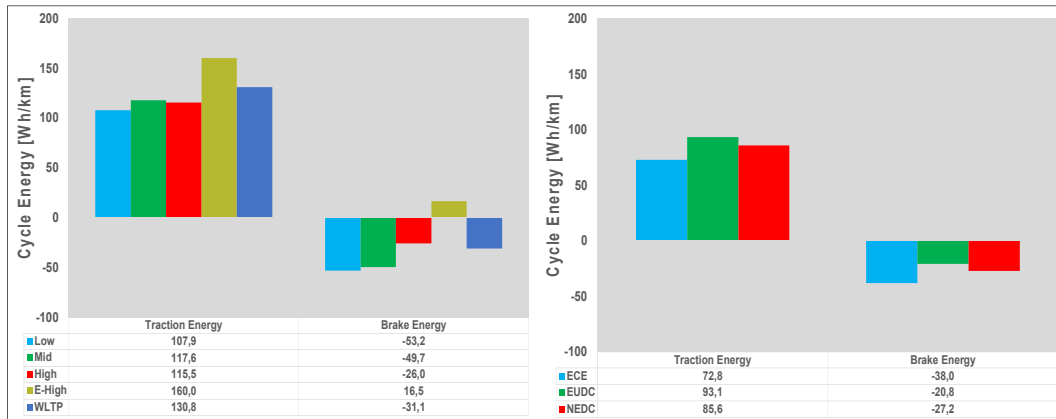


**Figure 27:** Yaris Hybrid – Cycle energy demand along the WLTC (Left) and NEDC (Right)

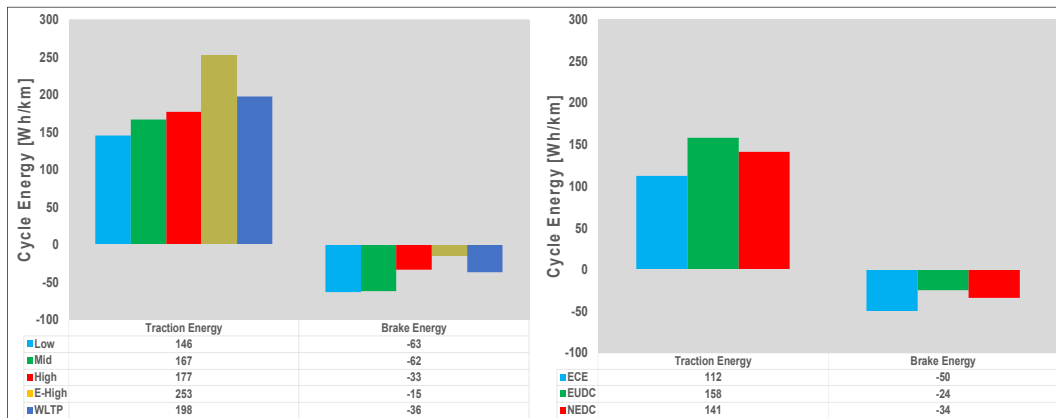


**Figure 28:** Golf GTE – Cycle energy demand along the WLTC (Left) and NEDC (Right)

This paragraph will introduce the test procedure adopted for the two vehicles, which differs from HEVs to PHEVs due to the different use of the battery energy. In the first case the battery operates as an energy buffer, while in the second is the primary energy source of the vehicle.

### 2.4.1 HEVs protocol

The European TA procedure requests the correction of the measured CO<sub>2</sub>, since the declared value should correspond to a neutral energy balance of the battery [28]. This correction is necessary to take into account the effect of battery recharge made by the ICE, since HEVs do not allow the external recharge of the high voltage battery. The correction coefficient is called K-Factor.

The K-Factor is defined inside the Regulation 101 [29] and its computation requests the measurement of two parameters: the CO<sub>2</sub> emissions at the end of the

cycle in g/km and the battery energy expressed as the integral of the battery current in Ah. The formulation of K-Factor is reported in Equation 3.

$$K = \left( n \cdot \sum_{i=1}^n Q_i \cdot M_i - \sum_{i=1}^n Q_i \cdot \sum_{i=1}^n M_i \right) / \left[ n \cdot \sum_{i=1}^n Q_i^2 - \left( \sum_{i=1}^n Q_i \right)^2 \right]$$

**Equation 3:** K-Factor definition

Where  $Q_i$  is the electricity balance measured during the  $i$ -th manufacturer's test,  $M_i$  represents the CO<sub>2</sub> emissions measured during the  $i$ -th test and  $n$  is the total number of measurements. Therefore, it is necessary to perform at least two tests to evaluate the correction coefficient, considering different starting energy levels of the battery to cover as much as possible the operating domain of the hybrid powertrain.

Due to the tight schedule of the project, the Yaris Hybrid was tested considering only two opposite levels of battery energy at the beginning of the cycle: battery fully charged and completely discharged. The battery conditioning was done driving at constant speed on the chassis dynamometer until the complete charge or discharge of the battery. The evolution of the battery energy level was monitored through the battery indicator on the cockpit, represented in Figure 29.



**Figure 29:** Example of battery indicator for Toyota Hybrids [30]

The discharging of the high voltage battery was done driving at a constant speed of 50 km/h. In this condition the EMS allows the electric driving until the reaching of the minimum battery level, corresponding to the engine ignition. The battery recharge was done driving the car at 70 km/h, since in this condition the EMS allows the Smart Charge. The charging procedure was stopped unto the battery indicator was full. The discharge/charge operations requested an average time of 15 minutes.



After the battery conditioning, the car was left in soak condition at a constant temperature between 20 and 30 °C until the engine oil temperature and the coolant are within +/- 2K of the temperature of the room.

Since hybrid vehicles available on the market have different operating modes selectable by the driver, the Regulation 83 requests that “*the vehicle testing shall be carried out in the mode which is automatically set after turn on of the ignition key (normal mode)*”[24].

The TA CO<sub>2</sub> emissions are computed using the formulation reported in Equation 4 [24].

$$M_0 = M - K \cdot Q$$

**Equation 4:** TA CO<sub>2</sub> for HEVs

Where  $M_0$  is the TA CO<sub>2</sub> in g/km,  $M$  refers to the CO<sub>2</sub> emissions in g/km at the end of the test,  $Q$  is the battery electricity balance measured during the test in Ah and  $K$  is the K-Factor.

### 2.4.2 PHEVs protocol

The test procedure adopted for the Golf GTE follows the requirements of Regulation 83 [24], which for PHEVs requests the execution of two different test:

1. **Condition A** (Charge Depleting (CD) Test): the high voltage battery should be fully charged;
2. **Condition B** (Charge Sustaining (CS) Test): the high voltage battery should be at minimum battery SOC.

The choice between the different driving modes (E-Mode, Hybrid, GTE, etc.) was done according to the actual regulation, applying the procedure described in Table 10. Therefore, the E-Mode was tested applying the Condition A, while the GTE mode, which is suitable for a more aggressive driving style, was characterized through the Condition B test.

**Table 10:** Driving mode selection [24]

Hybrid Modes	
<b>Condition A – Fully Charged</b>	Most Electric Hybrid Mode
<b>Condition B – Minimum SOC</b>	Most Fuel Consuming mode

During the Condition A and Condition B tests the CO<sub>2</sub> emissions, respectively called  $M_1$  and  $M_2$ , and the current from the high voltage battery should be recorded.

The presence of an externally rechargeable battery request the correct condition of the battery SOC for both tests according to Regulation 101 [29]. The evolution

of the SOC profile under the Condition A test is illustrated in Figure 30 and it is based on 6 steps:

1. Initial SOC of the high voltage battery;
2. The high voltage battery is discharged according to the speed profile in Figure 31;
3. The vehicle shall be conditioned driving one complete NEDC cycle followed by a EUDC;
4. The high voltage battery must be charged during the night soak at a constant temperature between 20 and 30°C;
5. Vehicle test;
6. Battery charge and measure of the charge energy  $e_1$ .

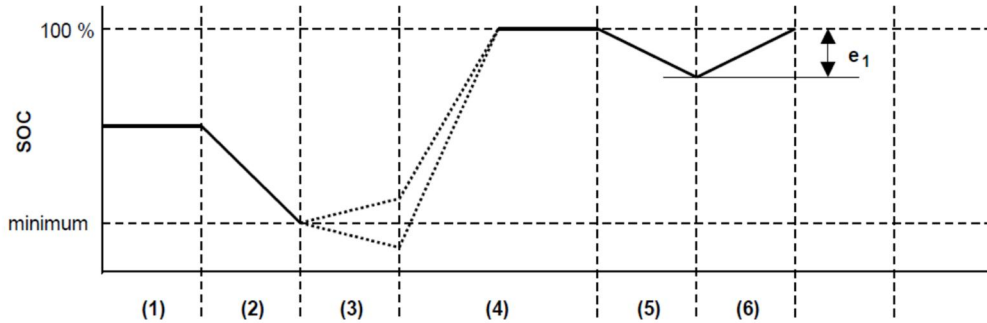


**Figure 30:** An example of SOC profile during the Condition A test [29]

The SOC profile during the Condition B test is depicted in Figure 32 and it is made up of 8 steps:

1. Initial SOC of the high voltage battery;
2. The vehicle shall be conditioned driving one complete NEDC cycle followed by a EUDC;
3. The high voltage battery is discharged according to the profile in Figure 31;
4. Vehicle soak at constant temperature between 20 and 30 °C until the engine oil temperature and the coolant are within +/- 2K of the temperature of the room.
5. Vehicle test;
6. Battery charge and measure of the charge energy  $e_2$ ;
7. The high voltage battery is discharged according to the profile in Figure 31;
8. Battery charge and measure of the charge energy  $e_3$ .



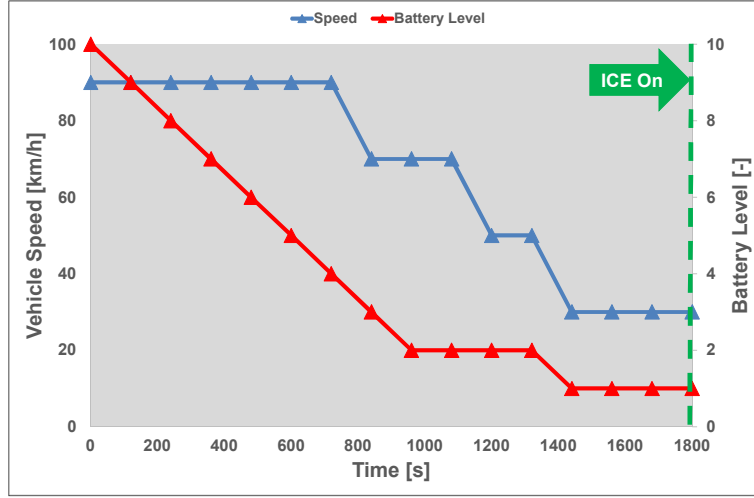


**Figure 31:** Golf GTE - Speed steps used for the battery discharge

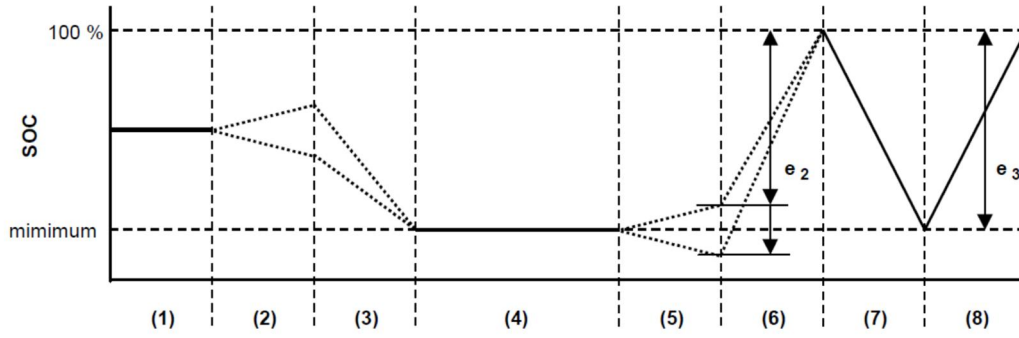


**Figure 32:** An example of SOC profile during the Condition B test [29]

The Golf GTE in E-Mode mode was tested through the repetition of four NEDC and two WLTC cycles. The number of cycles to be considered during the CD test is defined by the TA procedure. It asserts that the minimum SOC is reached in the  $N$  cycle if the electricity balance measured during the  $N+1$  cycle does not exceed 3% of the nominal capacity of the battery [24]. In other words if the engine charges heavily the high voltage battery along the  $N+1$  cycle, this cycle will be discarded from the CD analysis, as shown in Equation 5:

$$\frac{\int_0^{t_{end}} Idt}{3600 \cdot C_{nom}} < 0.03$$

**Equation 5:** Brake-off criterion

Where  $I$  is the battery current integrated between the beginning and the end of the individual cycle and  $C_{nom}$  is the battery nominal capacity expressed in Ah.

The CO<sub>2</sub> final value combines the results from the Condition A and the Condition B tests, weighed respectively with the electric range and the average distance between two battery recharges [24], as shown in Equation 6:

$$M = \frac{(D_{OVC} \cdot M_1 + D_{av} \cdot M_2)}{(D_{OVC} + D_{av})}$$

**Equation 6:** TA CO<sub>2</sub> emissions for PHEVs

where  $M$  is CO<sub>2</sub> TA value in g/km,  $M_1$  and  $M_2$  are the CO<sub>2</sub> emissions in g/km respectively in CD and CS,  $D_{OVC}$  is the electric range and  $D_{av}$  is the average distance between two battery recharges, assumed to be equal to 25 km as prescribed by the TA procedure [29]. The assessment of the electric range, as illustrated in Figure 33, excludes from the computation the portions travelled in electric mode thanks to the Load Point Shift, indicated with  $\Delta a$ , and to the energy recovered during the regenerative braking at speeds above the engine-on threshold, represented by  $\Delta b$ .

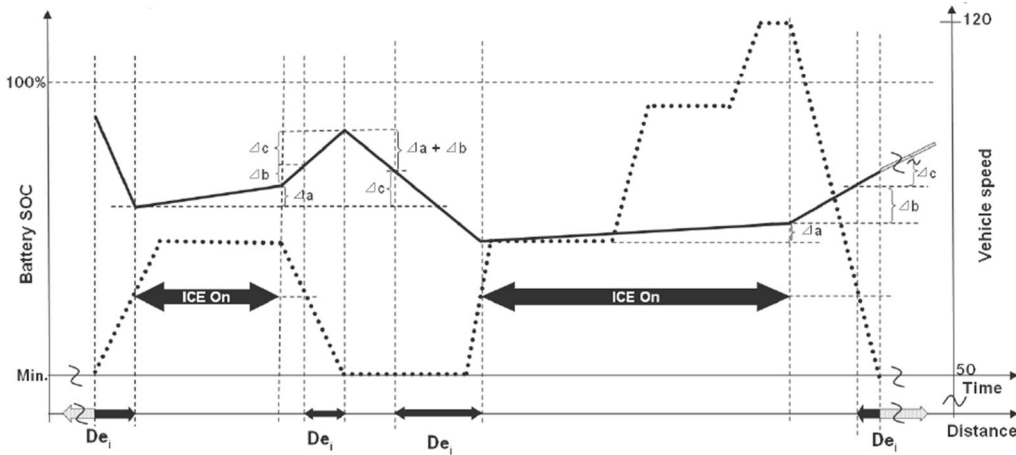


**Figure 33:** Electric distance computation along the NEDC cycle according to [29]

## 2.5 Energy management analysis

The EMS generates high-level control signals, which determine the overall behavior of the hybrid vehicle. Its characterization was carried out by means of engine and battery measurements combined with the vehicle speed, acceleration and load demand to identify the operating logic.

The outcomes of the EMS analysis are fundamental for the development of the Meta-Model, since they are used to design the mathematical models capable to reproduce the operating logic of the different vehicles along the NEDC cycle.

The first part will present the EMS analysis applied to the Yaris Hybrid considering two opposite initial battery energy levels. The vehicle operating

parameters such as the battery SOC, the vehicle speed, acceleration and the motive power are related to each other to identify the engine enabling strategy and the use of peculiar modalities of hybrid vehicles such as the Load Point Moving or the Electric Boost.

The second part will apply the same analytical procedure to the Golf GTE for the CD and CS tests, which were performed using respectively the E-Mode and the GTE.

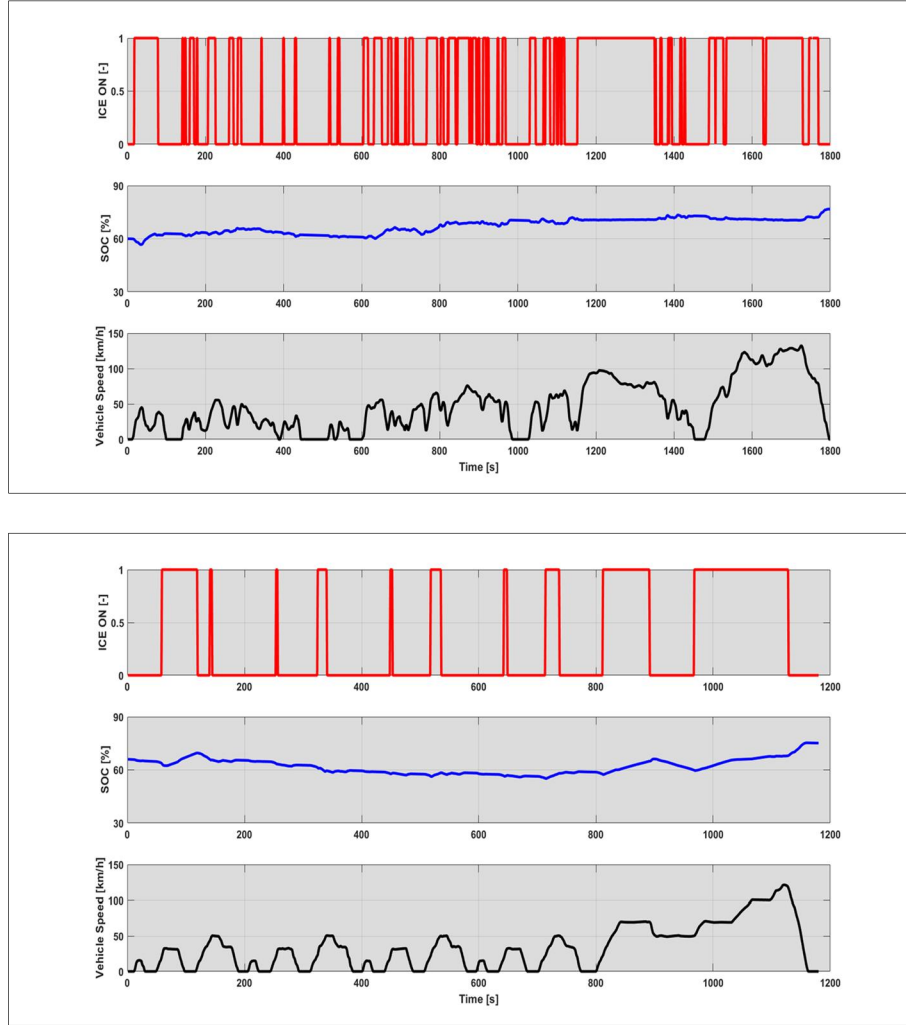
The use of the same analytical procedure applied to two opposite technical solutions is imposed by the necessity to find a common modelling platform, simplifying the code implementation and making more robust the mathematical modelling, which must be effective for a wide range of architectures and technical solutions [31].

### **2.5.1 Yaris Hybrid: EMS analysis**

This section analyses the EMS behavior of the Yaris Hybrid considering two opposite battery levels at the beginning of the cycle for two different reasons:

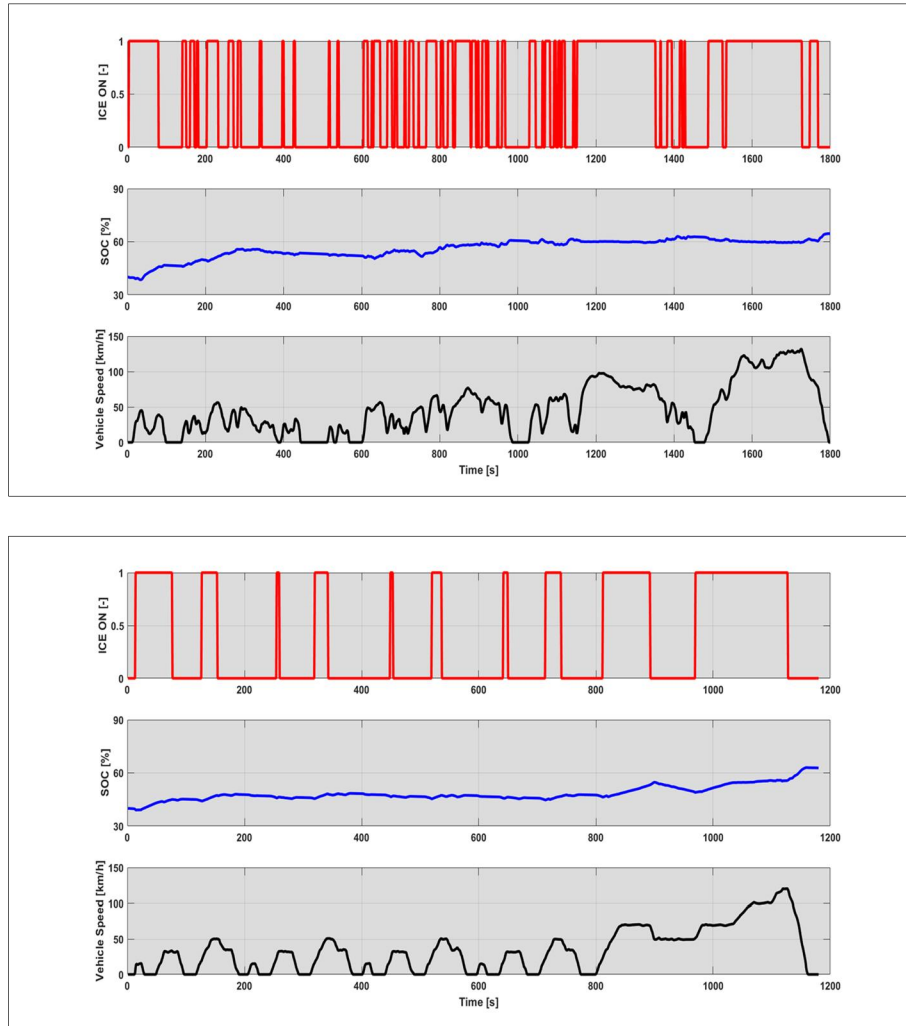
1. The Meta-Model shall be able to reproduce correctly the hybrid control logic, regardless of the initial battery level;
2. The code must compute correctly the K-Factor for the NEDC cycle.

Figure 34 illustrates the time dependency of the ICE On/Off logic, represented through a Boolean variable (0 = Off, 1 = On), and of the battery SOC, considering the battery fully charged at the beginning of the WLTC and NEDC cycles, hereinafter referred to as “High SOC”. In this case, the EMS enables the electric driving at low/medium speeds and consequently the use of ICE is more frequent along the WLTC respect to the NEDC, as remarked by the cycle energy increase shown in Figure 27. The SOC variation of 15% on WLTC and of 10% on NEDC confirms the enabling of the Smart Charge for the “High SOC” case when the ICE is enabled.



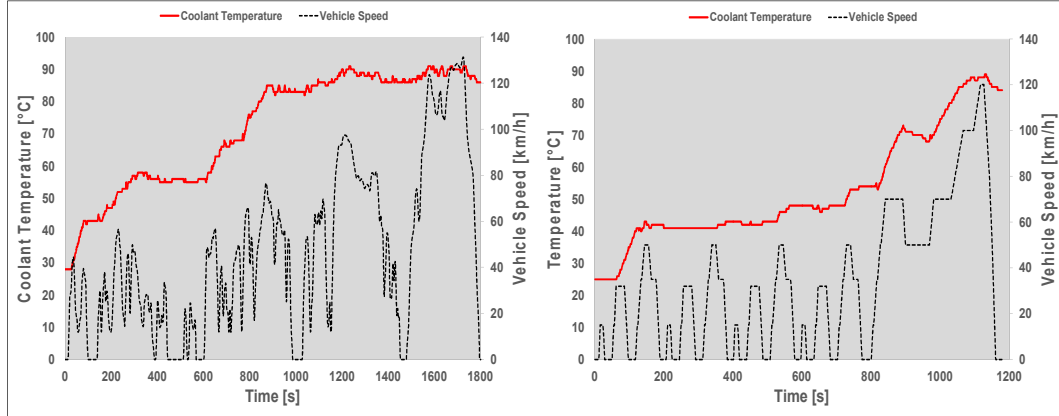
**Figure 34:** Yaris Hybrid - On/Off and battery SOC for the “High SOC” case along the WLTC (Top) and NEDC (Bottom)

Figure 35 presents the case of the battery fully discharged at the beginning of the cycle, hereinafter referred to as “Low SOC”. It is evident a wider use of the ICE along both cycles in the first 200 seconds compared to the “High SOC”. In this particular condition, the EMS enables the battery recharge to reach quickly a “normal” battery energy level, as confirmed by the fast growth of the SOC, bringing the EMS to operate as in the “High SOC” case.



**Figure 35:** Yaris Hybrid - On/Off and battery SOC for the “Low SOC” case along the WLTC (Top) and NEDC (Bottom)

In the first 200 seconds both for the “High SOC” and “Low SOC”, even though the load demand and the vehicle speed are low, the engine is on for approximately 100 seconds to warm-up the after-treatment system, as evident from the temperature profiles reported in Figure 36. During this condition, the cut-off and the stop-start are disabled.



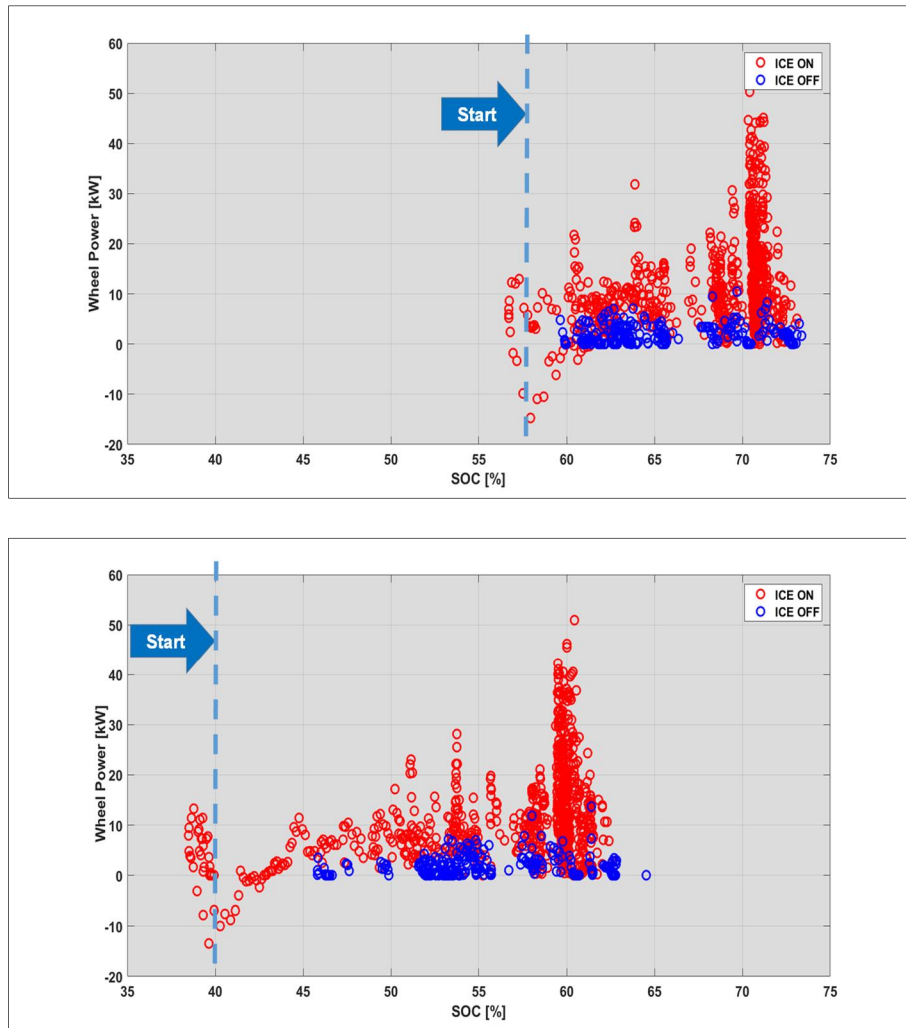
**Figure 36:** Yaris Hybrid - Engine coolant temperature profiles along the WLTC (Top) and NEDC (Bottom) for the “High SOC” case

The understanding of the EMS logic requires a detailed analysis of the measurements of the main parameters, which characterize the hybrid powertrain operating logic. Therefore, the battery and the engine measurements were correlated with the key vehicle parameters, such as the vehicle speed, acceleration and traction power, thus obtaining an interesting insight of the hybrid powertrain control logic [32].

A key control parameter for HEV/PHEVs is the battery SOC [33]. Figure 37 and Figure 38 report the ICE state (On/Off) for all the operating points as a function of battery SOC and motive power respectively along the WLTC and the NEDC. The blue points represent the ICE Off condition, the red points correspond to the ICE On and finally the blue arrow indicates the battery starting condition. Figure 37 highlights that the EMS in “High SOC” condition along the WLTC enables the electric driving up to 10 kW. In “Low SOC” the EMS promotes the aggressive battery recharge, limiting the electric drive to 2.5 kW, until the reaching of normalized SOC values (approximately 55%), allowing in this situation the “zero emission” drive in the same area of the “High SOC”. At the beginning of the cycle in both operating conditions, the EMS disables the cut-off, as evident in the negative motive powers region, and the stop-start to quicken the warm-up of the after-treatment system. The EMS behavior along the NEDC cycle is quite similar to the WLTC as shown in Figure 38.

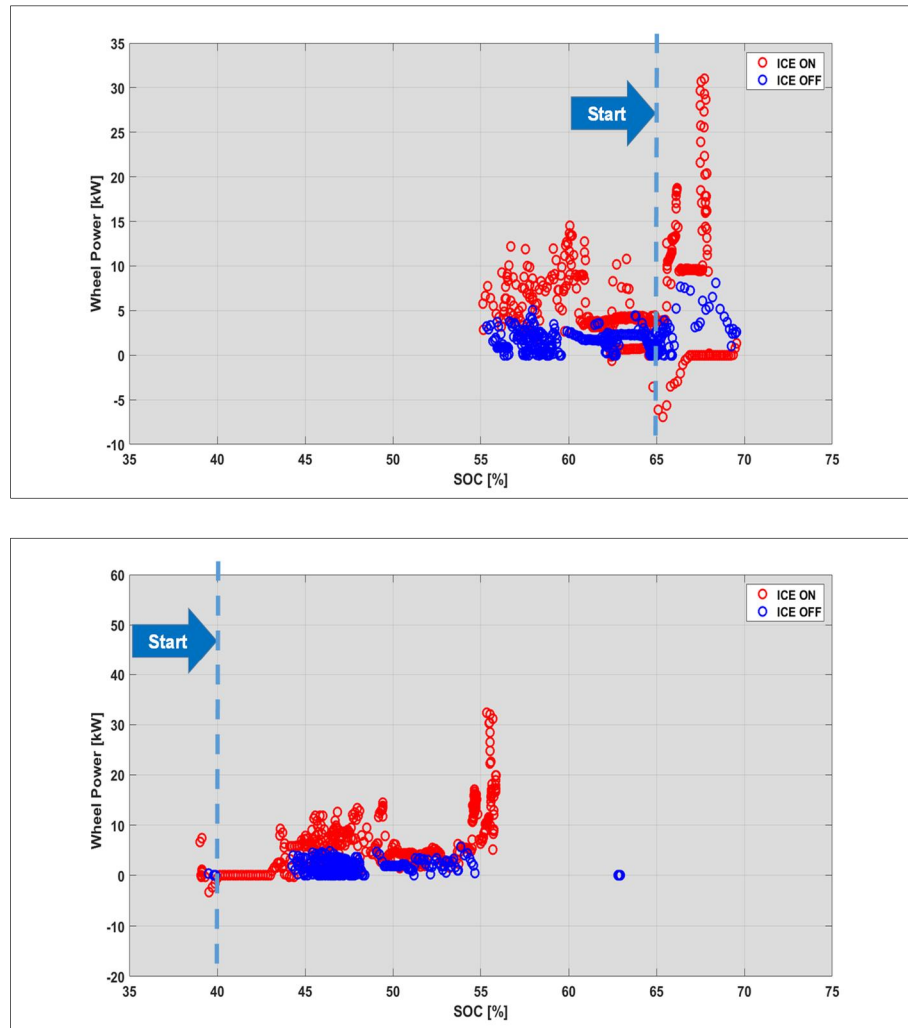
Figure 37 and Figure 38 demonstrate the importance of the SOC as a HEVs key control parameter for two different reasons:

1. The EMS limits the output battery power to control the SOC swing;
2. The EMS when the high voltage battery is depleted promotes the aggressive recharge until the reaching of normal operating conditions.



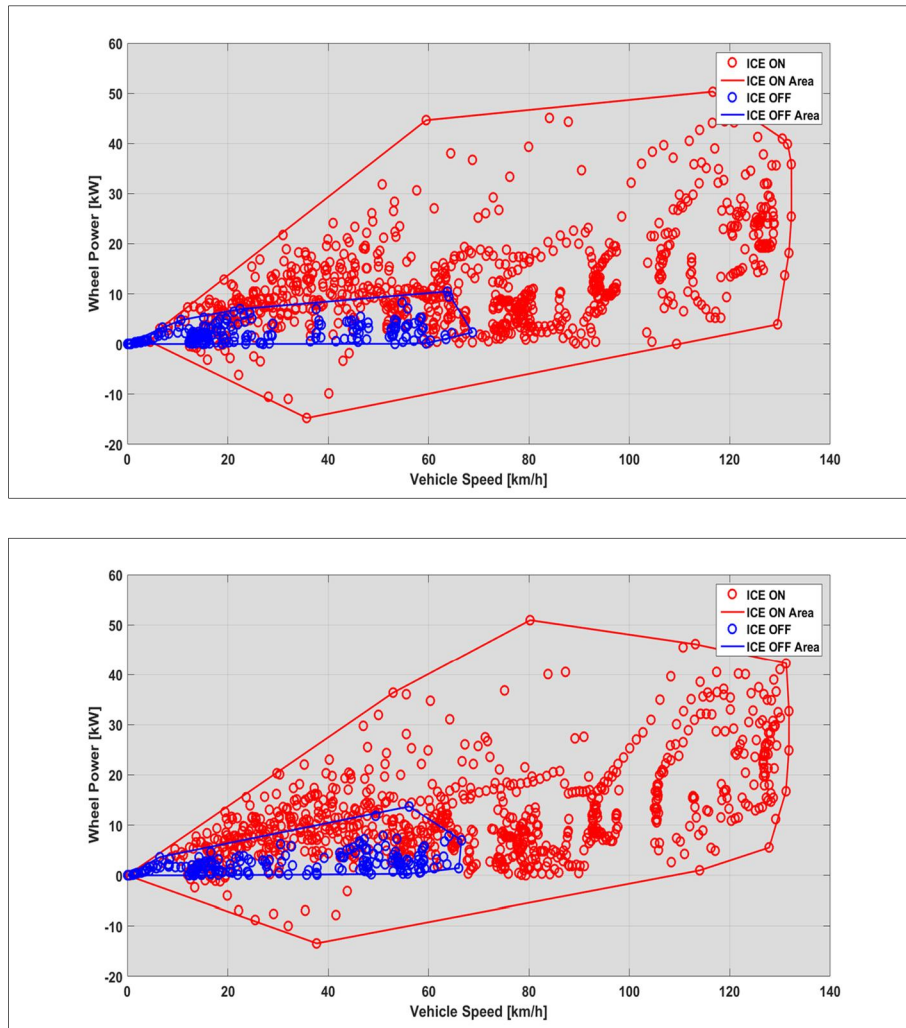
**Figure 37:** Yaris Hybrid – ICE actuation as a function of battery SOC for the “High SOC” (Top) and for the “Low SOC” (Bottom) along the WLTC

Figure 39 and Figure 40 show the influence of the vehicle speed on the EMS behavior respectively along the WLTC and NEDC cycles. Both the “High SOC” and “Low SOC” demonstrate the importance of the vehicle speed, since the EMS limits the electric driving until 60 km/h, confirming that the Yaris Hybrid enables the “zero emissions” drive in urban driving conditions.



**Figure 38:** Yaris Hybrid: ICE actuation as a function of battery SOC for the “High SOC” (Top) and for the “Low SOC” (Bottom) along the NEDC





**Figure 39:** Yaris Hybrid - ICE actuation as a function of vehicle speed for the “High SOC” (Top) and the “Low SOC” (Bottom) along the WLTC

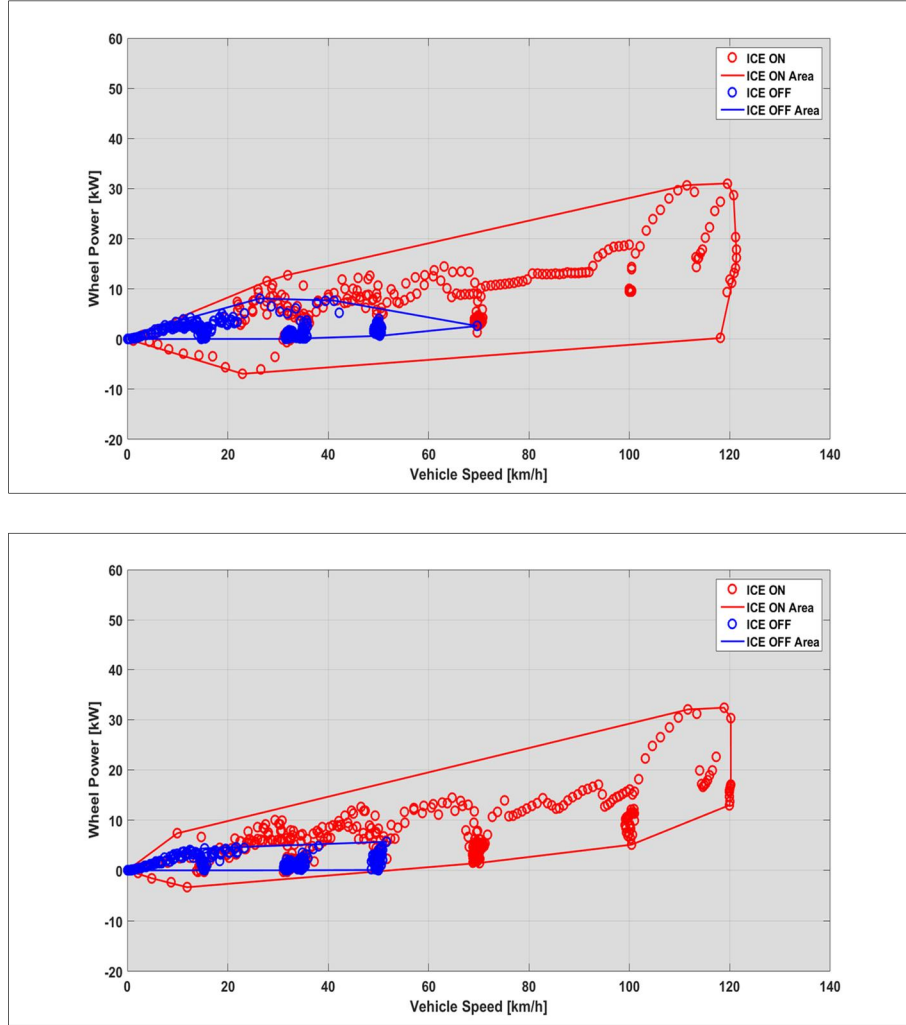


**Figure 40:** Yaris Hybrid - ICE actuation as a function of vehicle speed for the “High SOC” (Top) and the “Low SOC” (Bottom) along the NEDC

Finally, Figure 41 and Figure 42 show the impact on the powertrain control logic of the product between the vehicle speed and acceleration. The electric drive for the “High SOC” and “Low SOC” cases along the WLTC, reported in Figure 41, is circumscribed in a well-defined region between  $-3.5 \text{ m}^2/\text{s}^3$  and  $4.5 \text{ m}^2/\text{s}^3$ , demonstrating the similarities between the two test case. A similar condition is evident along the NEDC cycle.

Therefore, the EMS limits the electric drive when:

1. When vehicle speeds are in the medium range (until 60 km/h) and the accelerations are very low (below  $0.5 \text{ m}/\text{s}^2$ );
2. When accelerations are moderate (until  $1 \text{ m}/\text{s}^2$ ) and speeds are low (below 20 km/h).

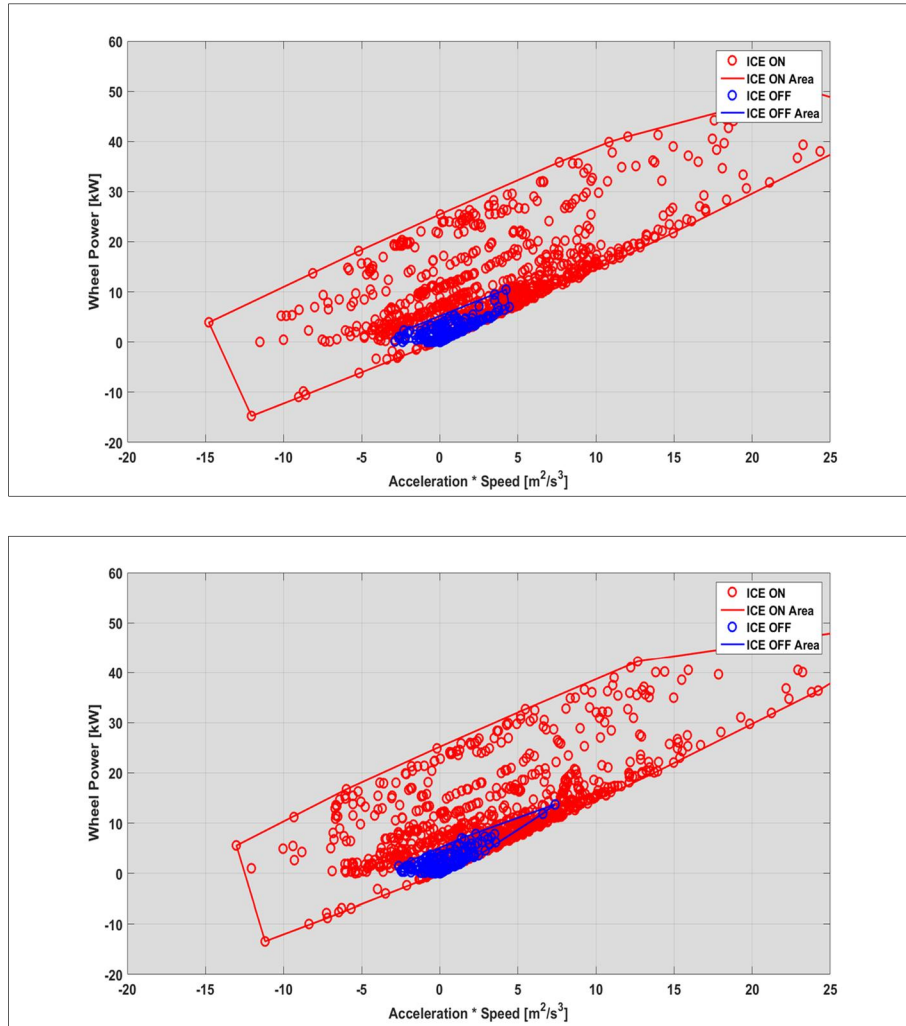


**Figure 41:** Yaris Hybrid - ICE actuation as a function of the product between vehicle speed and acceleration for the “High SOC” (Top) and the “Low SOC” (Bottom) along the WLTC

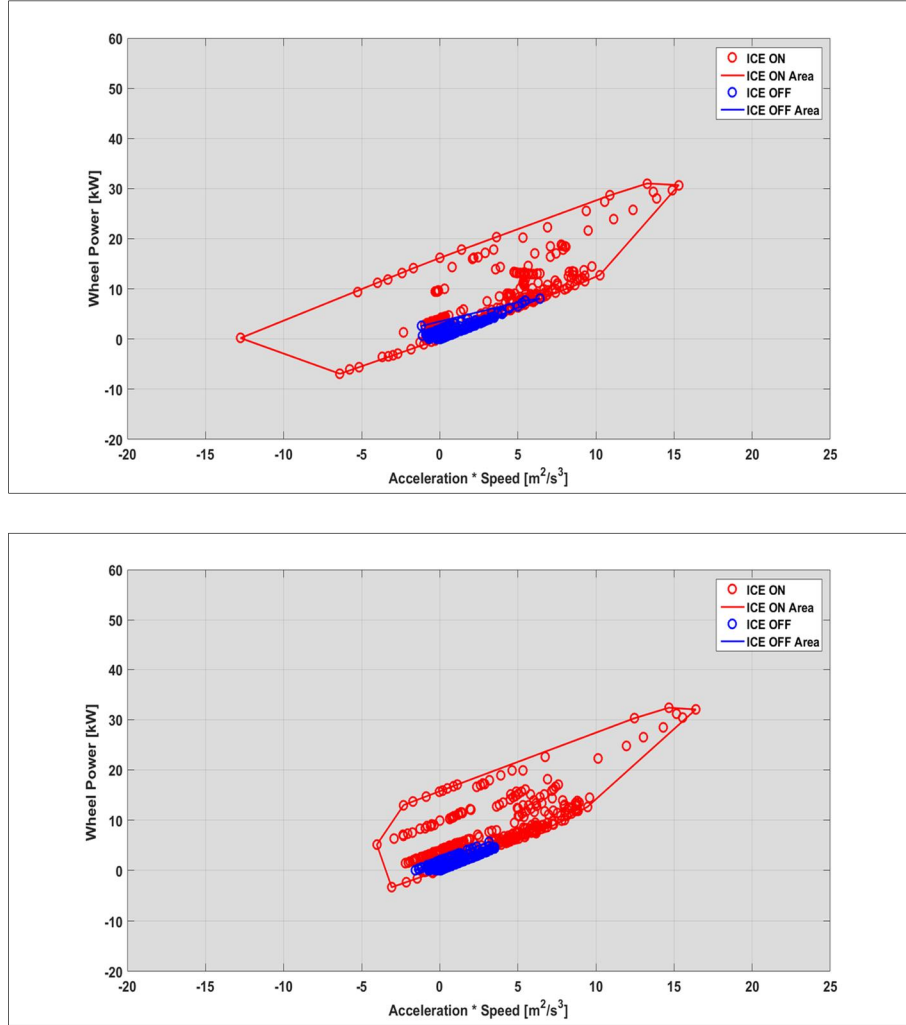
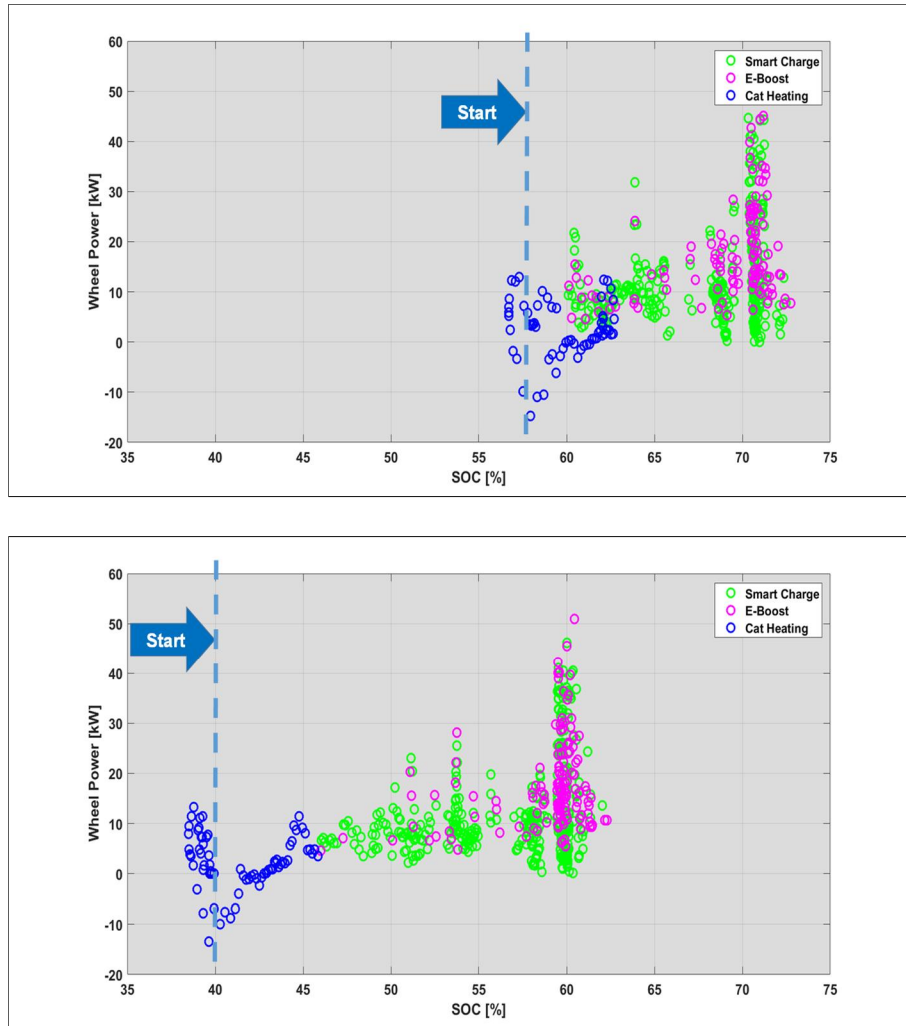


**Figure 42:** Yaris Hybrid - ICE actuation as a function of the product between vehicle speed and acceleration for the “High SOC” (Top) and the “Low SOC” (Bottom) along the NEDC

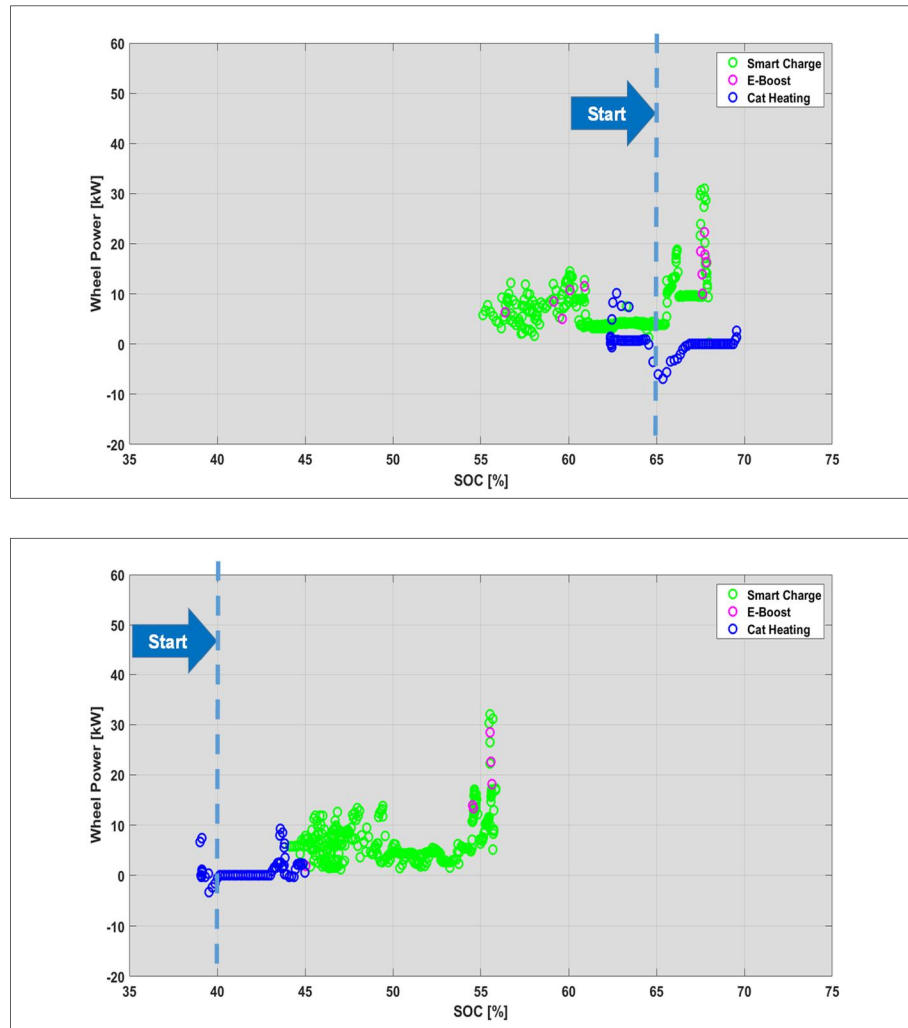
The last section of this paragraph analyses ICE behavior when enabled, focusing on the actuation of the E-Boost and Smart Charge through the overlapping of the engine On/Off condition with the current signal.

From Figure 43 to Figure 46, the green points represent the Smart Charge condition, while the blue indicate the Cat-Heating and the magenta stand for the E-Boost. Along the WLTC cycle, the engine most frequent operating condition is the Smart Charge as evident in Figure 43, but the E-Boost for both test cases is not negligible. In particular, it is evident its use from 10 to 50 kW when the battery SOC is above 60%. Instead, the Smart Charge is widely diffuse along all operating domain, especially when the battery SOC is below 55%, where the EMS enables the battery recharging, as seen in the SOC profile reported in Figure 35. Therefore,

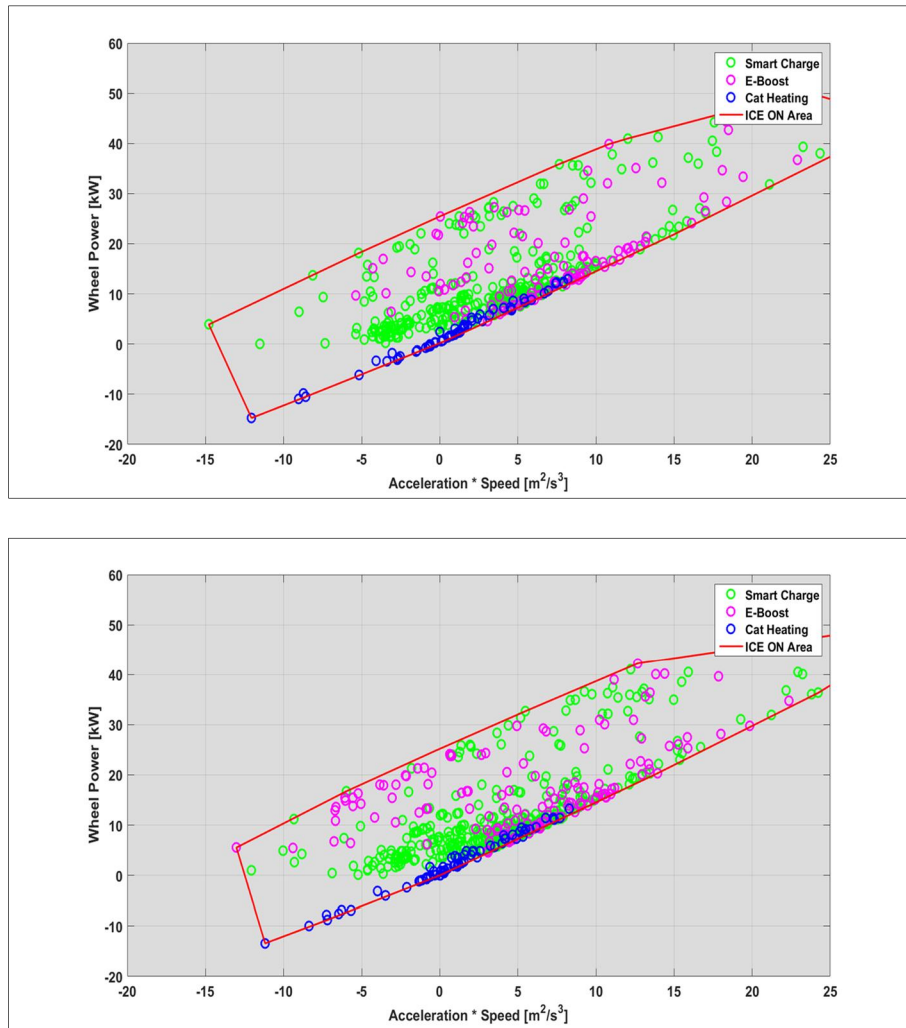
the SOC is a key parameter for the correct detecting and modelling of these two engine operations, but it is not enough. Figure 45 confirms the importance of Smart Charge, but the E-Boost along the WLTC is present in a small region from 5 to 20  $\text{m}^2/\text{s}^3$ , which is limited to high accelerations and medium-high powers, corresponding to a sudden variation of accelerator pedal. Instead, along the NEDC the EMS enables always the Smart Charge along the NEDC for both test cases and the use of E-Boost is negligible due to the limited load demand peaks, as evident from Figure 44 and Figure 46.



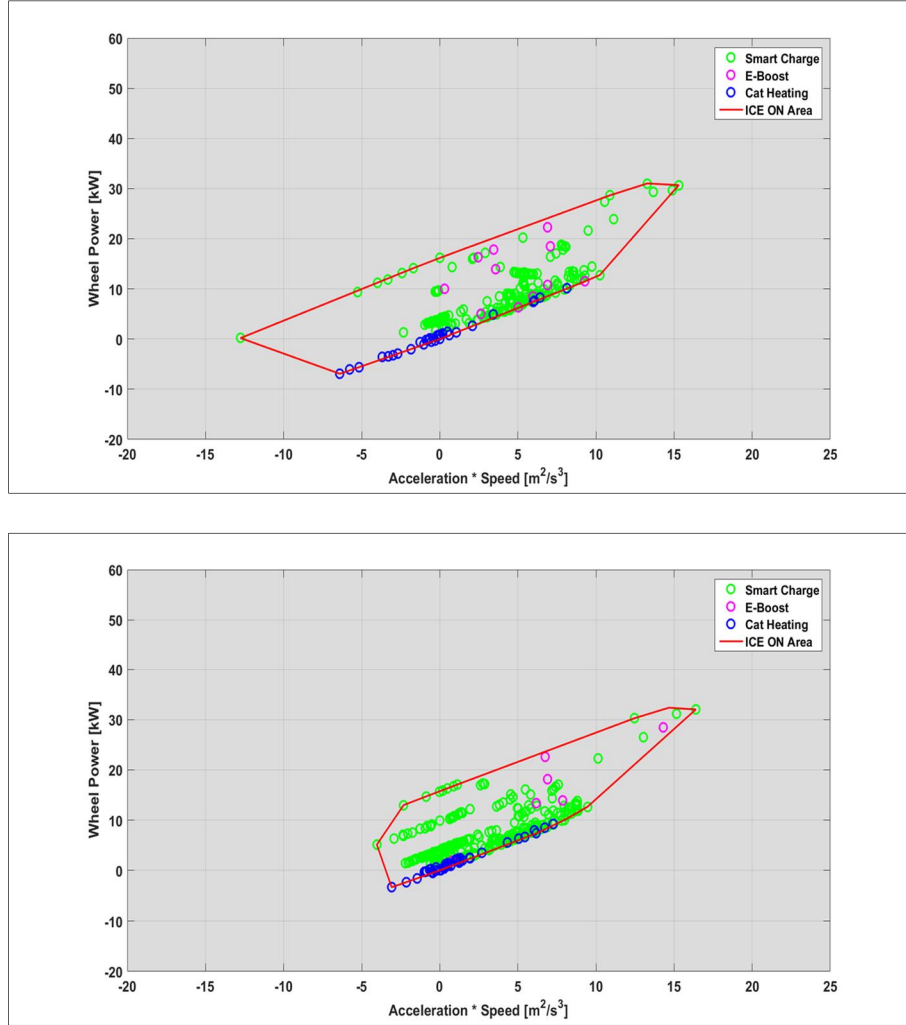
**Figure 43:** Yaris Hybrid - Identification of the ICE operating conditions for the “High SOC” (Top) and the “Low SOC” (Bottom) as a function of battery SOC along the WLTC



**Figure 44:** Yaris Hybrid - Identification of the ICE operating conditions for the “High SOC” (Top) and the “Low SOC” (Bottom) as a function of battery SOC along the NEDC



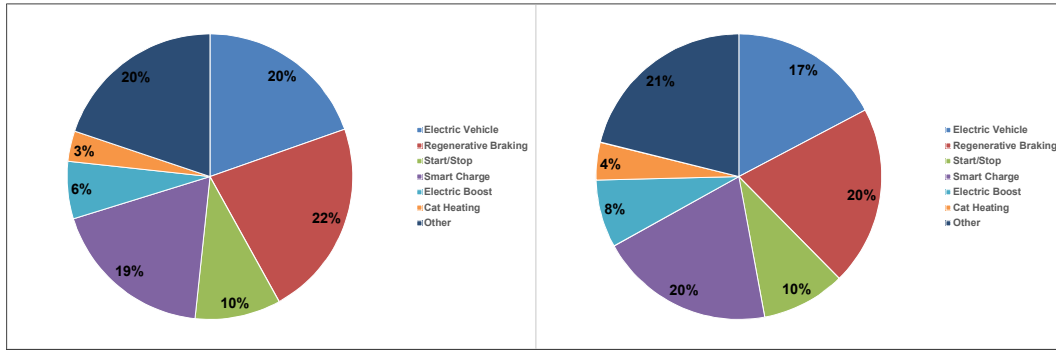
**Figure 45:** Yaris Hybrid - Identification of the ICE operating conditions for the “High SOC” (Top) and the “Low SOC” (Bottom) as a function the product between vehicle speed and acceleration along the WLTC



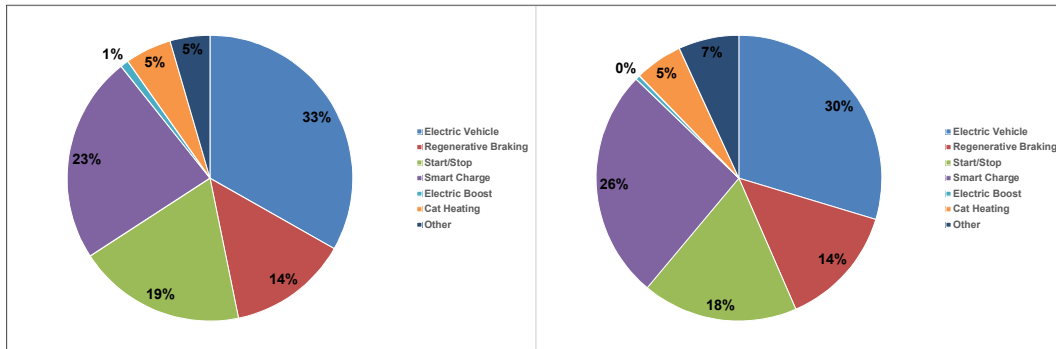
**Figure 46:** Yaris Hybrid - Identification of the ICE operating conditions for the “High SOC” (Top) and the “Low SOC” (Bottom) as a function the product between vehicle speed and acceleration along the NEDC

Figure 47 and Figure 48 show the share of the different operating modes along the WLTC and NEDC respectively (the term “Other” refers to not specific operating conditions such as the engine cranking, or to the impossibility to associate a measurement to a particular mode due to problems of signal phasing). The reduction of electric drive from NEDC to WLTC is around 13%, both in “High SOC” and “Low SOC”. Both graphs confirm that the usage of Smart Charge is wider than the E-Boost, which is not negligible along the WLTC cycle, having an average share of 7%. Along the NEDC, the use of E-Boost is negligible, since its use is below 1% of the cycle. The cat-heating weighs only 3% on WLTC and 5% on NEDC, confirming the reduced impact of “Cold Start”.





**Figure 47:** Yaris Hybrid - Vehicle operating mode share along the WLTC cycle for the “High SOC” (Left) and the “Low SOC” (Right)



**Figure 48:** Yaris Hybrid - Vehicle operating mode share along the NEDC cycle for the “High SOC” (Left) and the “Low SOC” (Right)

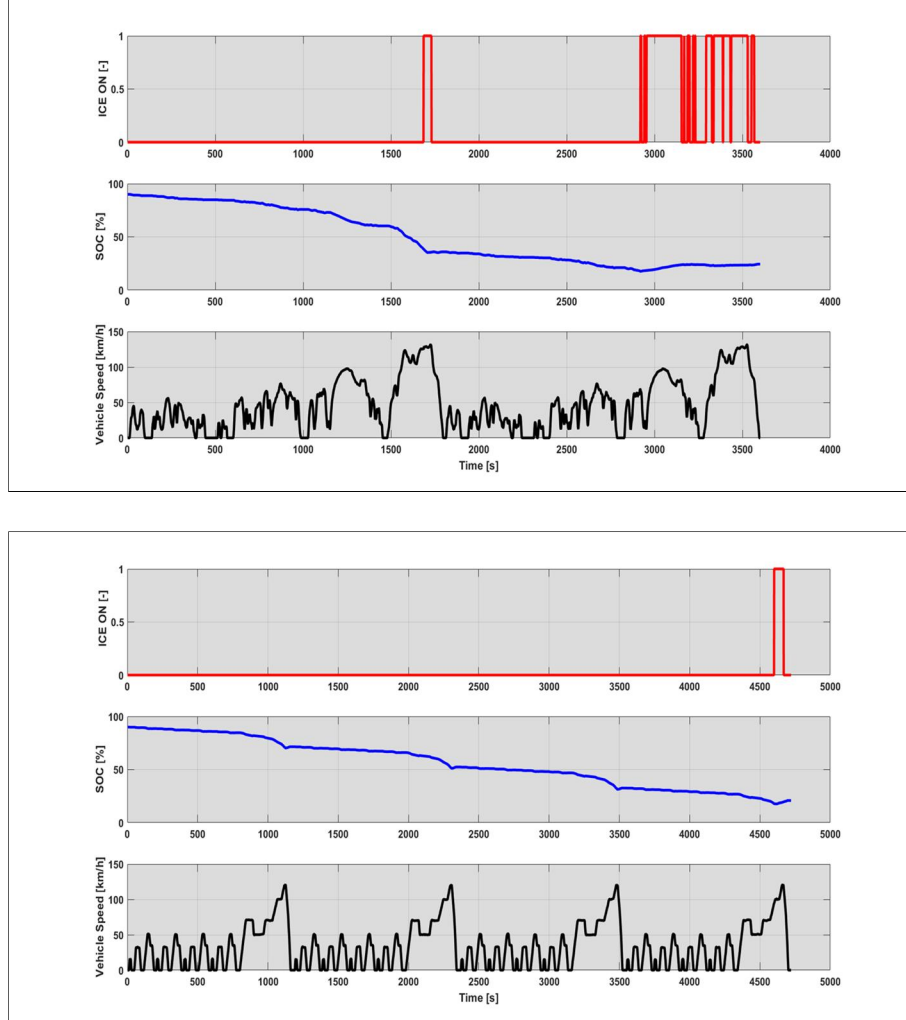
## 2.5.2 Golf GTE: EMS analysis

As the HEVs case, the Meta-Model should be able to reproduce correctly the behavior of different PHEVs according to the TA requirements. Therefore, the Golf GTE was characterized considering the two different test conditions, as described in 2.4.2. The E-Mode was tested in CD condition through the repetition of two WLTC and four NEDC cycles according to Equation 5. The GTE mode was characterized in CS condition, considering the battery fully depleted at the beginning of the cycle. The analytical procedure of the EMS applied to the Yaris Hybrid was extended to the Golf GTE [31].

### 2.5.2.1 E- mode analysis

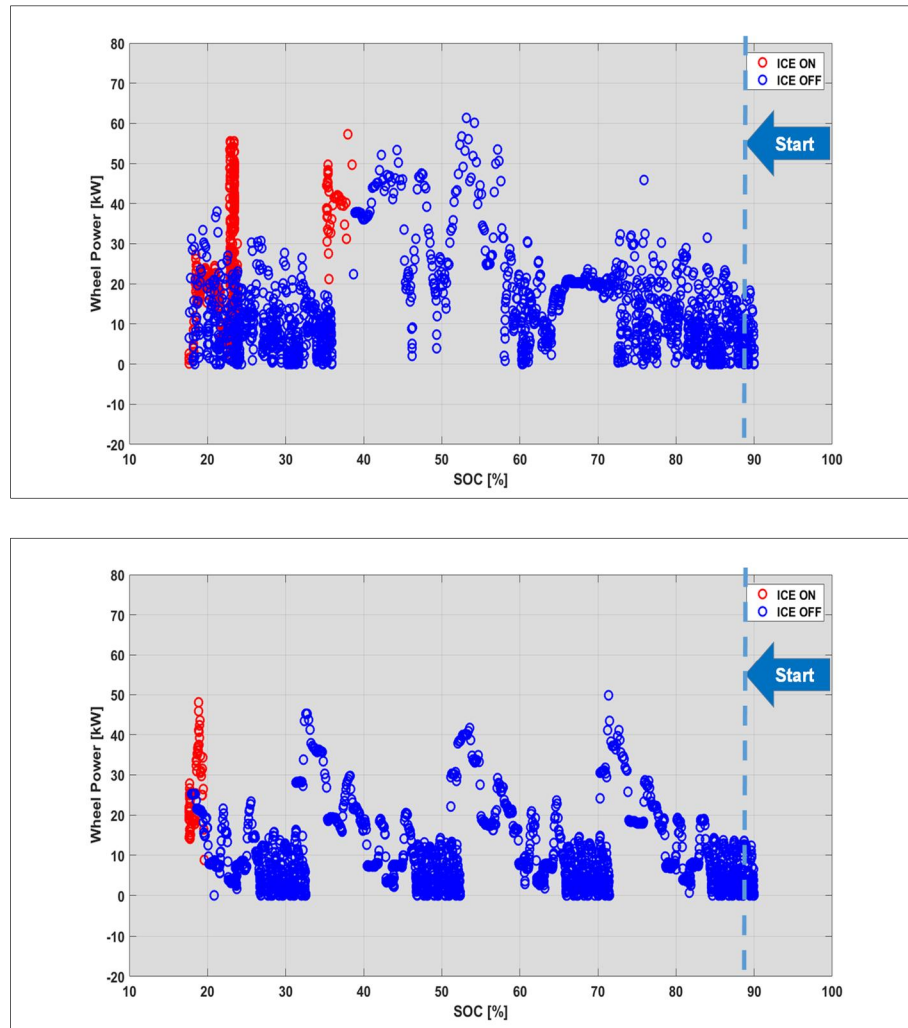
Figure 49 illustrates the time dependency of the ICE On/Off logic and of the battery SOC for the E-Mode mode along the WLTC and NEDC cycles. On the WLTC the control allows the electric drive for almost one complete cycle, except when the vehicle speed overcomes 130 km/h on the extra-high phase. The battery depletion ends at 2800 seconds at the beginning of the high phase of the second cycle. Hence, the EMS switches on the engine to charge the battery as evident from

the SOC profile. Along the NEDC instead, the car travels as an EV for almost four complete NEDC and the EMS turns on the ICE when battery is almost fully depleted.



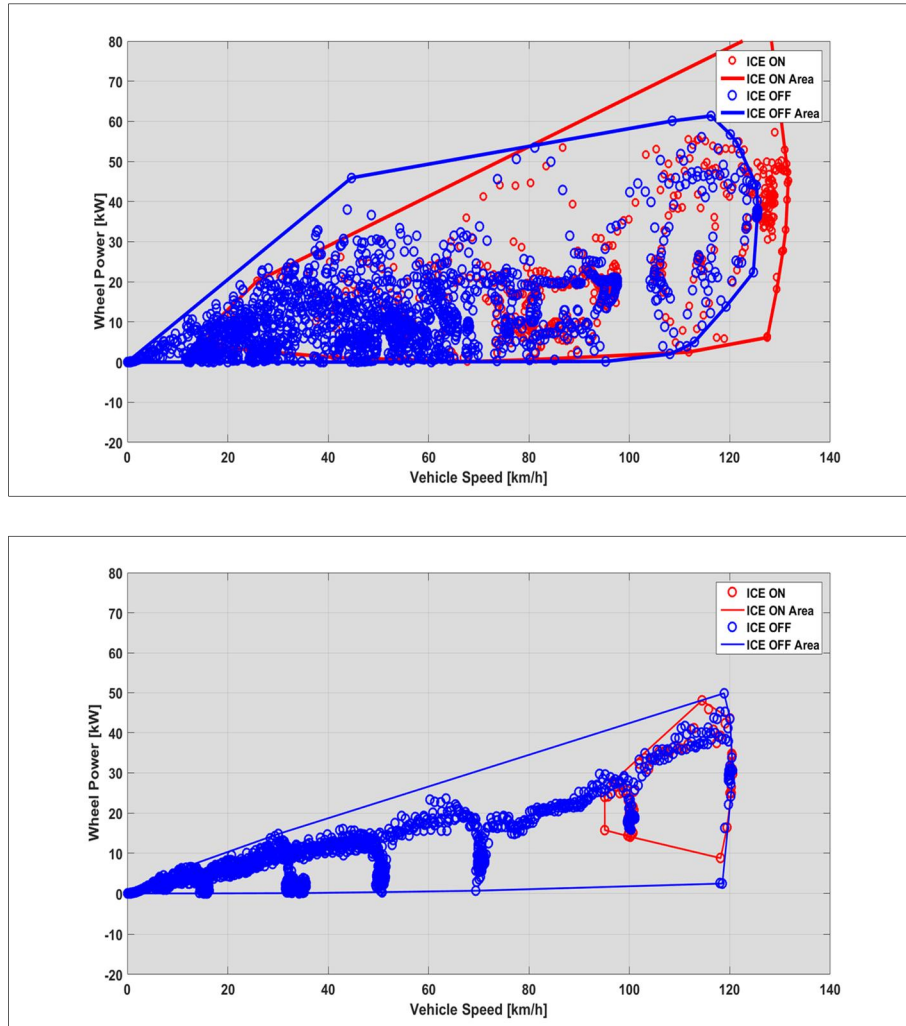
**Figure 49:** Golf GTE - ICE On/Off and battery SOC for the E-mode along the WLTC (Top) and NEDC (Bottom)

As like the Yaris Hybrid characterization, Figure 50 reports the ICE state (On/Off) for all the operating points as a function of battery SOC and motive power along the WLTC and the NEDC. In Figure 50 is evident that the E-Mode along the WLTC allows the electric drive until 60 kW, pushing the battery depletion until 25% of the SOC is reached. The powertrain behavior along the NEDC cycle is quite similar to the WLTC as shown in Figure 50. The E-Mode mode logic is simple, because it exploits as much as possible the electric energy stored in the battery, enabling the ICE only when the battery SOC is significantly depleted.



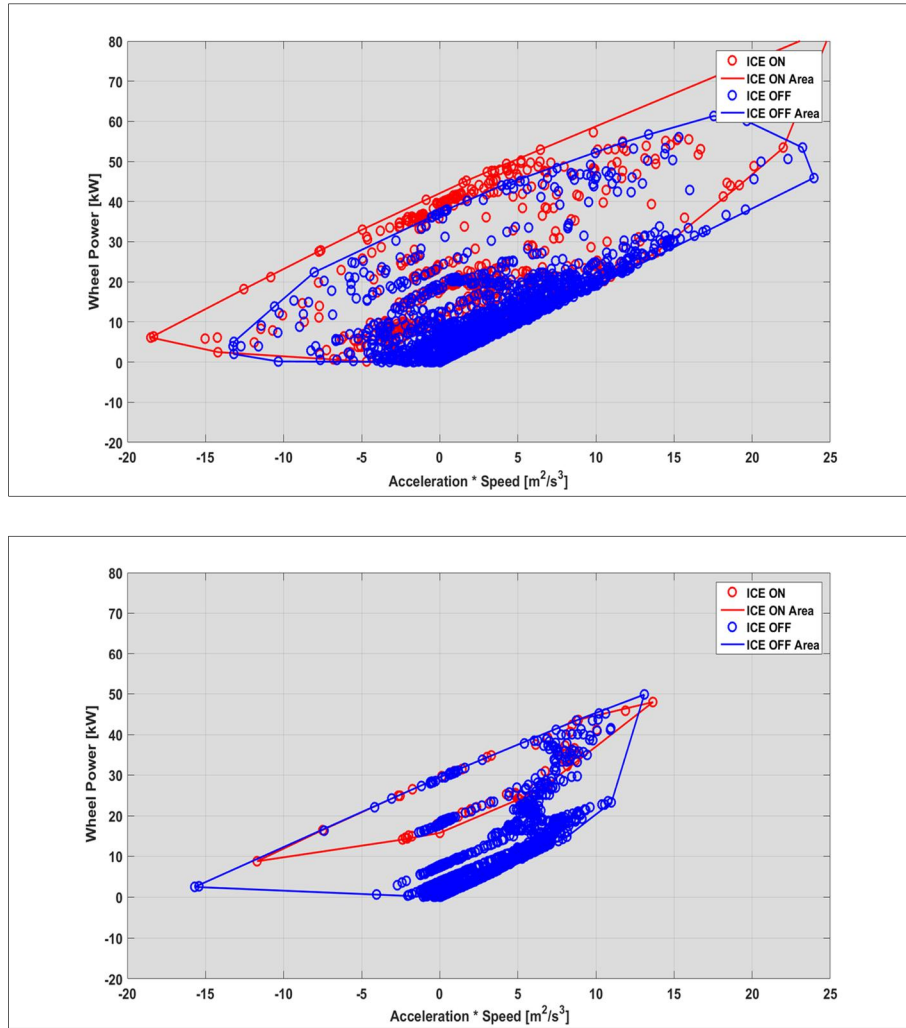
**Figure 50:** Golf GTE - ICE actuation as a function of battery SOC for the E-Mode along the WLTC (Top) and NEDC (Bottom)

Figure 51 analyses the influence of vehicle speed on the powertrain control. The E-Mode enables the electric driving until 60 kW and 120 km/h respectively, thus allowing zero tail pipe emissions for almost the first WLTC. The same behavior can be noticed on the NEDC, as illustrated in Figure 51.



**Figure 51:** Golf GTE - ICE actuation as a function of vehicle speed for the E-Mode along the WLTC (Top) and NEDC (Bottom)

Like the HEV analysis, the product between the vehicle speed and acceleration has an important influence on the EMS conduct. Figure 52 highlights the capabilities of E-Mode to enable the electric driving from  $-15$  to  $25 \text{ m}^2/\text{s}^3$  and from  $0$  to  $60 \text{ kW}$  along the WLTC, which is similar also along the NEDC.



**Figure 52:** Golf GTE - ICE actuation as a function of vehicle speed for the E-Mode along the WLTC (Top) and NEDC (Bottom)

The last part of this paragraph analyses the parallel mode, so the Smart Charge and the Electric Boost enabling, using the same approach of the Yaris Hybrid. As shown in Figure 53, the E-Mode enables always the Smart Charge along the WLTC and NEDC when the battery reaches the minimum SOC level, while the E-Boost is always negligible. Figure 54 confirms that the ICE operates always in Smart Charge condition in the range of powers, speeds and accelerations expected for the NEDC and WLTC, while the exploitation of the E-Boost is negligible, due to the limited load demand peaks.

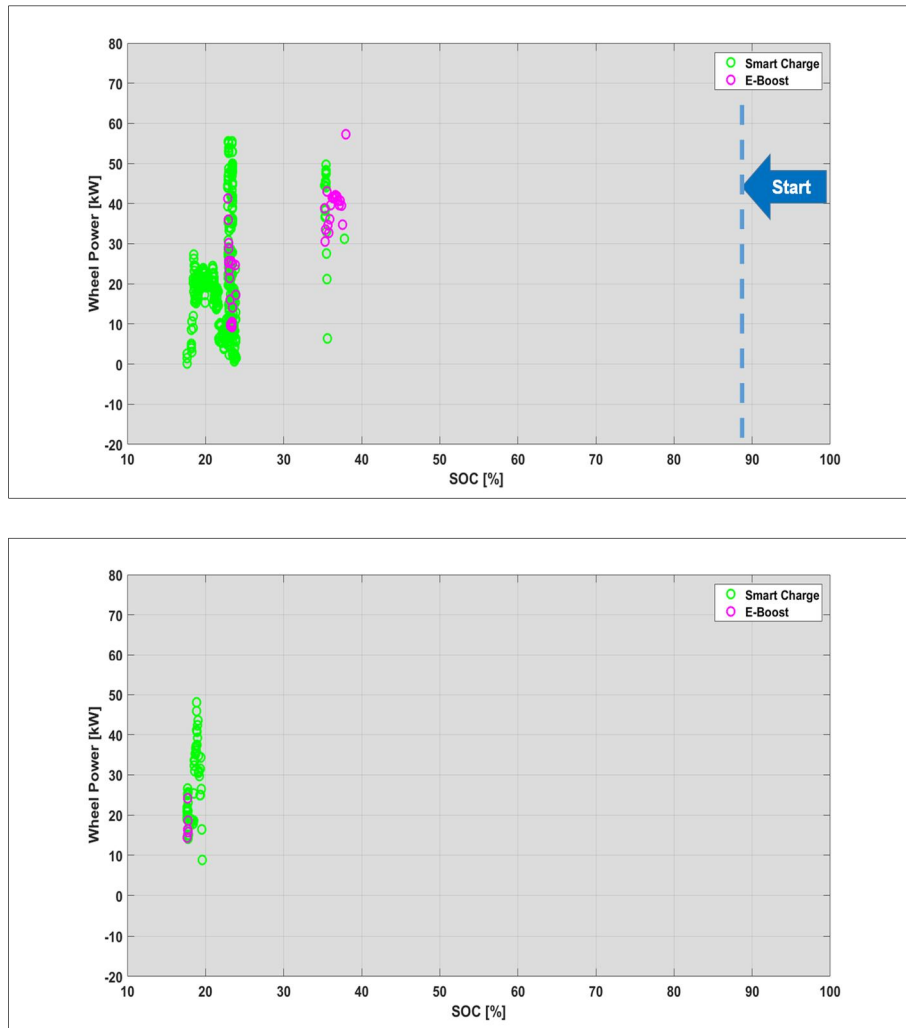


**Figure 53:** Golf GTE - Identification of the ICE operating conditions for the E-Mode along the WLTC (Top) and NEDC (Bottom) as a function of battery SOC

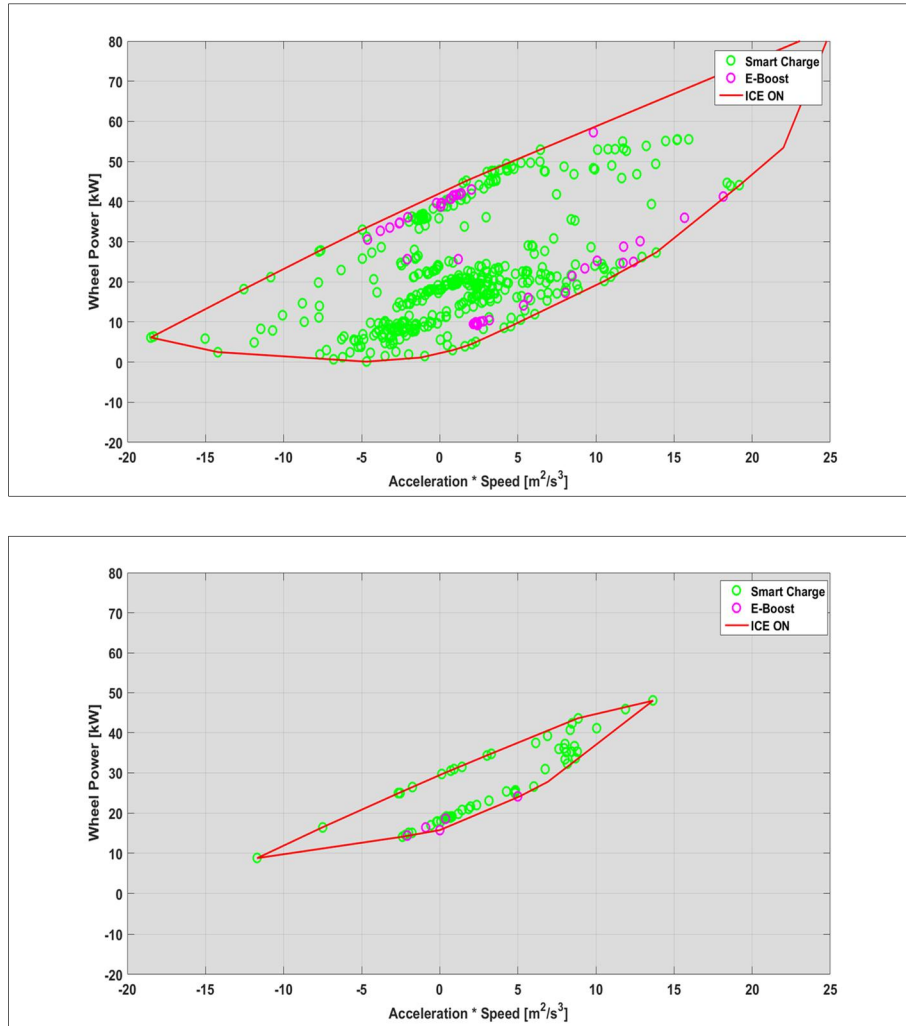


**Figure 54:** Golf GTE - Identification of the ICE operating conditions for the E-Mode along the WLTC (Top) and the NEDC (Bottom) as a function the product between vehicle speed and acceleration

Finally, Figure 55 shows the share between the different operating modes along the WLTC and the NEDC respectively. The reduction of electric driving is around 10% from NEDC to WLTC and the Electric Boost usage is negligible compared to the Smart Charge. The term “Other” refers to other vehicle operating conditions, such as the engine cranking

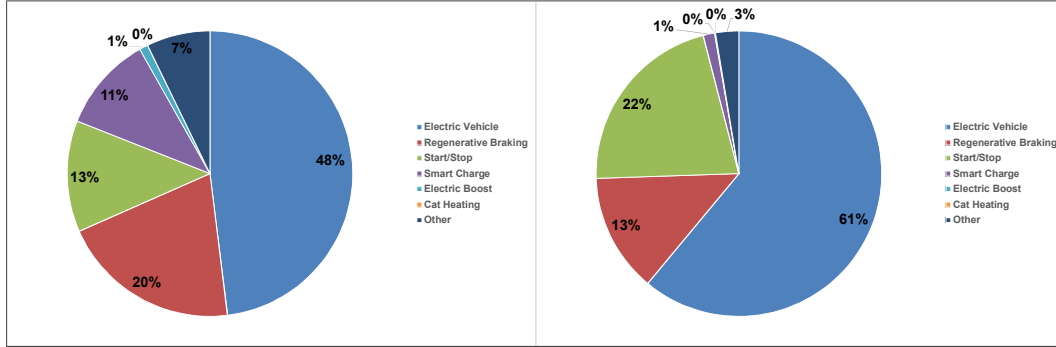


**Figure 55:** Golf GTE - vehicle operating mode share for the E-Mode along the WLTC (Left) and NEDC (Right)

#### 2.5.2.2 GTE analysis

The GTE mode was tested in CS condition starting with the high voltage battery fully discharged, as prescribed by the TA procedure. The data analysis follows the same approach adopted for the CD test. The ICE status and the battery SOC profiles along the WLTC and NEDC are shown in Figure 56.

As expected, the EMS uses frequently the ICE to propel the vehicle and charge the battery, but unexpectedly the charge is aggressive, showing in both cases a SOC variation of almost 15%. Moreover, at the beginning of the cycles, the engine cut-off and stop-start are disabled to accelerate the warm-up of the after-treatment system, as like the Yaris Hybrid. Like the CD test, the role of battery SOC in the control logic was investigated, by plotting the ICE status (On/Off) as a function of SOC and traction power, as shown in Figure 57. It is evident that the EMS in both cycles allows the electric driving only when the battery SOC is above 25% and the power demand is below 10 kW.

As far as the vehicle speed role in the control logic is concerned, data reported in Figure 58 clearly show that the EMS permits the electric driving until a threshold speed of about 60 km/h is reached.



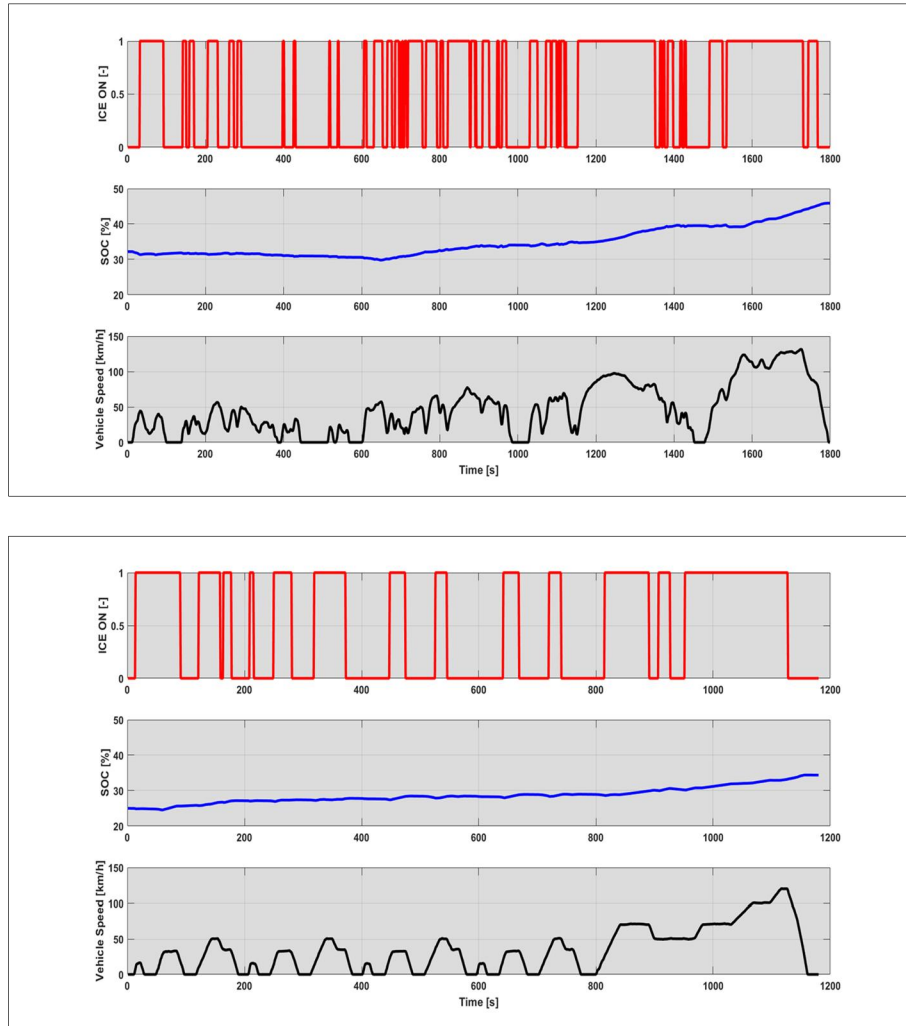


**Figure 56:** Golf GTE - ICE On/Off and battery SOC for the GTE mode along the WLTC (Top) and NEDC (Bottom)

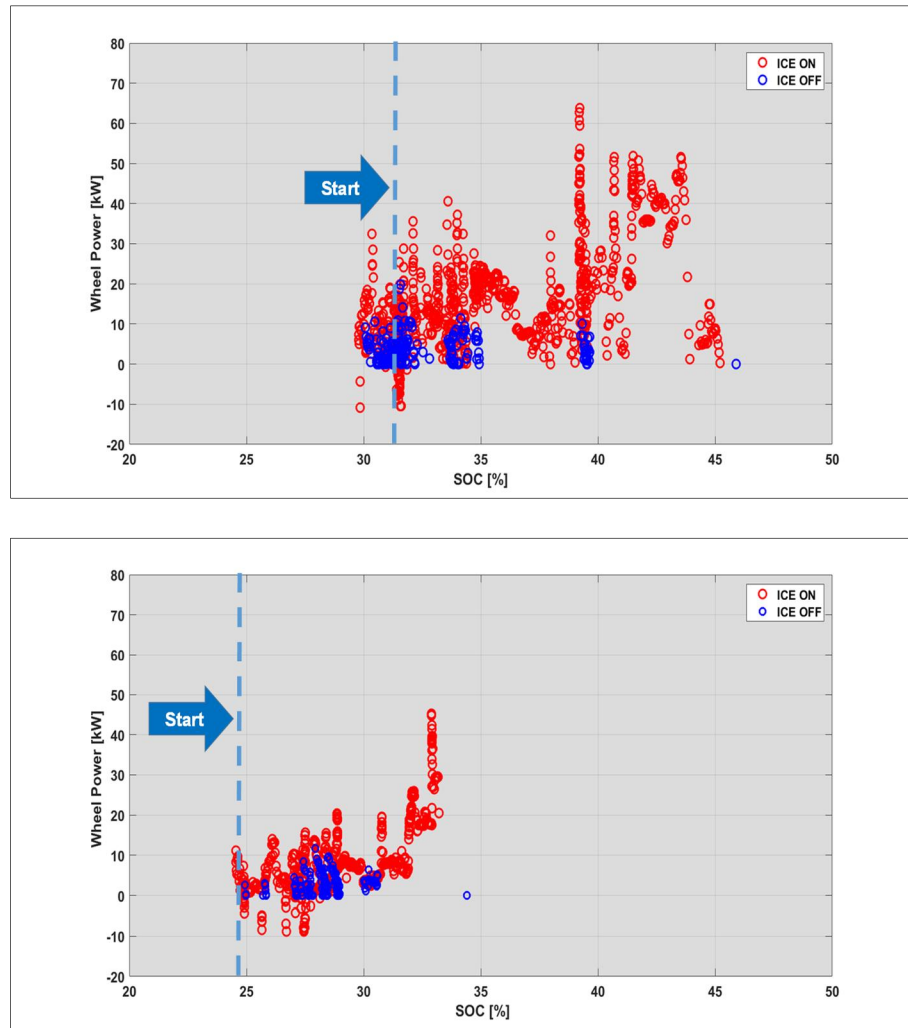


**Figure 57:** Golf GTE - ICE actuation as a function of battery SOC and traction power for the GTE mode along the WLTC (Top) and NEDC (Bottom)

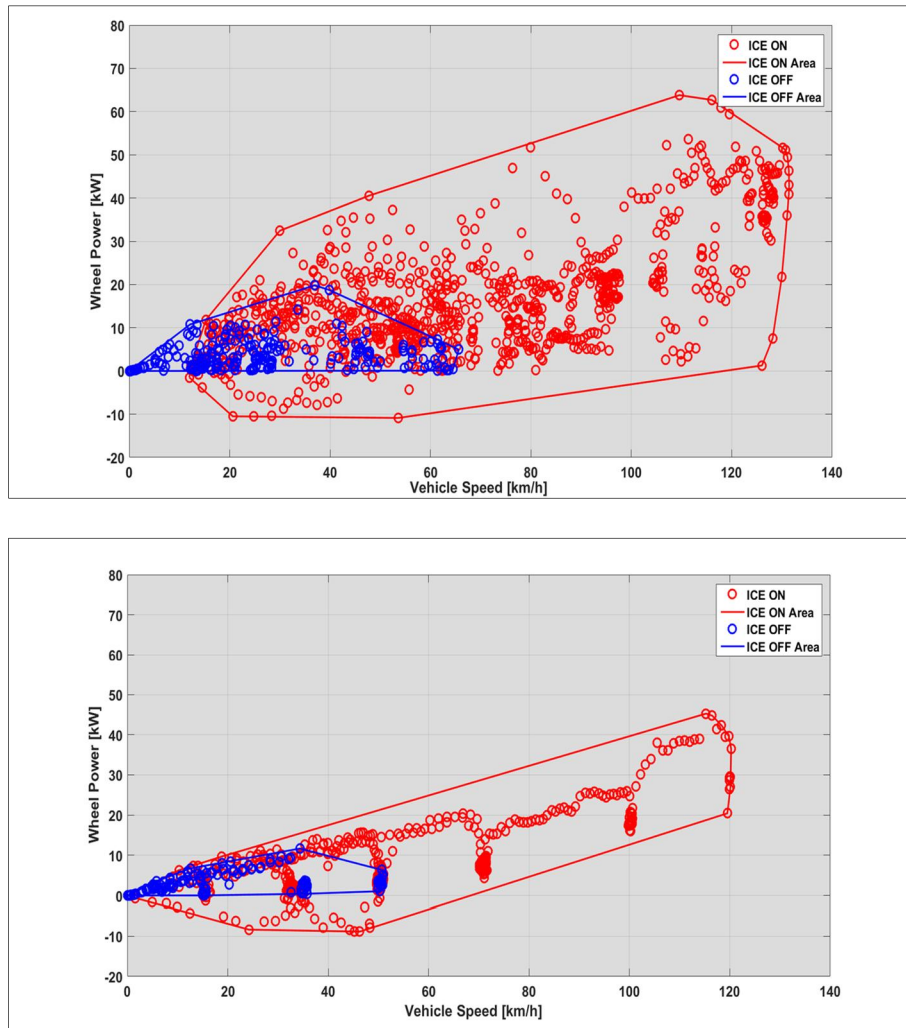


**Figure 58:** Golf GTE - ICE actuation as a function of vehicle speed and traction power demand for the GTE mode along the WLTC (top) and NEDC (Bottom)

Finally, Figure 59 points out that in the speed per acceleration domain the “zero emissions” drive is allowed between  $-5$  to  $10 \text{ m}^2/\text{s}^3$ , permitting the electric drive to steady state speed segments and drive away.

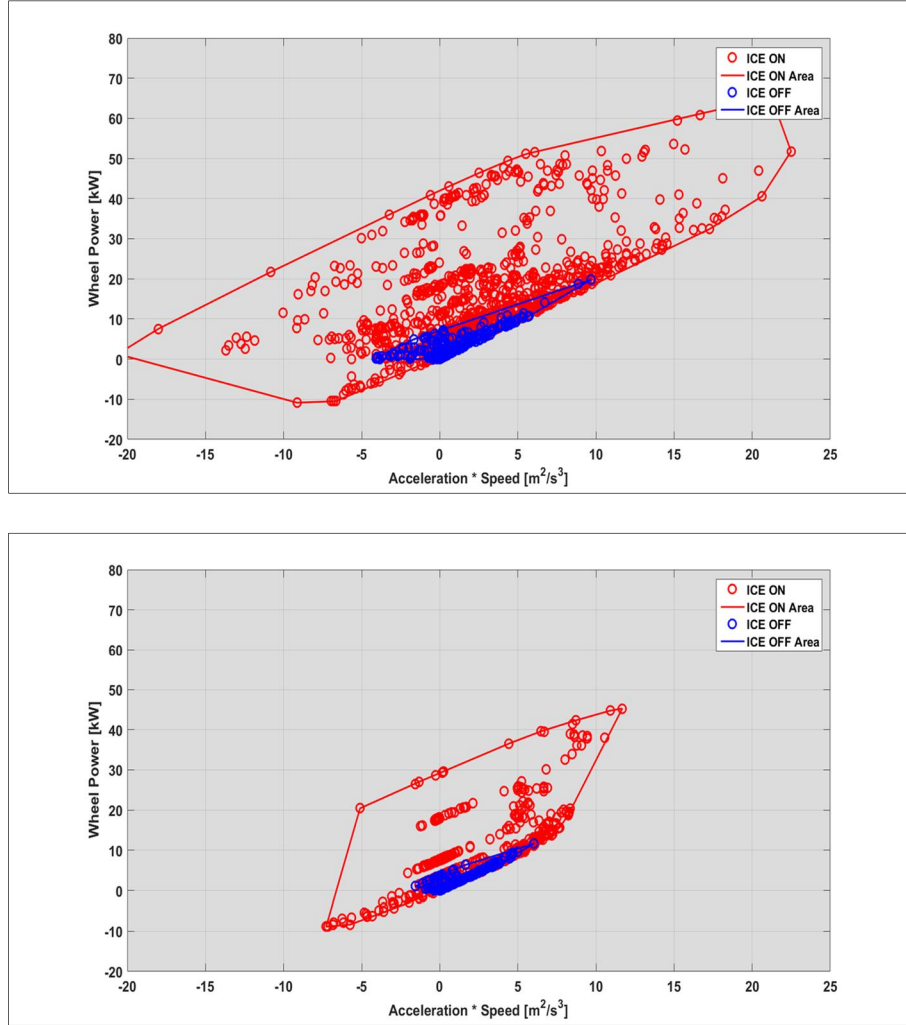


**Figure 59:** Golf GTE - ICE actuation as a function of the product between vehicle speed and acceleration and traction power demand for the GTE mode along the WLTC (Top) and NEDC (Bottom)

Focusing the attention on the parallel mode, the continuous increase of the battery SOC shown in Figure 56 highlights the massive use of the ICE for vehicle propulsion and battery recharge throughout the Load Point Moving strategy. The actuation of Smart Charge and E-Boost modes as function of the battery SOC and of the traction power demand is shown in Figure 60. The EMS enables always the battery recharge for both driving cycles, except at the beginning where the cat-heating strategy is applied. Similar to the E-Mode tests, the E-Boost use is negligible.

Further confirmations can be found in Figure 61, where the ICE operating conditions are plotted as a function of the speed per acceleration term versus the motive power.

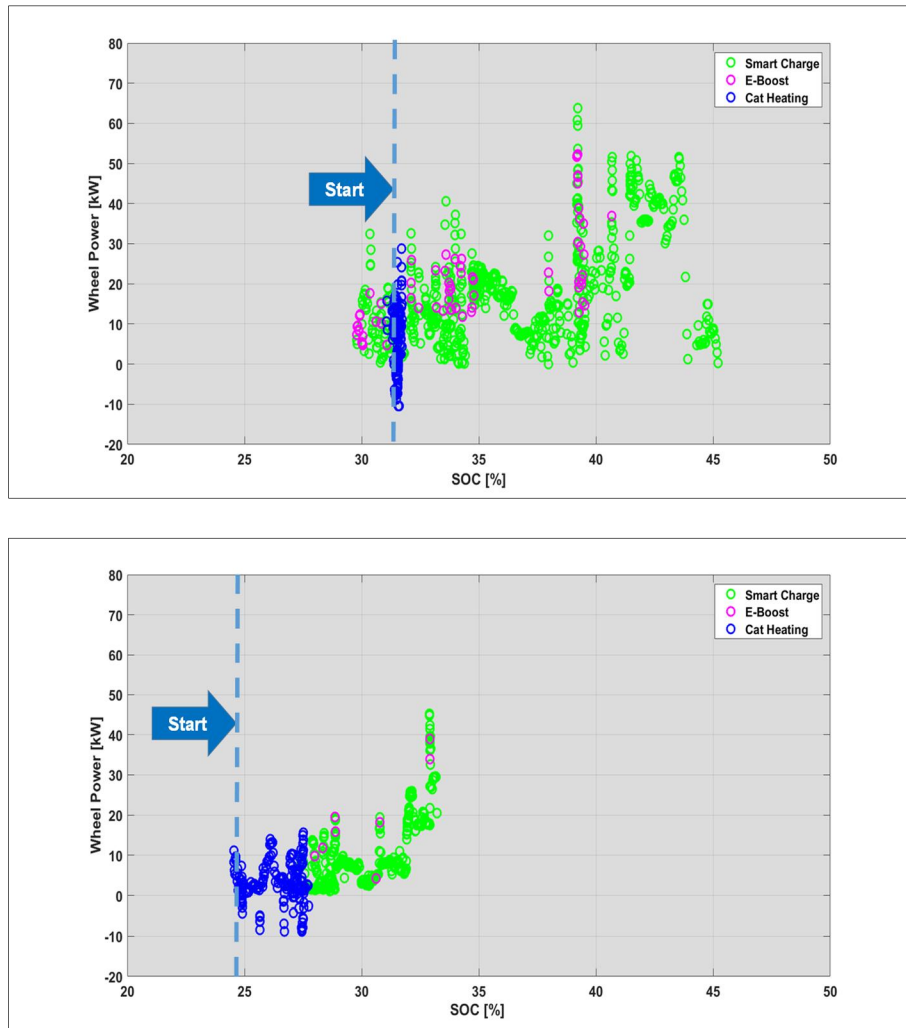


**Figure 60:** Golf GTE - Identification of the ICE operating conditions in GTE mode as a function of battery SOC along the WLTC (Top) and NEDC (Bottom)

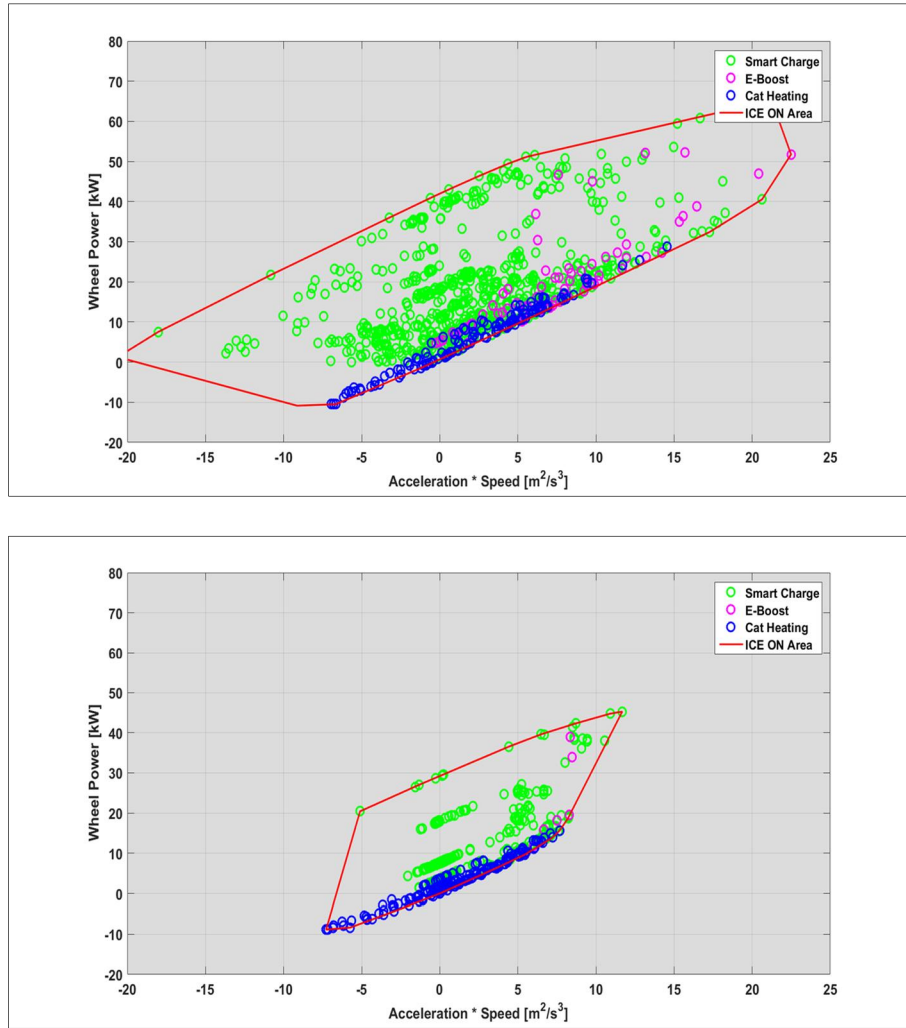


**Figure 61:** Golf GTE - Identification of the ICE operating conditions as a function of the product between vehicle speed and acceleration for the GTE mode along the WLTC (Top) and NEDC (Bottom)

Figure 62 shows that the percentage of EV driving does not differ significantly from the NEDC to WLTC, as opposed to the CD case, and it highlights a comparable use of the Smart Charge mode for both driving cycles.

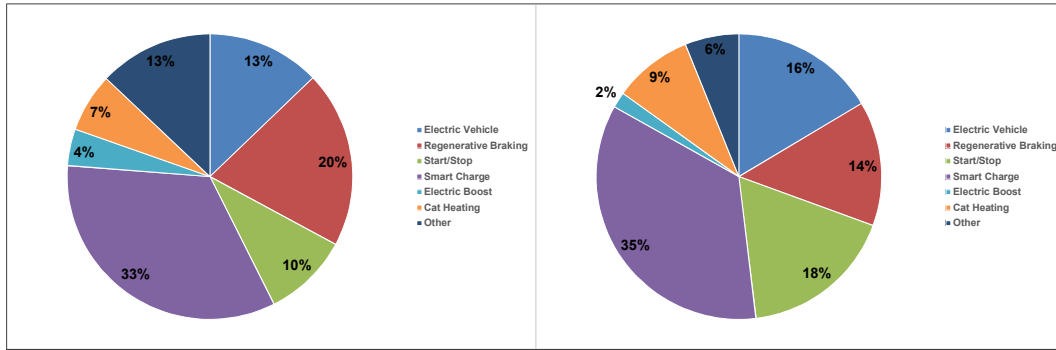


**Figure 62:** Golf GTE - Vehicle operating mode share for the GTE mode along the WLTC (Left) and NEDC (Right)

## 2.6 CO<sub>2</sub> emissions

The CO<sub>2</sub> emissions for the Yaris Hybrid and the Golf GTE were calculated applying the procedure described in [29] and summarized in 2.4, which is currently used for the TA of passenger cars. All the results presented in this section will be used off course to assess the predictive capabilities of the code, but also to analyze incisively the impact of different test conditions on the CO<sub>2</sub> emissions.

In the first part, the main results for the Yaris Hybrid will be presented, focusing on the computation of the K-Factor and on the correction of the measured CO<sub>2</sub> values according to the TA procedure. The second part will be focused on the Golf GTE, analyzing the impact of the different test procedure on the electric range and consequently on the TA CO<sub>2</sub>.

### 2.6.1 Yaris Hybrid: K-Factor and CO<sub>2</sub> emissions

The change to more severe test conditions and the different battery energy level at the beginning of the cycles affect the EMS capabilities to exploit the electric driving and consequently the CO<sub>2</sub> emissions, as illustrated in Figure 63. The change of the test condition from NEDC to WLTC leads to an average increase of CO<sub>2</sub> emissions of 26 g/km independently from the starting SOC. Instead, the different starting conditions of the battery entails an average increase of 6.5 g/km on the same cycle.

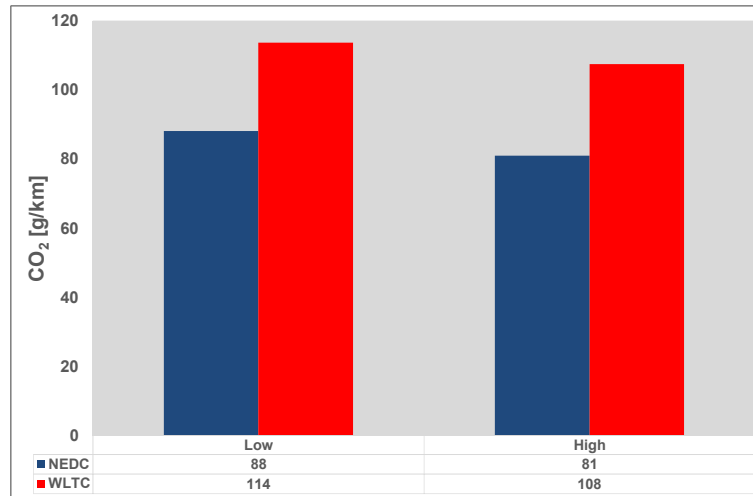


**Figure 63:** Yaris Hybrid - CO<sub>2</sub> emissions for the “Low SOC” and “High SOC” cases

The computation of K-Factor was done according to Equation 3 and, as illustrated in Table 11, the two values are divergent. The different share of electric driving due to the increasing cycle energy demand from NEDC to WLTC produces this situation. Therefore, the wider use of the ICE impacts on the CO<sub>2</sub> emissions, but also on the battery energy balance at the end of the cycle, due to the diffuse usage of Smart Charge strategy, as demonstrated in Figure 47 and Figure 48.

**Table 11:** Yaris Hybrid - comparison between the K-Factors calculated along the NEDC and WLTC cycles

	NEDC	WLTC
<b>K Factor [g/(km•Ah)]</b>	-8.06	-12.16

The corrected CO<sub>2</sub> emissions for the NEDC and WLTC are reported in Figure 64. The red triangular and the blue squared markers represent the CO<sub>2</sub> emissions in g/km respectively at the end of the WLTC and NEDC, related to the “High SOC” and “Low SOC” cases, as a function of the battery current integral. The slopes of the two straight lines correspond to the K-Factor. Finally, the green markers represent the CO<sub>2</sub> corrected values according to Equation 4, which are reported in Table 12.



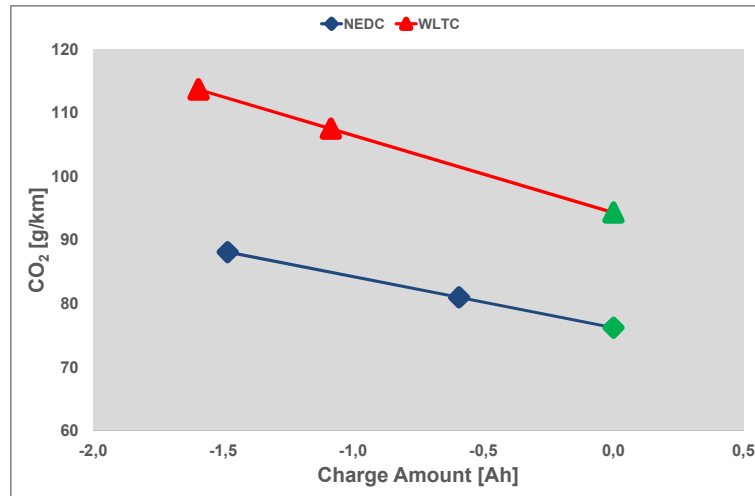


**Figure 64:** Yaris Hybrid - K-Factor correction

**Table 12:** Yaris Hybrid - CO<sub>2</sub> TA values

	NEDC	WLTC
CO <sub>2</sub> [g/km]	76.2	94.3

The new test conditions show an increase of CO<sub>2</sub> emissions from NEDC to WLTC of 18 g/km, corresponding to an increment of 23%.

### 2.6.2 Golf GTE: electric range and CO<sub>2</sub> emissions

The assessment of the electric range was done according [29] and the results along the NEDC and WLTC cycle are reported in Table 13.

**Table 13:** Golf GTE - Values of the electric range for the NEDC and the WLTC

	NEDC	WLTC
Dovc [km]	41.7	32.7

The higher energy demand of the WLTC compared to the NEDC, as shown in Figure 28, produces a reduction of electric range of 20%, thus significantly affecting the final CO<sub>2</sub> value, as shown in Figure 65, where the TA emissions are obtained through the weighing of the E-Mode with the GTE, according to Equation 6.

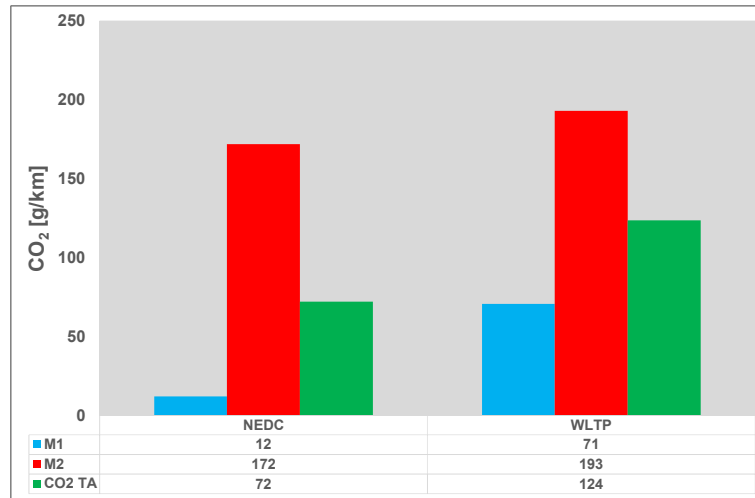


**Figure 65:** Golf GTE - CO<sub>2</sub> emissions along the NEDC and the WLTC combining the E-Mode with the GTE

The CO<sub>2</sub> emissions increase of 58 g/km in E-Mode, indicated as  $M_1$ , from NEDC to WLTC. The growth of the energy demand entails the complete discharge of the battery in the middle of the second repetition of WLTC, forcing the EMS to charge the battery during the High and Extra-High phases. The CS test, labelled with  $M_2$ , betrays less the influence of the test procedure, showing a CO<sub>2</sub> increase of 21 g/km. The final value conveys the superposition of the reduced electric range and the increase of CO<sub>2</sub> emissions in CD, leading to a growth of 70% from NEDC to WLTC.

## Chapter 3

# Hybrid Meta-Model

### 3.1 Introduction

The experimental campaign carried out on two different hybrid vehicles, described in Chapter 2, is the base for the development of the Hybrid Meta-Model. Inside this chapter, the design of the mathematical model capable to estimate the CO<sub>2</sub> emissions along the NEDC cycle for HEVs and PHEVs vehicles, based on the detection of the EMS throughout a limited number of data, available from the TA test along the WLTC cycle, will be presented. The code should be able to reproduce correctly the powertrain behavior along the NEDC cycle, recognizing the actuation logic of the typical operating conditions of HEV and PHEV, as illustrated in Figure 66. Both HEVs and PHEVs, independently by the hybrid architecture layout, can work in four different ways:

- ***Electric Vehicle***: the ICE is shut down and all the energy necessary for the vehicle propelling needs is provided by the high voltage battery;
- ***Regenerative Braking***: during the braking event the kinetic energy is recovered through the electric machines connected to the wheels and stored inside the high voltage battery, instead of being dissipated using the mechanical brakes;
- ***Smart Charge or Load Point Moving***: the ICE is turned on and its operating points are shifted up closed to the optimal efficiency area and the power exceeding the vehicle propulsion needs is used to recharge the battery through the on board electric machines;
- ***E-Boost***: the available electric machines support the ICE in case of sudden load demand, improving the overall efficiency and the kick-down response.

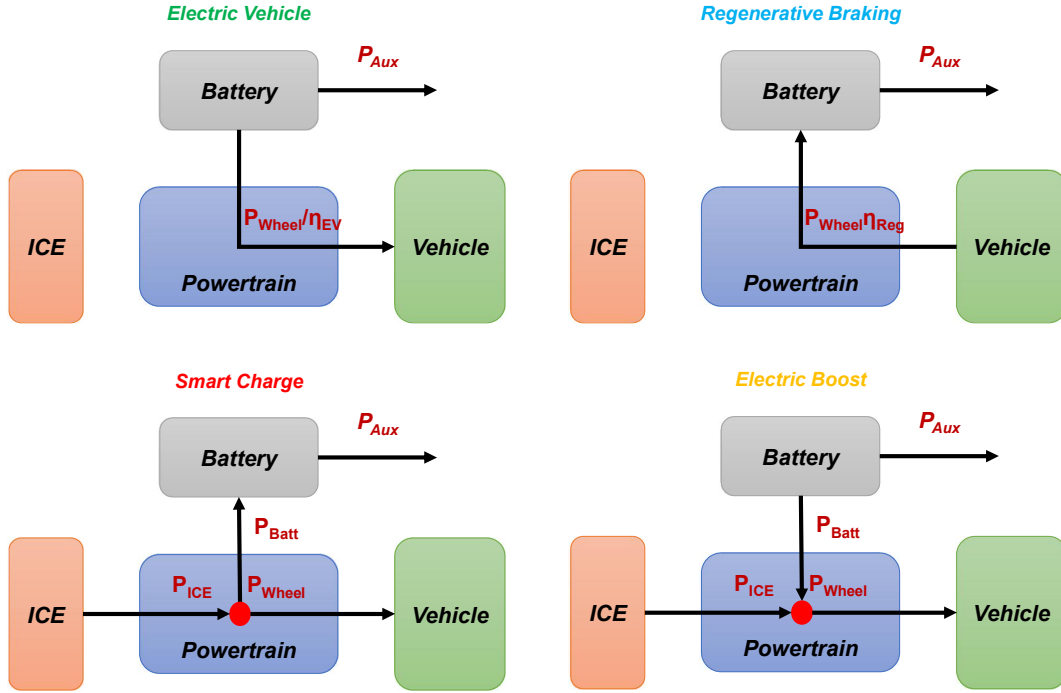


**Figure 66:** Normal operating conditions of HEV/PHEV vehicles [34]

The selection of one mode instead of another depends on different vehicle operating parameters, such as the battery SOC, the vehicle speed, the driver's power demand, etc., as illustrated in Chapter 2.

The Meta-Model should discern between the different operating modes, identifying a list of parameters representative of the EMS logic:

- **ICE operating strategy** (Engine On/Off);
- **Actuation logic and power released/adsorbed** by the battery during the **E-Boost/Smart Charge** events;
- **Battery parameters**, such as the internal resistance and the Open Circuit Voltage (OCV);
- **ICE warm-up strategy** during the “Cold Start” event;
- **Powertrain efficiencies** during the electric propulsion and regenerative braking operations, indicated in Figure 66 respectively as  $\eta_{EV}$  and  $\eta_{Reg}$ ;
- Power absorption from the **auxiliary components**, such as the cockpit, the Engine Control Unit (ECU), etc.

The detection of the EMS through the Meta-Model and the correct simulation of the powertrain along the NEDC cycle requests a limited number of information coming from the TA test such as:

1. **Vehicle speed**;
2. **Engine speed**;

3. **High Voltage battery measurements**, such as the current, the voltage and the SOC;
4. **Engine coolant temperature**;
5. **Instantaneous CO<sub>2</sub> emissions**.

In addition to the experimental acquisitions, it is necessary to provide few information related to the test case such as:

1. **Vehicle test mass and RLs** both for WLTC and NEDC cycles;
2. **Engine WOT curve**;
3. **High Voltage battery capacity**.

This chapter will present the design of the Meta-Model, focusing on its logic and on the approach applied for the identification of the main operating parameters of hybrid vehicles.

## 3.2 The Meta-Model logic

Before the detailed explanation of the methodology used for the identification and modelling of the operating parameters, this paragraph illustrates the operations sequence applied by the model to simulate the EMS of HEV and PHEV vehicles.

The simulation of HEVs does not differ much from the PHEVs, because as shown in Figure 66, they share the same operating conditions and the EMS for both technologies relies on the same parameters like the battery SOC, the vehicle kinematic and the traction power. The main difference is the computation of CO<sub>2</sub> emissions, as described in Chapter 2.

In HEVs, the battery represents an energy buffer, since the electric energy used during the discharge phase should be supplied afterwards through the engine load point moving or through the regenerative braking. On the contrary, the PHEVs rely on an externally rechargeable battery, allowing the pure electric traction for medium distances.

The computation of CO<sub>2</sub> emissions along the NEDC cycle should reflect the requirements of Regulation 83 [24], presented in Chapter 2.

### 3.2.1 HEV simulation logic

The computation of CO<sub>2</sub> emissions from HEVs requests the definition of the K-Factor, which is used to correct the emissions depending on the battery energy balance. Therefore, the K-Factor represents the slope of a straight line on a plane defined by the battery energy balance and the CO<sub>2</sub> emissions, requesting for its evaluation at least two cycles' measurements, with opposite initial battery energy levels. As demonstrated in Chapter 2, the K-Factor detected along the WLTC test is different from the NEDC one due to a different usage of the battery energy.

Whereas the K-Factor for the NEDC cycle will be not available, the model should be able to compute it from the measurements on WLTC cycle. Therefore, it needs at least two acquisitions with different initial battery SOC levels, simulating the EMS on the NEDC for each SOC level and computing the K-Factor from the simulated cycles.

The basis is the correct detection of the engine enabling for each measure carried out on WLTC, indicated in Figure 67 as  $n$ , at different initial SOC levels.

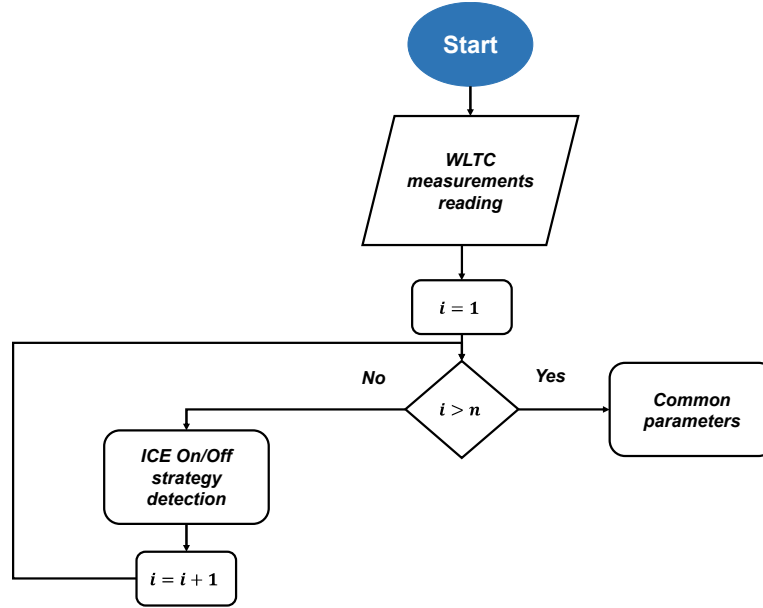


**Figure 67:** Meta-Model flow chart - Detection of the ICE On/Off strategy for HEVs

The second step is the modelling of powertrain efficiencies, of the power adsorbed by auxiliary components, and of Smart Charge/E-Boost. This section is called “*common parameters*”, as indicated in Figure 67. The term “*common*” indicates the absence of dependencies from the battery SOC level at the beginning of the cycle. For example, the powertrain efficiencies during the electric drive or the regenerative braking are mainly dependent from the physical characteristics and on the operating conditions of the electric machines. It is possible to build a well-defined map using all the available acquisitions, assuming a limited influence of the battery SOC. The same approach is applied to evaluate the power absorption from the auxiliary components, which is almost the same for each test condition, since components like the Heating, Ventilating and Air conditioning (HVAC) and the on board infotainment, characterized by a variable absorption, are off during the test. Furthermore, the actuation of the Smart Charge/E-Boost and the power adsorbed/released during these conditions can be modelled with the same approach, since their actuation, as seen in Chapter 2, is strictly dependent by the engine operating conditions. Therefore, the gathering of all the acquisitions can be helpful for the construction of maps and volumes dependent on traction power, battery SOC

and vehicle speed/acceleration, representative of the power absorbed/released by the battery and of the actuation logic, covering a large portion of the powertrain domain.

The third step is the modelling of the ICE speed and of its conduct throughout the “Cold Start”, as shown in Figure 68. The modelling is subject to the power generated by the ICE, computed thanks to the knowledge of the driveline and electric efficiencies evaluated in the second step. As like the engine On/Off detection, the computation of such parameters is made for each WLTC measurement.

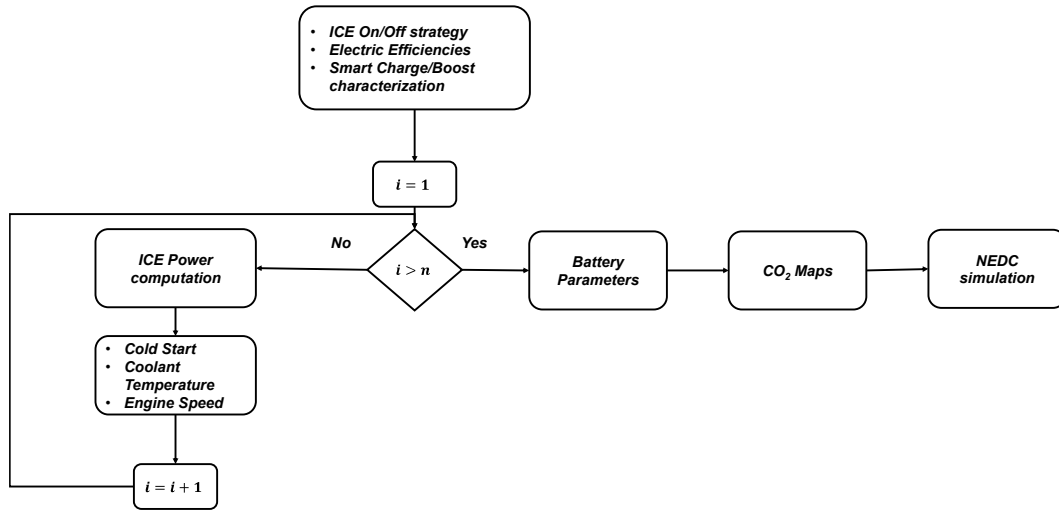


**Figure 68:** Meta-Model flow chart - Detection of the “Cold Start” strategy and calibration of the engine speed and coolant temperature empirical relations for HEVs

The battery parameters, like the internal resistance and the OCV, are evaluated for each WLTC acquisition, because the accumulator behavior relies on the SOC profile, which varies from cycle to cycle.

Finally, the Meta-Model computes the CO<sub>2</sub> emissions maps depending on the engine thermal status (Cold or Hot), applying an approach similar to the definition of the electric machines efficiencies. The engine calibration is unique for each repetition of the WLTC cycle and it does not change depending on battery energy level, as instead its actuation. So all the operating conditions along the various WLTC tests are gathered for the map building.

All the models defined in the previous steps are used to simulate the EMS along the NEDC cycle for the different initial levels of battery SOC, indicated as  $j$  in Figure 69, to compute the K-Factor necessary for the correction of CO<sub>2</sub> emissions, as illustrated in Figure 69.

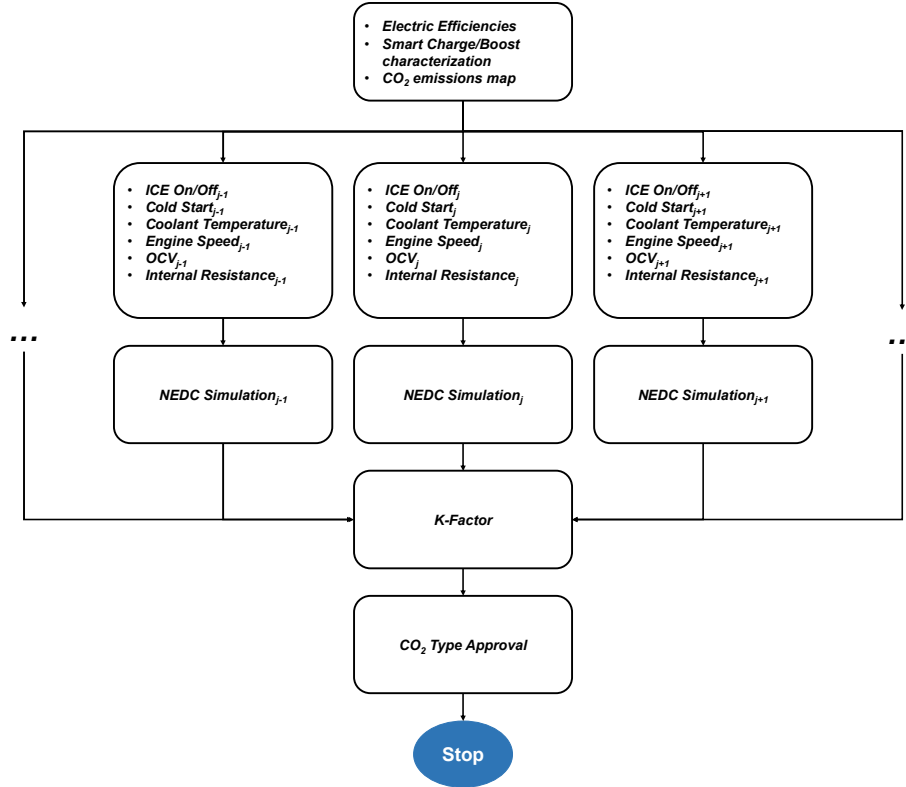


**Figure 69:** Meta-Model flow chart - Simulation of NEDC cycle and TA CO<sub>2</sub> emissions computation for HEVs

### 3.2.2 PHEV simulation logic

The modelling of PHEVs follows a similar approach of HEVs, but the TA assessment of CO<sub>2</sub> emissions requests the execution of two tests, one in CD and the other one in CS, as described in Chapter 2. The TA procedure weighs the CD and CS emissions respectively with the electric range and the average distance between two battery recharges, which is a fixed value equal to 25 km. Therefore, the model should evaluate correctly along the NEDC the “electric distance” in CD and the CO<sub>2</sub> emissions for both test conditions. Furthermore, as seen in Chapter 2 the TA procedure requests the test of the CD in the “most hybrid electric mode”, than the CS in the “most fuel consuming mode”. For this reason, the Meta-Model should detect and reproduce correctly two different EMS logics, operating at different levels of battery SOC.

Like the HEVs case, the PHEVs Meta-Model identifies the ICE On/Off strategy for the two tests along the WLTC cycle, as outlined in Figure 70.



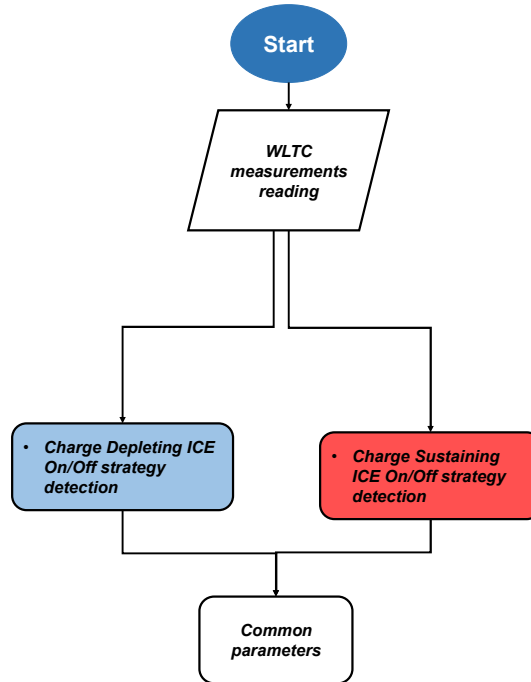


**Figure 70:** Meta-Model flow chart - Detection of the ICE On/Off strategy for PHEVs

The ensemble of “*common operating parameters*” made by the powertrain efficiencies, the characterization of the Smart Charge/Boost and the detection of the power adsorbed by auxiliary components is structured in the same way of HEVs.

The “Cold Start” modelling and the calibration of the coolant temperature relation follow the same methodology of HEVs, but their application is limited exclusively to the CS case, as depicted in Figure 71. The reason is ascribable to the negligible impact of engine “Cold Start” in PHEVs during the CD test along the NEDC cycle. As evident from Chapter 2, modern PHEVs are able to travel in pure electric driving for more than one cycle and the engine ignition takes place when the battery is depleted. Therefore, the EMS does not actuate warm up strategies in CD, such as for example the cut-off disabling at the beginning of the CS test. The simulation of “Cold Start” and consequently of the coolant are neglected for the CD test. Finally, the modelling of the engine speed and the computation of the ICE power, the detection of the battery operating parameters and of CO<sub>2</sub> maps follow the same approach adopted for HEVs vehicles. The logic passages are illustrated in the flow chart reported in Figure 71.

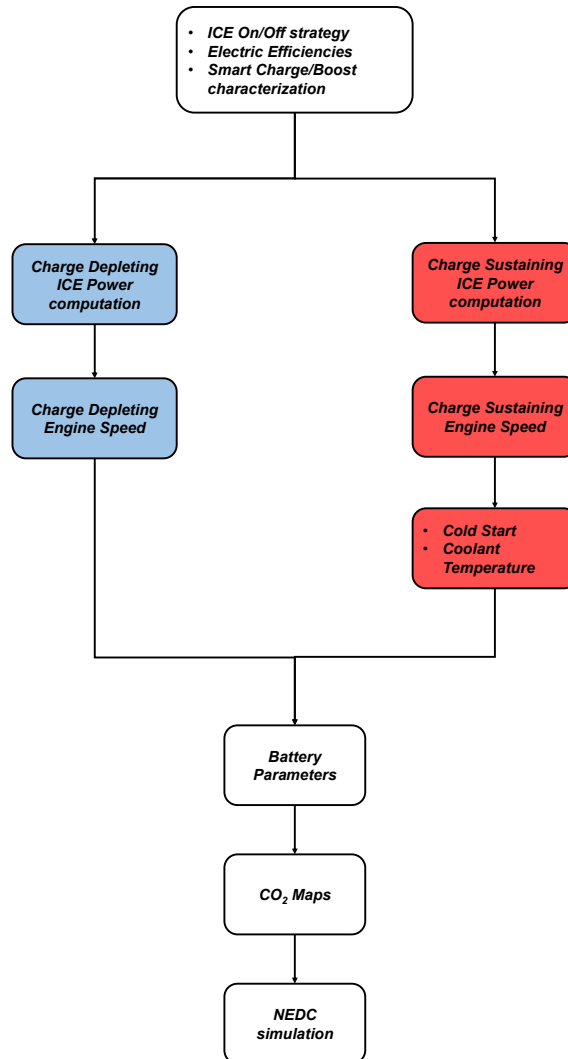


**Figure 71:** Meta-Model flow chart - Detection of the “Cold Start” strategy and calibration of the engine speed and coolant temperature empirical relations for PHEVs

All the mathematical models defined for the CD and the CS are used to simulate the EMS along the NEDC cycle, providing as output all the information necessary to compute the CO<sub>2</sub> emissions according to the TA procedure, as summarized in Figure 72.

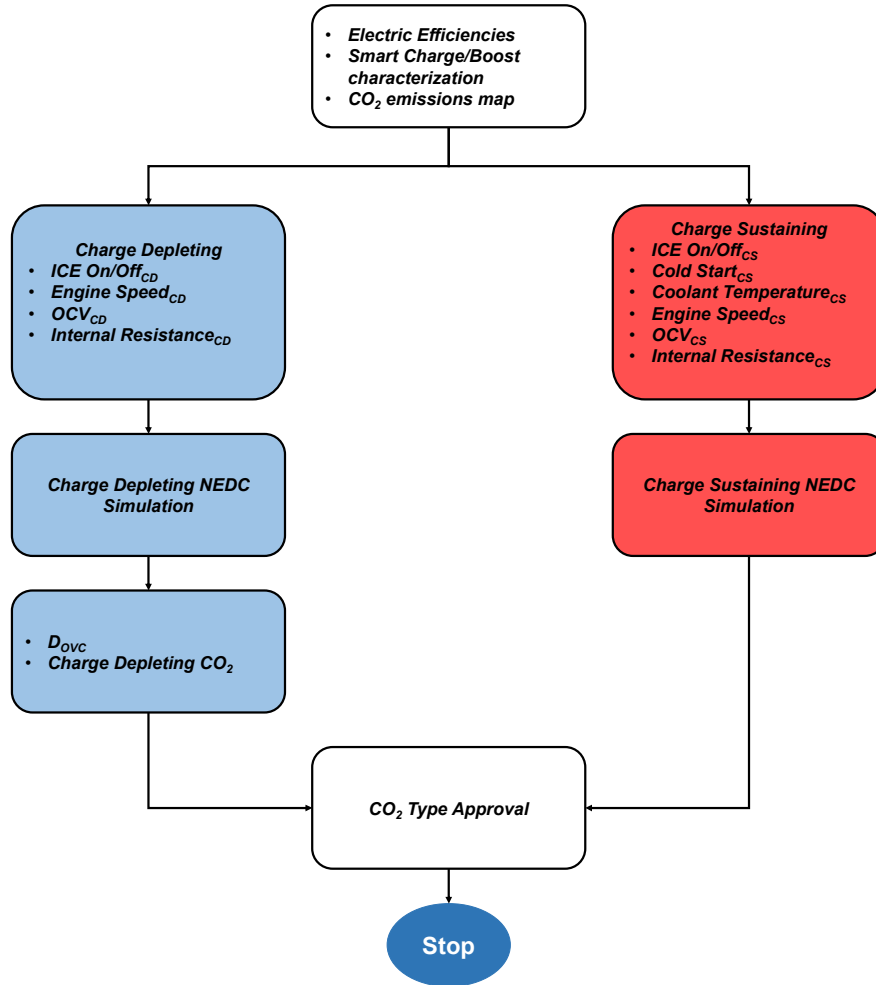


**Figure 72:** Meta-Model flow chart – Simulation of NEDC cycle and TA CO<sub>2</sub> emissions computation for PHEVs

### 3.3 Energy Management System identification

The use of a correlation model to estimate the CO<sub>2</sub> emissions from hybrid vehicles is based on a simple consideration: the powertrain operating area along the NEDC falls within the WLTC. Figure 73 shows the vehicle operating points as function of vehicle speed and power demand for the Yaris Hybrid. The red points define the WLTC area, while the blue one the NEDC.

The NEDC area is a proper subset of the WLTC for two different reasons:

1. The dynamic of the NEDC cycle is lower compared to the WLTC, because it is characterized by limited speeds and accelerations;
2. The WLTC test conditions (mass and RLs) are more severe than the NEDC, leading the powertrain to operate in a wider range.

The identification of the powertrain behavior relies on this two important condition, permitting the correct simulation of NEDC cycle.

The next paragraphs will describe the mathematical approach used for the identification of the principal operating parameters and their modelling for HEVs and PHEVs.

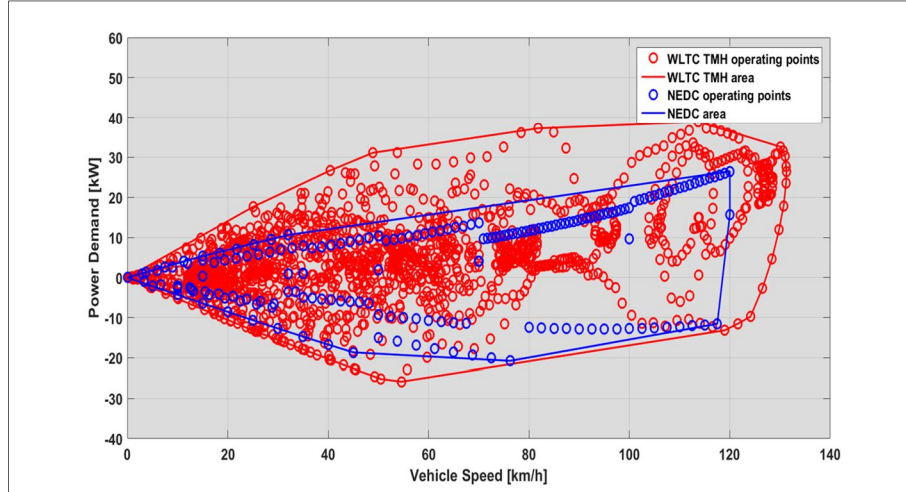


**Figure 73:** Vehicle operating area for the Yaris Hybrid

### 3.3.1 Internal Combustion Engine operating strategy

The actuation logic of the ICE in hybrid powertrains, as seen in Chapter 2, relies on the battery SOC, on driver's power demand and on kinematic parameters like the vehicle speed and acceleration.

The detecting of the ICE enabling strategy along the WLTC cycle is done using mathematical curves defined as function of the physical parameters listed before, applying different methodologies depending on whether a HEV or a PHEV powertrain.

#### 3.3.1.1 Hybrid Electric Vehicle

In case of hybrid powertrains, the ICE actuation is dependent certainly on battery SOC and traction power. The decision to model the engine On/Off strategy also as function of vehicle speed instead of acceleration derives from the code validation for different HEV applications.

The On/Off curves are modelled organizing the powertrain operating points for different levels of SOC to take into account the weight of the battery's energy level, simplifying as much as possible the modelling. The definition of level's number is a critical issue, because a limited number could lead the model to miss some engine ignitions during the NEDC simulation. Otherwise, a large number could generate fake ignitions, influencing the computation of CO<sub>2</sub> emissions.

As seen in Chapter 2, when the battery energy level is high at the beginning of the cycle the EMS limits the electric drive depending on the physical limits of the powertrain, neglecting the influence of the battery energy status. On the contrary, the SOC plays an important role when the battery energy level is low, because the control should actuate particular strategies to charge the battery and to limit the electric drive. Therefore, the Meta-Model designs the number of bands setting a minimum number of vehicle operating points within it, variable as a function of the starting SOC, as shown in the flow chart in Figure 74.

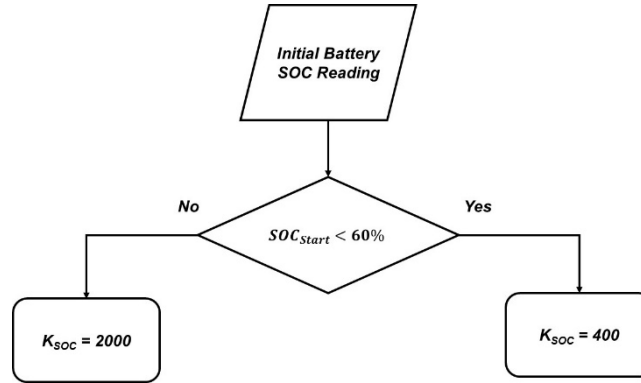


**Figure 74:** Definition of the minimum number of points per each SOC band depending on the battery initial energy level

$K_{SOC}$  represents a multiplicative coefficient of the data sampling frequency, defining together the minimum number of points per each SOC band, as shown in Equation 7. Figure 75 shows an example of band definition, where all the operating points are represented according to the engine state as function of vehicle speed and traction power, excluding the breaking event. The light blue points represent the electric vehicle condition, while the black one the hybrid driving.

$$N_{SOC} = K_{SOC} \cdot Input_{freq}$$

**Equation 7:** Calculation of the minimum number of points per each SOC band

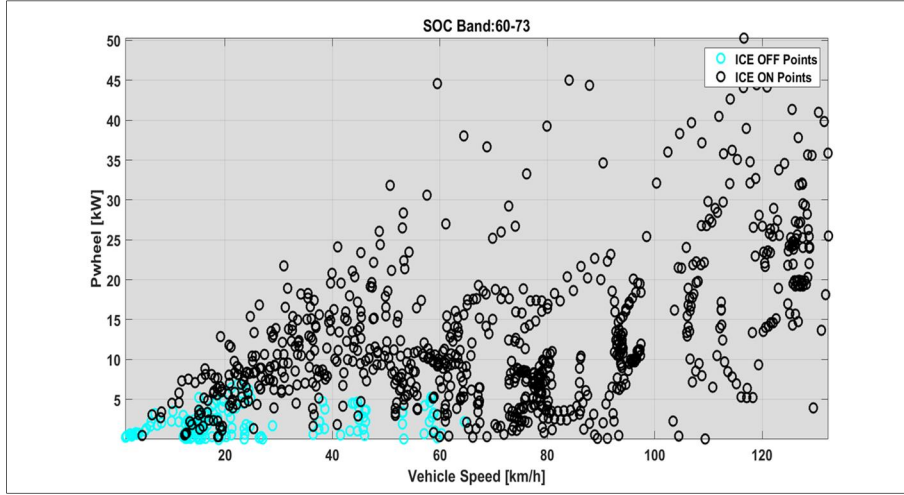


**Figure 75:** Example of SOC band organization for an HEV with battery fully charged

For each SOC band, the Meta-Model defines the engine On/Off curves to prevent high frequency oscillations of the engine status, affecting the quality of the results. The code splits the powertrain domain in different speed band, likely the SOC case, and it identifies for each one the maximum traction power during the electric drive and the minimum one during the hybrid mode. These two values are associated to the average vehicle speed of the band to shape the engine On/Off curves.

The length of each speed band is variable and its size depends by a minimum number of points likely the SOC case as defined by the Equation 8.

$$N_{Speed} = K_{Speed} \cdot Input_{freq}$$

**Equation 8:** Calculation of the minimum number of points per each speed band

The multiplicative coefficient  $K_{Speed}$  is set to 20.

The model applies specific filters to prevent the definition of curves without physical meaning, such as for example when the switch off limit is higher than the ignition. This condition happens when all the hybrid points inside the speed band are above the electric drive one. The model corrects these points applying the minimum traction power of the vehicle in hybrid mode within the SOC band.

Figure 76 and Figure 77 represent for two different levels of initial battery SOC how the code design the engine On/Off, represented respectively by the red and the blue lines curves.

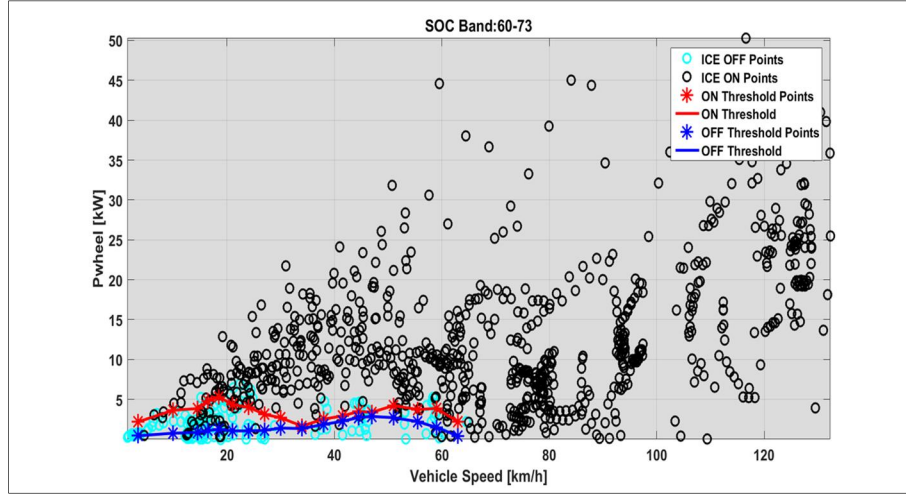


**Figure 76:** Example of On/Off curves for a HEV with the battery fully charged at the beginning of the cycle

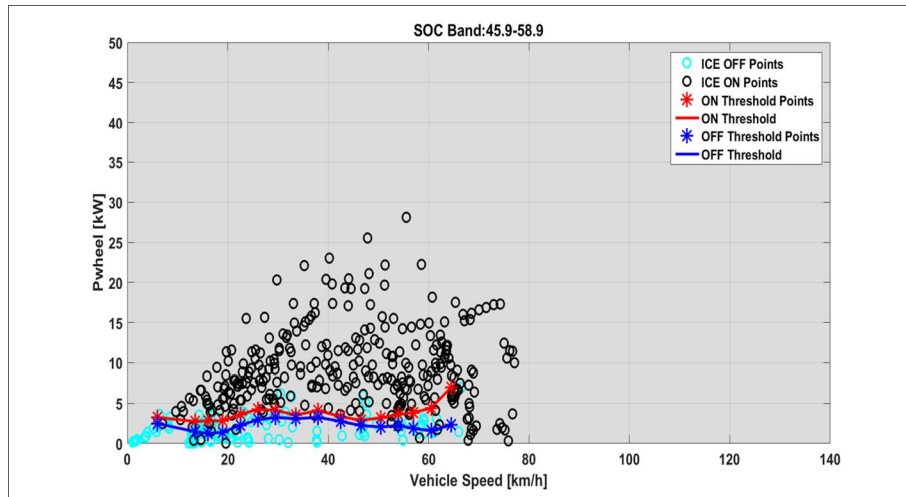


**Figure 77:** Example of On/Off curves for a HEV with the battery discharged at the beginning of the cycle

### 3.3.1.2 Plug-In Hybrid Electric Vehicle

The ICE ignitions curves are designed using the same approach of HEVs powertrains. However, the model uses different methodologies depending on the test conditions, discerning between CD and CS.

#### 3.3.1.2.1 Charge Depleting

The use of the ICE during the CD test is dependent from the battery SOC and from the traction power, similarly to the HEVs, but the model uses the vehicle acceleration instead of speed as a kinematic landmark parameter.

The organization of SOC bands follows the same methodology as HEV according to Equation 7, where  $K_{soc}$  in this case is equal to 500. However, the design of the SOC bands in this way generates two different scenarios, as illustrated in Figure 78.

- The top figure represents the typical behavior of a PHEV along the WLTC cycle when the EMS uses always the electric drive since the battery SOC has not yet reached the bottom level, except when the pedal demand exceeds the physical limits of the powertrain;
- The bottom graph shows the final part of the CD test where the battery is discharged and the ICE is switched on for almost the time.

These two opposite situations make the NEDC simulation difficult. If the ICE ignition curves are modelled applying the HEV methodology when the number of hybrid points is limited, as it happens in the top graph of Figure 78, it will generate fake ignitions. Therefore, the Meta-Model should discriminate between these two different conditions, evaluating in each acceleration bands the ratio between the number of hybrid points and the electric drive. If the ratio is below 0.5, the engine on threshold is set equal to the maximum traction power along the WLTC, than the off to zero. Otherwise, the curve shaping follows the same methodology applied to the HEV case in the acceleration domain. Equation 9 calculates the length of each acceleration band, setting  $K_{Acceleration}$  to 20.

$$N_{Acceleration} = K_{Acceleration} \cdot Input_{freq}$$

**Equation 9:** Calculation of the minimum number of points per each acceleration band



The engine On/Off curves for PHEVs generated with this methodology are illustrated in Figure 79.

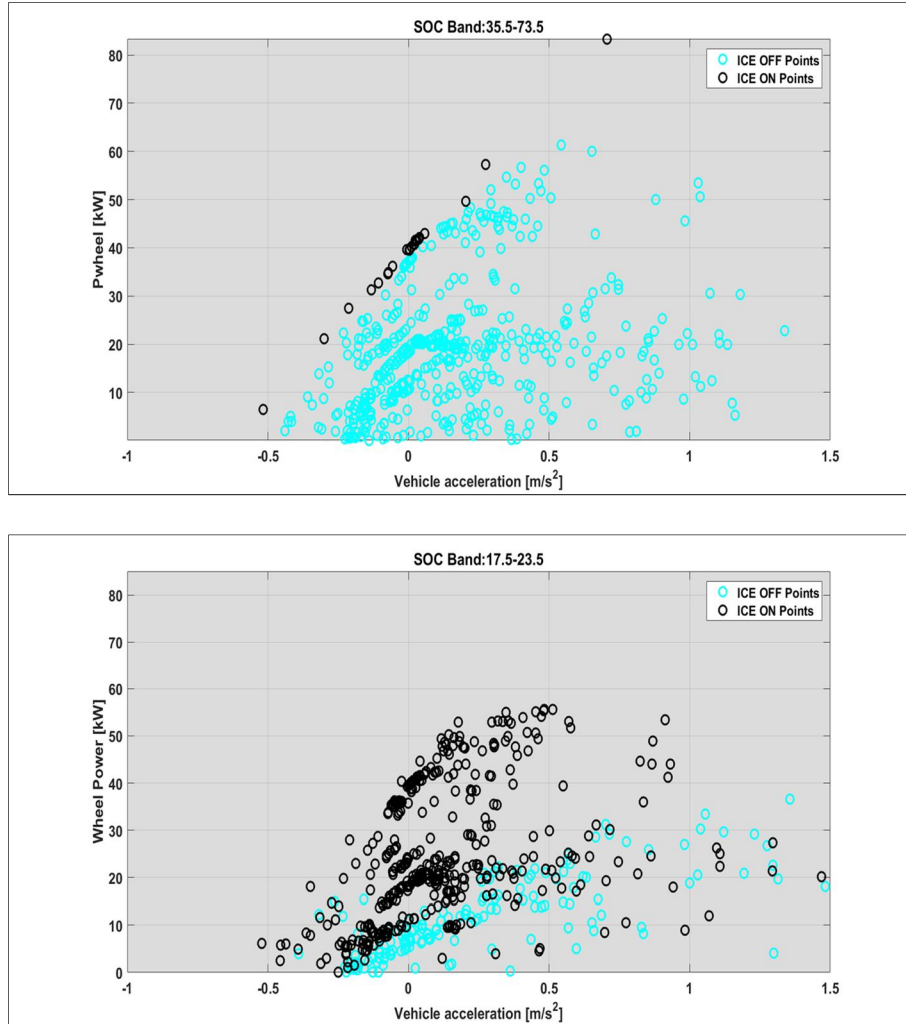


**Figure 78:** Example of SOC band organization for a PHEV in CD

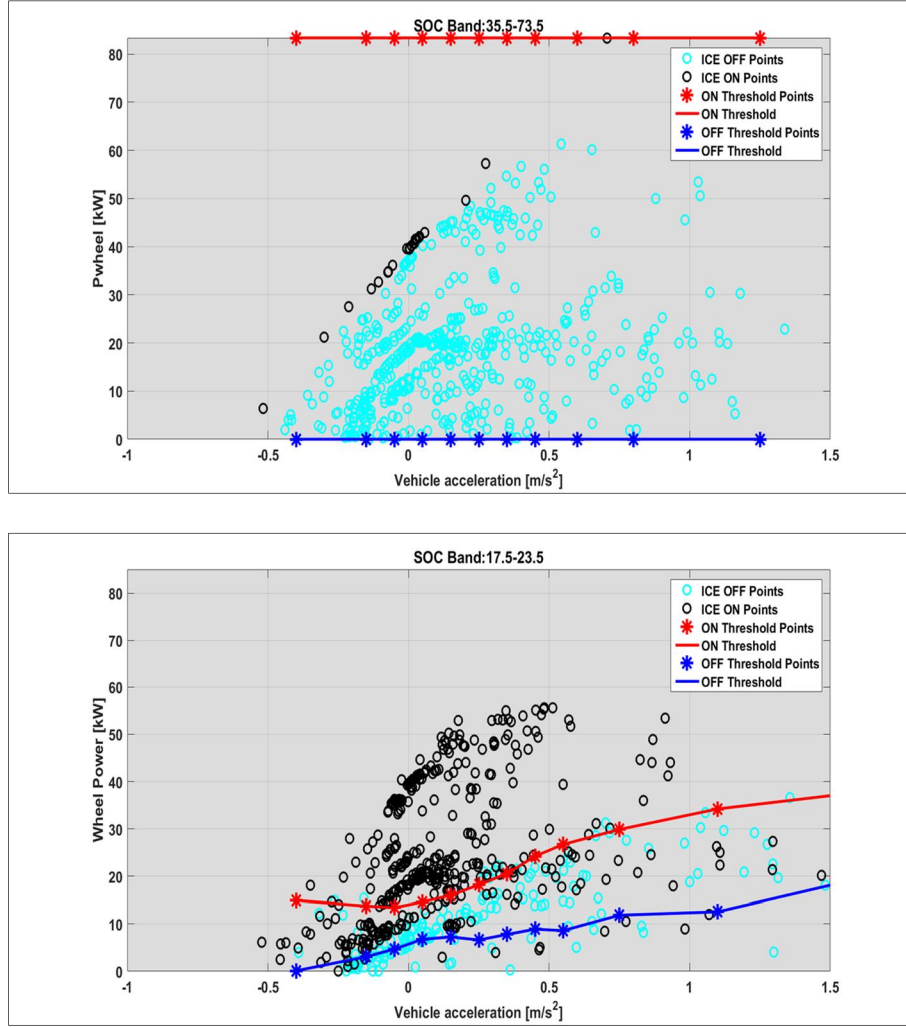


**Figure 79:** Example of On/Off curves for a PHEV in CD

### 3.3.1.2.2 Charge Sustaining

In this case, the definition of engine On/Off curves is identical to the HEVs approach. The EMS behavior during the CS condition, as evident from Chapter 2, is similar to the HEV when the battery is discharged. In both situations, the EMS limits the electric drive and forces the engine to recharge the battery. Therefore, the sizing of SOC and vehicle speed bands follows the same methodology and almost the same calibration of HEVs. The only remarkable differences are the values of the multiplicative coefficients  $K_{SOC}$  used in Equation 7, which is set to 250, and the  $K_{Speed}$  used in Equation 8, which is equal to 10. The engine On/Off curves generated by the Meta-Model are reported in Figure 80.

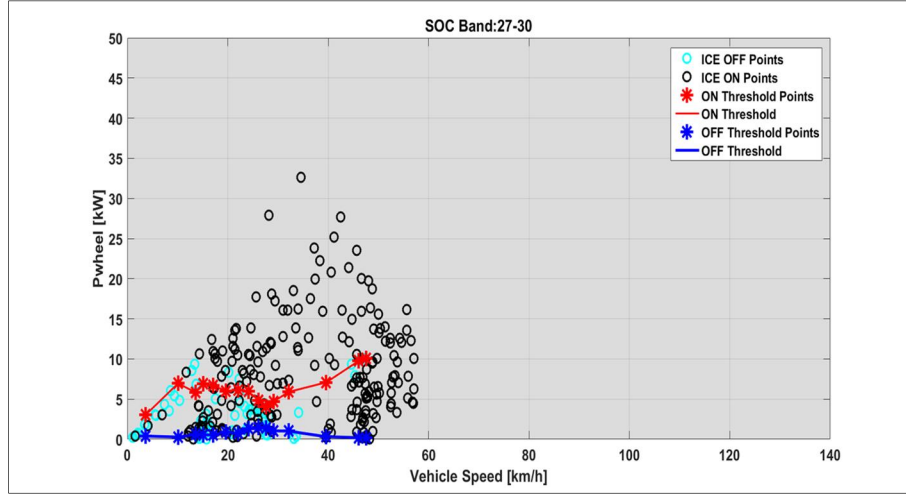


**Figure 80:** Example of On/Off curves for a PHEV in CS

### 3.3.2 Powertrain efficiency and regenerative braking

The powertrain efficiencies represent one critical parameter for the modelling of hybrid especially for PHEVs, because a wrong evaluation during the CD simulation could lead to underrate the battery SOC and consequently to an early ignition of the ICE along the NEDC cycle, compromising the CO<sub>2</sub> emissions estimation.

The estimation of powertrain efficiencies is limited to two specific operating modes of the vehicles: the electric vehicle and the regenerative braking. In case of the parallel mode the direct evaluation of the powertrain efficiencies is not possible due to the impossibility to measure the ICE torque during the vehicle test.

The efficiency of the hybrid powertrain for the considered modes depends on the mechanical/electrical characteristics of the electrical machines. Since this information is not available, the characterization can be done using the measurements available from the high voltage battery and the knowledge of vehicle mass and RLs.

The measurements of battery current and voltage are used to compute the battery power as shown in Equation 10.

$$P_{Batt} = V_{Batt} \cdot I_{Batt}$$

**Equation 10:** Calculation of battery power

Where  $P_{Batt}$  is the battery power,  $V_{Batt}$  is the voltage and  $I_{Batt}$  is the continuous current. The vehicle mass and RLs are used to compute the traction power, as reported in Equation 11.

$$P_{Wheel} = [(F_0 + F_1 \cdot v_{Vehicle} + F_2 \cdot v_{Vehicle}^2) + 1.03 \cdot v_{Vehicle} \cdot a_{Vehicle}] \cdot v_{Vehicle} / 3.6$$

**Equation 11:** Calculation of motive power

Where  $P_{Wheel}$  is the traction power,  $F_0$ ,  $F_1$  and  $F_2$  are the RLs coefficients,  $v_{Vehicle}$  is the vehicle speed and  $a_{Vehicle}$  is the vehicle accelerations. In this formulation the contribution to vehicle inertia of rotating parts is assumed to be the 3% of the mass [24].

These two parameters together can describe the efficiency of the powertrain as illustrated in Equation 12.

$$\eta_{EV} = P_{Wheel} / P_{Batt}$$

$$\eta_{Reg} = P_{Batt} / P_{Wheel}$$

**Equation 12:** Calculation of the powertrain efficiencies during the electric drive ( $\eta_{EV}$ ) and the regenerative braking ( $\eta_{Reg}$ )

These efficiencies values are employed to build a map depending on vehicle speed and traction power. This modelling decision is supported by a physical observation on electric machine characterization: the efficiency is generally correlated with the revolution speed and the output torque/power for two different reasons:

1. the Joule effect is predominant at low speeds and high torque demand where the currents are high;
2. The impact of iron losses is significant at high revolution speeds.

Since the characteristics of the gearbox (such as the gear ratios) are not available, the best way is to correlate the revolution speed with the vehicle one and the output power with the motive, because they are correlated by kinematic relations. The efficiency maps are created using the scattered interpolation function “*scatteredInterpolant*” available from the Matlab library. An example of generated maps is reported in Figure 81.

The last parameter descriptive of the regenerative braking is the minimum power that can be recovered by the battery. This aspect is not negligible for two different reasons:

1. Physical limits of the battery: the current adsorbed during a charging phase is usually limited to prevent possible battery damages;
2. Electronic brake force distribution: this safety device available on modern passenger cars distributes the brake force between the front and rear axle to prevent the lock up of the wheels causing the vehicle skid.

Such value corresponds to the minimum motive power value where the regenerative braking event is enables, as shown in Figure 82.

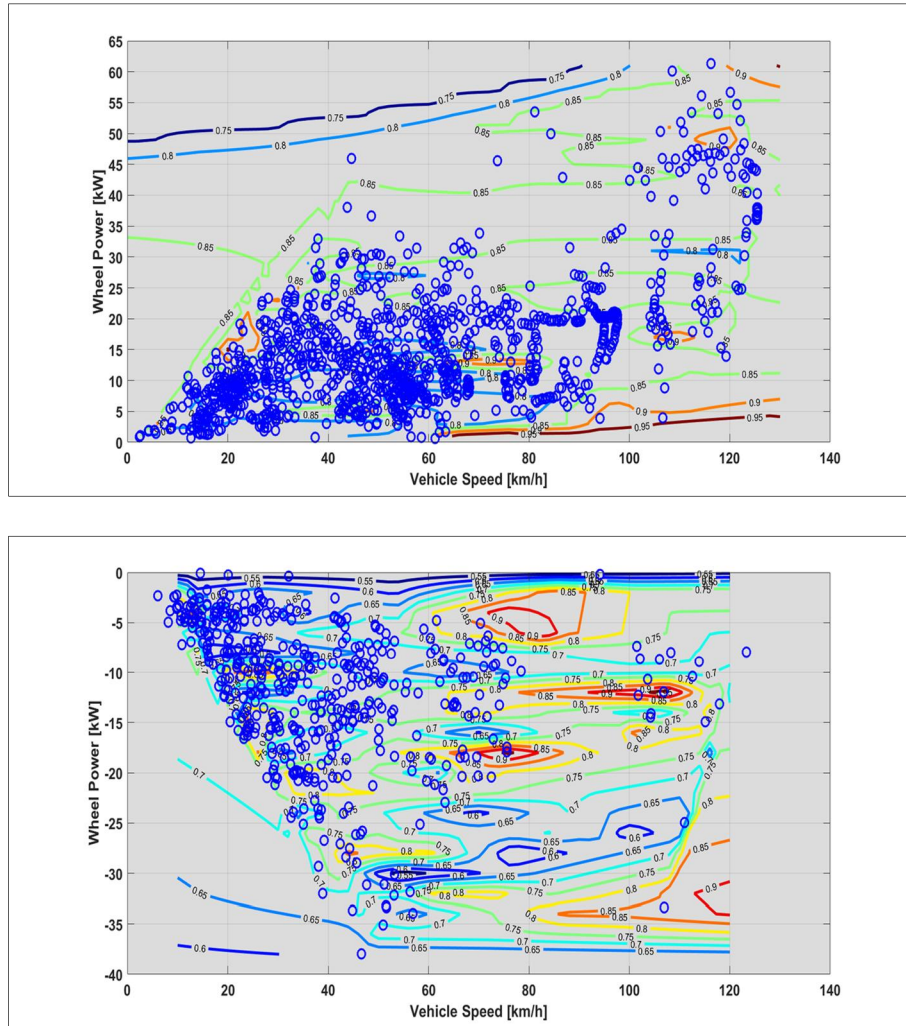


**Figure 81:** Example of efficiency maps generated by the Meta-Model for a PHEV for the electric driving (Top) and the regenerative braking (Bottom)

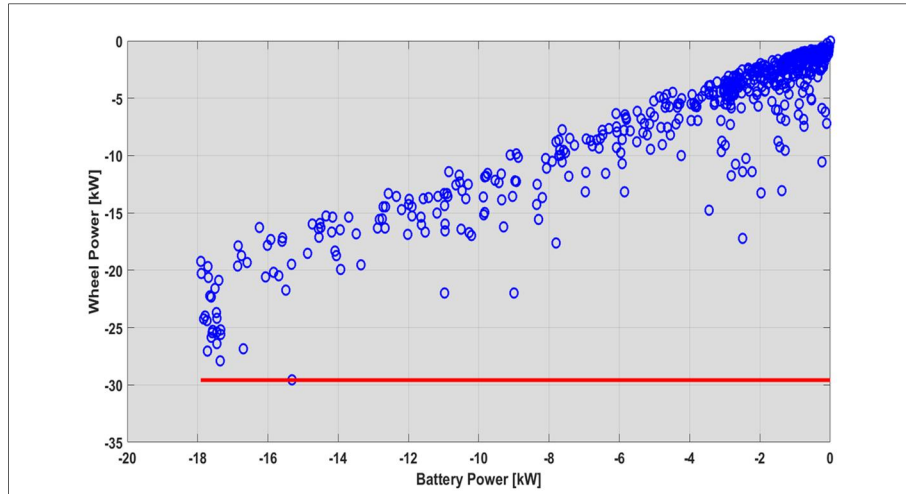


**Figure 82:** Detection of the minimum power recovered during the regenerative braking event

### 3.3.3 Power adsorption from auxiliary components

Inside a passenger car there are many electrical components supplied by the 12 V battery such as the infotainment system, the power electronic, the headlights, etc. In case of hybrid vehicles, all these components are still supplied by the 12V battery, however it is charged by the high voltage battery through a DC/DC converter, allowing the removal of the alternator and consequently reducing the weight of the accessory loads on the ICE. Furthermore, in hybrid cars the high voltage battery supplies the compressor used for the air conditioning and the cooling systems used for the battery thermal management, as illustrated in Figure 83.

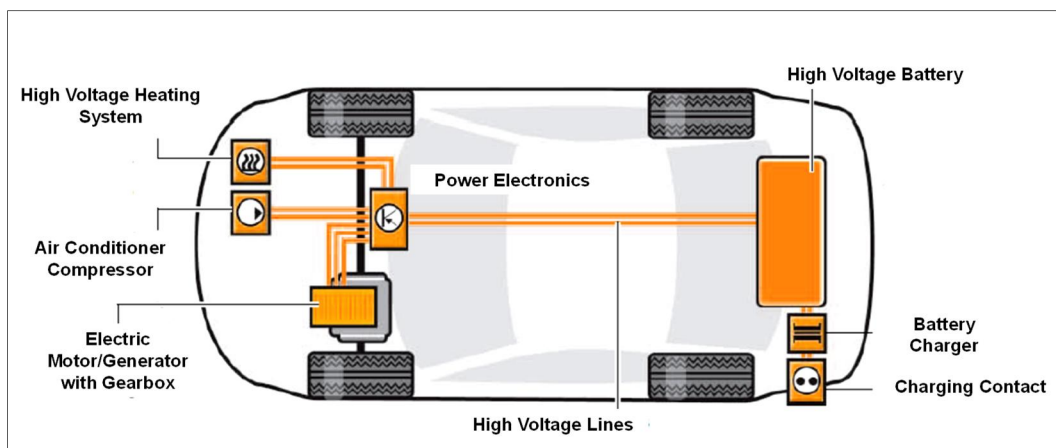


**Figure 83:** Example of high voltage circuit for hybrid cars [35]

During the TA test, as described in Chapter 2, auxiliary components like air conditioning system and the infotainment are off, but it is still necessary to detect correctly the adsorption from power electronics, the cockpit, etc. When the vehicle is running, the high voltage battery supplies both the electric machine and the auxiliaries making difficult a net distinction between the different components. Hence, the simplest way to insulate the auxiliary load is the computation of battery power when the vehicle is stopped along the cycle, where only the auxiliaries weigh on the high voltage battery, as evident from Figure 84.

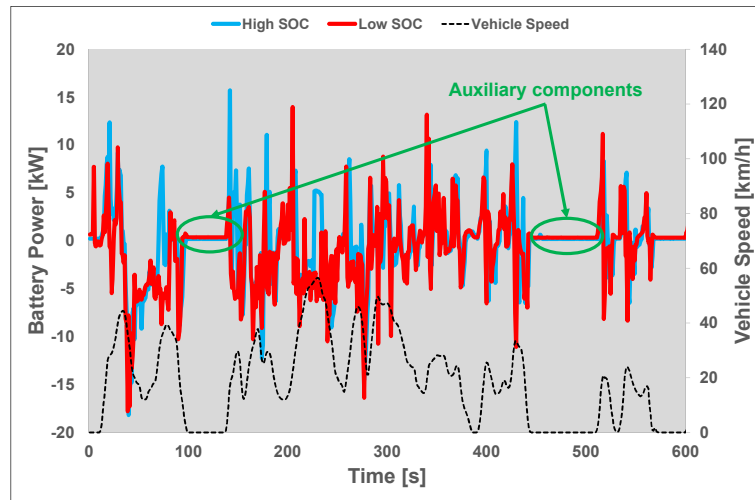


**Figure 84:** Example of detection of power adsorption from auxiliary components for two different test along the Low phase of WLTC cycle

### 3.3.4 E-Boost and Smart Charge identification and modelling

Hybrid powertrains are designed to optimize the efficiency of the ICE increasing the vehicle fuel economy thanks to the flexibility guarantee by the presence of the battery. When the ICE is turned on, the EMS, depending on the load demand, can actuate two different modalities: the E-Boost and the Smart Charge [36].

The modelling of the hybrid status is problematic due to the lack of crucial information such as the engine efficiency map. The simplest way is to insulate and analyze the battery measurements when the ICE is working, trying to identify:

1. When the EMS enables the Smart Charge and E-Boost events;
2. The power adsorbed or released by the high voltage battery.

The code collects all the data available from the different experimental acquisitions, for example it gathers for PHEVs all the acquisition from the CD and CS tests, and it isolates the measurements of current, voltage, SOC, vehicle speed, acceleration and traction power when the engine is working. The gathering of all



the available tests from the same vehicle gives the possibility to analyze the EMS behavior for a wide range of operating conditions.

The actuation logic of the E-Boost/Smart Charge is detected throughout the correlation between the battery SOC, the product between vehicle speed and acceleration and the traction power, because as seen in Chapter 2 they represents the keystone of the EMS logic. Figure 85 shows how the model organizes these parameters in a volume defined by the battery SOC, traction power and product speed/acceleration according to the EMS status, representing with the green points the Smart Charge condition and in magenta the Electric Boost. The Meta-Model splits this volume in different sub-volumes, evaluating the weight of the E-Boost and Smart Charge events within each portion. Therefore, depending on the speed, acceleration, battery SOC and power demand the code goes in the proper volume and it chooses the correct operating condition, comparing the weight of the two modes.

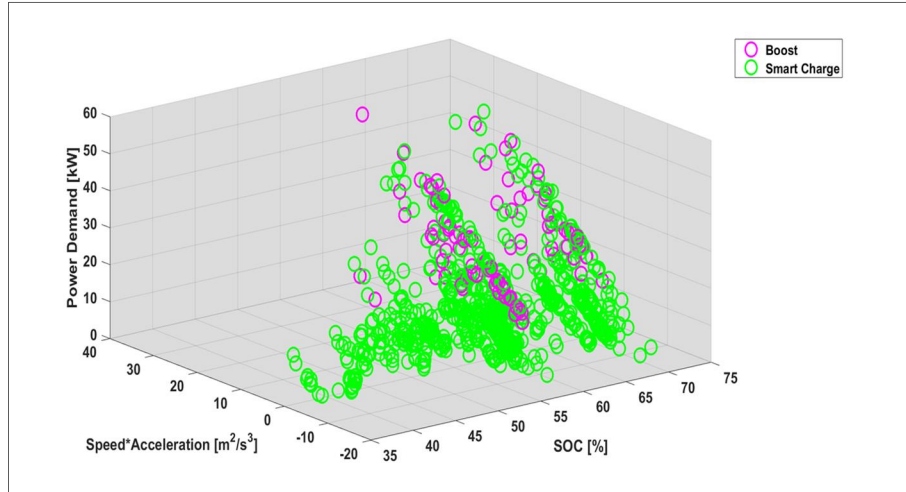


**Figure 85:** Example of measurements organization in hybrid conditions for the E-Boost/Smart Charge detection

The sub-volumes generation employs a similar approach used to design the engine On/Off thresholds, by splitting the operating domain in many bands of different length, representing each of them the edges of a parallelepiped. Each SOC band corresponds the depth of one single sub-volume and it should contain a minimum number of points, as described in Equation 13.

$$N_{SOC,hybrid} = K_{SOC,hybrid} \cdot Input_{freq}$$

**Equation 13:** Definition of the depth of the sub-volume

Where  $N_{SOC, hybrid}$  is the minimum number of points inside the SOC band and  $K_{SOC, hybrid}$  is the multiplicative coefficient of the experimental sampling frequency,



which is equal to 200 for HEVs and PHEVs models. The resulting sub-volume's width is shown in Figure 86.

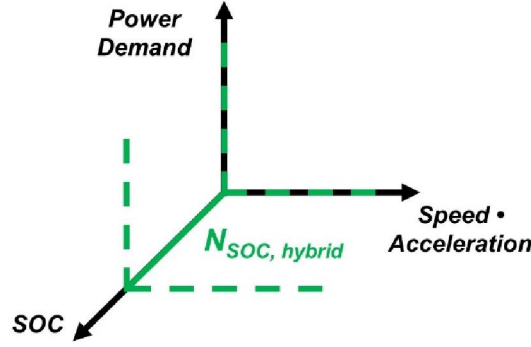


**Figure 86:** Depth of the sub-volume

In Equation 14  $N_{SA, hybrid}$  represents the minimum number of operating points in the speed/acceleration domain, defining the width of the parallelepiped.

$$N_{SA, hybrid} = K_{SA, hybrid} \cdot Input_{freq}$$

**Equation 14:** Definition of the width of the sub-volume

Where  $K_{SA, hybrid}$  is the multiplicative coefficient of the experimental sampling frequency equal to 50 for HEVs and PHEVs. The resulting base of the sub-volume is depicted in Figure 87.

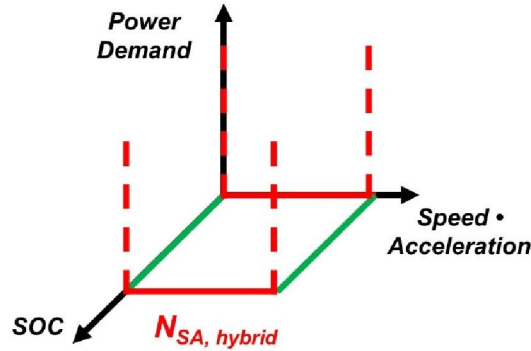


**Figure 87:** Base of the sub-volume

Finally, the Meta-Model computes the height of the sub-volume, which is defined in Equation 15, where  $K_{Pwheel, hybrid}$  is the multiplicative coefficient of the experimental sampling frequency set for HEVs and PHEVs to 200. The complete sub-volume is represented in Figure 88.

$$N_{P_{Wheel,hybrid}} = K_{P_{Wheel,hybrid}} \cdot Input_{freq}$$

**Equation 15:** Definition of the height of the sub-volume

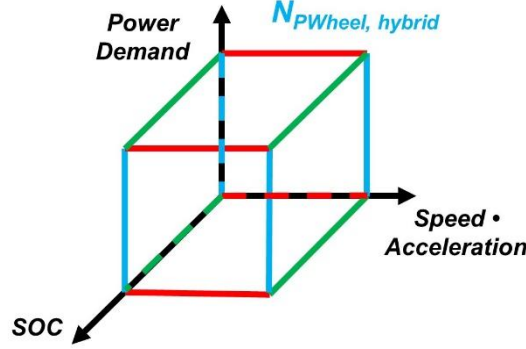


**Figure 88:** Complete sub-volume

This procedure is repeated many times within the operating domain, obtaining as the results the plot in Figure 89.

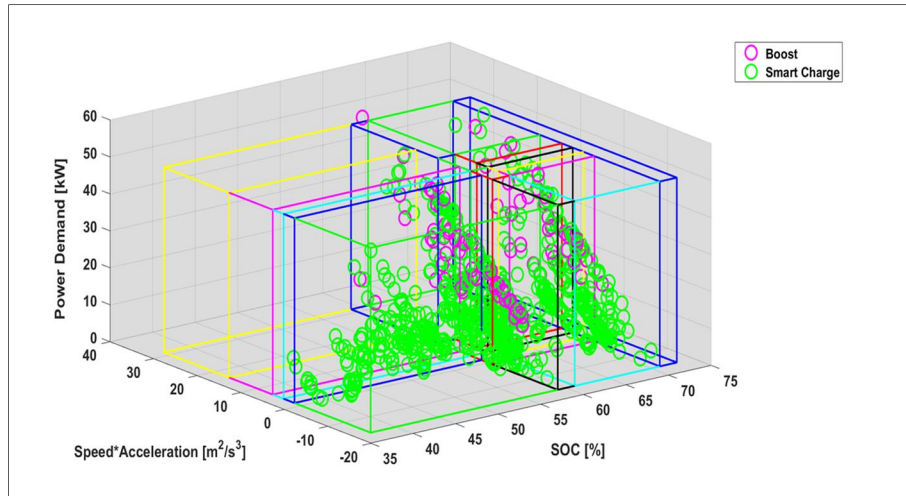


**Figure 89:** Example of the volume splitting for an HEV to identify the E-Boost/Smart Charge modes

The power adsorbed or released by the battery during the Smart Charge and the E-Boost modes for both HEVs and PHEVs is modelled through the design of maps, which correlate the battery SOC and the traction power to the battery power. The surface fitting from scattered data uses the function “*gridfit*” [37]. The examples of Smart Charge and E-Boost surfaces are depicted respectively in Figure 90 and Figure 91 for an HEV test case.

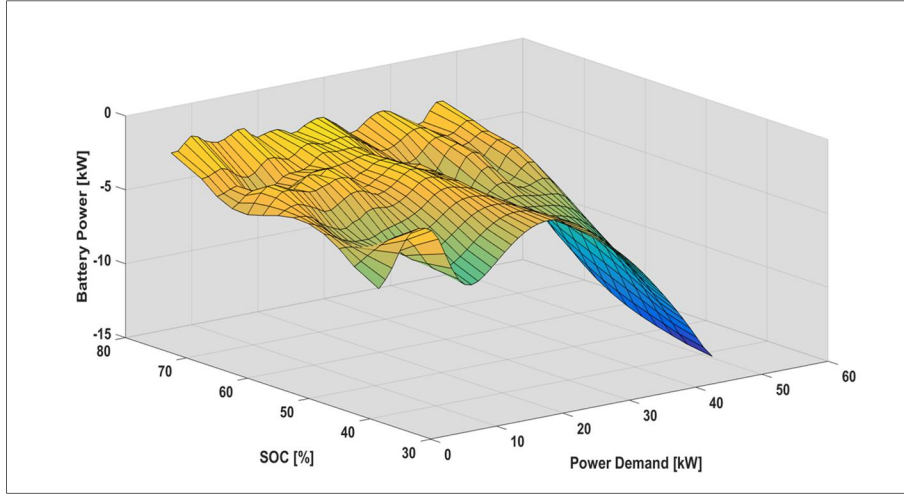


**Figure 90:** Example of Smart Charge map for an HEV vehicle

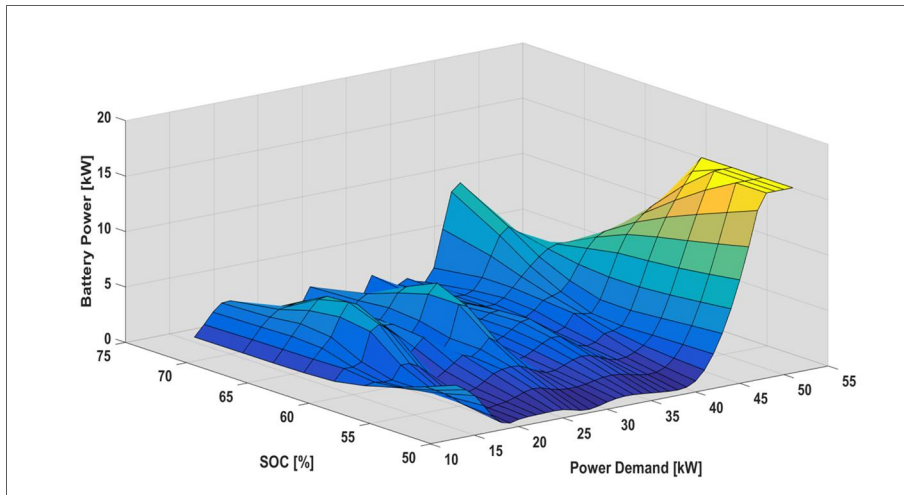


**Figure 91:** Example of E-Boost map for an HEV vehicle

### 3.3.5 Engine power evaluation

The estimation of the engine power is crucial to model the “Cold Start”, the coolant temperature, the engine speed and finally the CO<sub>2</sub> emissions map. The main problem is represented by the lack of information related to the hybrid architecture and to the transmission’s efficiencies.

The engine power evaluation passes through the computation of battery and the motive powers, respectively defined by Equation 10 and Equation 11. The ICE power is obtained as the difference between these two quantities, taking into account the efficiencies of the transmission.

The transmission of a hybrid vehicle can be simplified using the model reported in Figure 92 where:

- $P_{ICE}$  is the power of the thermal engine;
- $P_{Batt}$  is the power of the high voltage battery;
- $\eta_{AVG}$  is the average efficiency of the electric powertrain computed from the maps presented in paragraph 3.3.2;
- $P'$  is the output power from the gear box;
- $P_{Wheel}$  is the traction power;
- $\eta_{Gb}$  is the average efficiency of the transmission assumed equal to 0.90;
- $\eta_{Fd}$  is the final drive average efficiency assumed equal to 0.98.

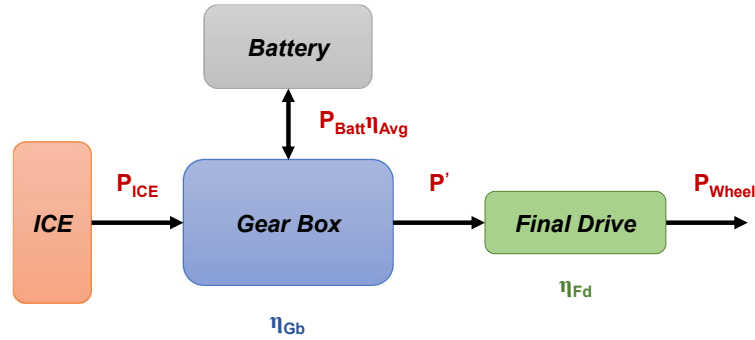


**Figure 92:** Modelling of the hybrid powertrain

The Equation 16 and Equation 17 describe the hybrid transmission.

$$P' = \eta_{Gb} P_{ICE} + P_{Batt} \cdot \eta_{Avg}$$

**Equation 16:** Output power from the gearbox

$$P' = P_{Wheel} / \eta_{Fd}.$$

**Equation 17:** Correlation between the motive power and the gearbox output

The correlation between the engine power and traction is obtained substituting Equation 17 in Equation 16, as reported in Equation 18.

$$P_{ICE} = P_{Wheel} / \eta_{Gb} \cdot \eta_{Fd} - P_{Batt} \cdot \eta_{Avg} / \eta_{Gb}$$

**Equation 18:** Computation of the ICE power

### 3.3.6 Engine coolant temperature modelling

The coolant temperature is modelled using a polynomial empirical relation [38], which correlates the increase of temperature with the engine speed and load, as reported in Equation 19.

$$\Delta\theta(t) = K_1 + K_2 \cdot \omega(t) + K_3 \cdot P_{ICE}(t) + K_4 \cdot \theta(t - t_{resp}) + K_5 \cdot \omega(t)^2 + K_6 \cdot \omega(t) \cdot P_{ICE}(t) + K_7 \cdot \omega(t) \cdot \theta(t - t_{resp}) + K_8 \cdot \theta(t - t_{resp})^2 + K_9 \cdot \omega(t)^3 + K_{10} \cdot T(t - t_{resp}) \cdot \omega(t)^2$$

**Equation 19:** Engine coolant temperature model

Where  $\omega$  is the engine speed,  $P_{ICE}$  is the engine power,  $\theta$  is the coolant temperature and  $t_{resp}$  is the thermal response time of the engine during the transient.

The coefficients  $K_1 \dots K_{10}$  are calibrated along the WLTC cycle using the experimental acquisitions, as shown in Figure 93.

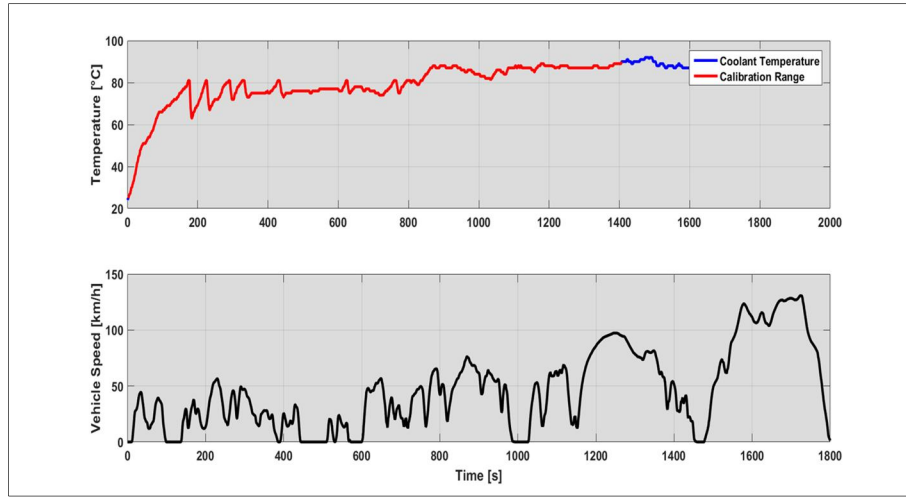


**Figure 93:** Temperature calibration range for a PHEV along the WLTC

The calibration range starts from the beginning of the cycle until the reaching of the temperature value of 90°C, represented by the red line in Figure 93, which corresponds to the standard engine operating condition. These coefficients are used by the Meta-Model to simulate the thermal transient during the NEDC simulation, which is crucial to take into account the effect of “Cold Start” on EMS behavior and consequently on CO<sub>2</sub> emissions.

### 3.3.7 Cold start modelling

The TA procedure requests the vehicle conditioning at constant temperature between 23 and 25°C until the engine coolant and the oil temperature are within  $\pm 2K$  of the temperature of the room. This is necessary to take into account the effect of “Cold Start” during the measurements of CO<sub>2</sub> and pollutants. The “Cold Start” affects both the friction losses and the efficiency of the after-treatment system. In particular, the ECU actuates particular strategies, such as fuel enrichment or stop-start disabling, to accelerate the warm-up of after-treatment systems until the achievement of the light-off temperature. Therefore, the resulting fuel penalty

cannot be neglected. This problem is more emphasized in hybrid vehicles due to the alternation of electric and hybrid driving, making more difficult the engine warm-up.

The modelling of this particular condition requests the analysis of the “Cold Start” impact along the WLTC driving cycle through the observation of the engine enabling along the Low and Medium phases, reported in Figure 94 and Figure 95.

These figures show the engine On/Off status expressed as a Boolean (0 = Off, 1 = On) depending on the engine thermal status. The red line represents the engine behavior during the “Hot Start”, while the blue one the “Cold Start”. For a meaningful comparison the two different engine thermal status were compared considering the same starting SOC, to avoid the superimposition of the battery management. The effect of “Cold Start” can be insulated in the first 100 seconds since the EMS disables the cut-off, as illustrated in Figure 96. When the coolant temperature reaches the threshold of 50 °C the EMS behavior is comparable in both thermal conditions, as evident from the engine status.

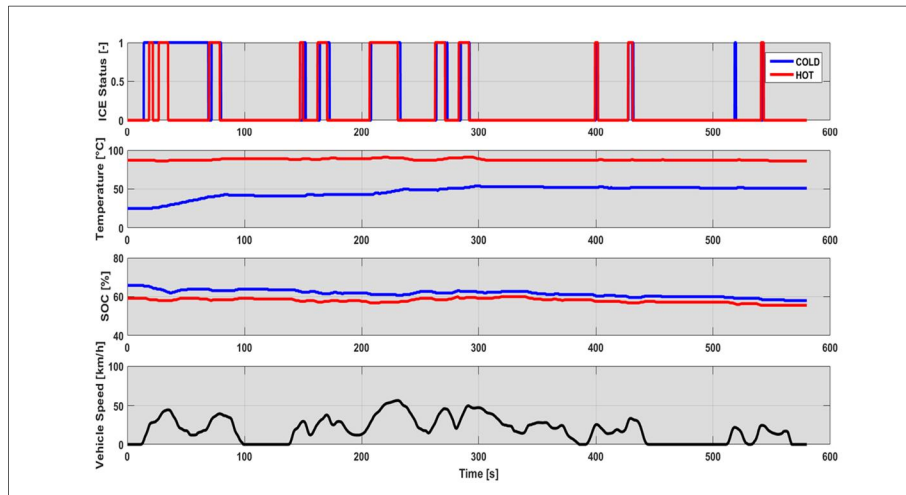


**Figure 94:** Engine status, engine coolant temperature and battery SOC profiles along the WLTC Low phase for an HEV

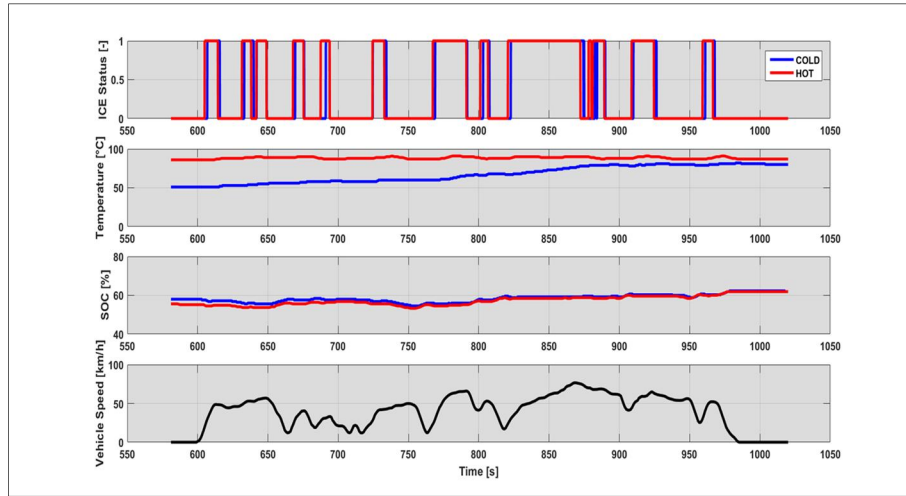


**Figure 95:** Engine status, engine coolant temperature and battery SOC profiles along the WLTC Medium phase for an HEV

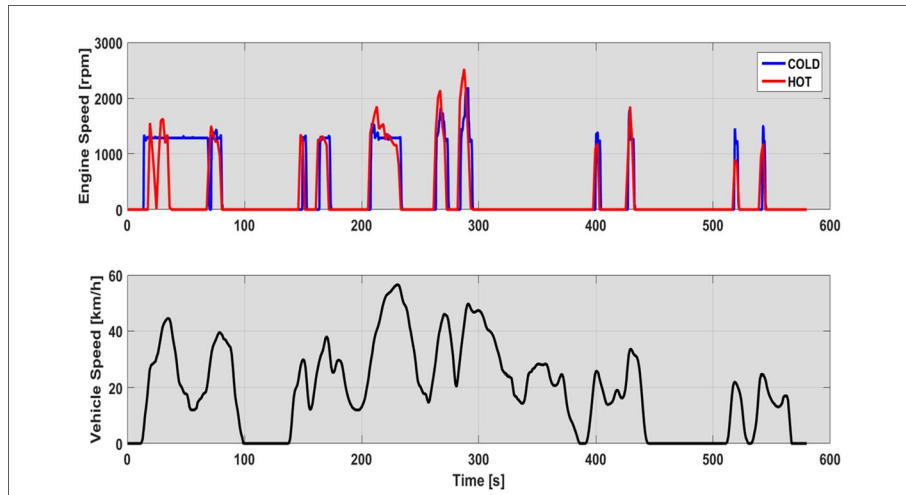


**Figure 96:** Engine speed profile along the WLTC Low phase for an HEV

During this particular situation, the engine enabling is controlled by the coolant temperature and by the motive power, neglecting the battery SOC. Therefore, the ICE power is evaluated as function of the motive power and of coolant temperature, to detect correctly the disabling of the cut-off and to compute the CO<sub>2</sub> emissions, as shown in Figure 96. This approach is adopted for both HEV and PHEVs, since, as shown in Chapter 2, the engine warm-up strategies are comparable. The effect of “Cold Start” is neglected for PHEVs during the CD test, because, as evident from the experimental outcomes, the use of ICE along the NEDC cycle is limited.

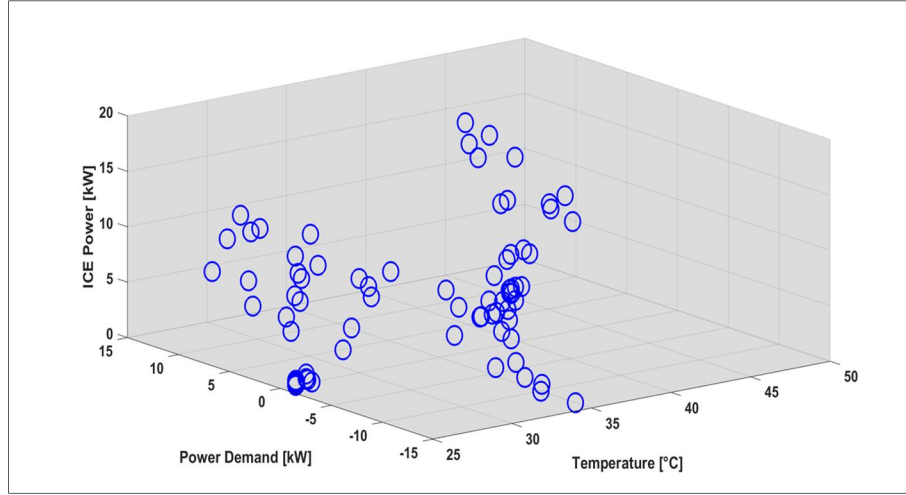


**Figure 97:** Example of “Cold Start” area for an HEV vehicle

The experimental points are fitted using the “*gridfit*” tool to generate a map representative of the engine power during the “Cold Start” as a function of coolant temperature and traction power, as illustrated in Figure 98. The generated map is used by the Meta-Model together with the simulated coolant temperature and the motive power to evaluate the ICE power during the first 100 seconds (assumed as the duration of “Cold Start” event) along the NEDC.

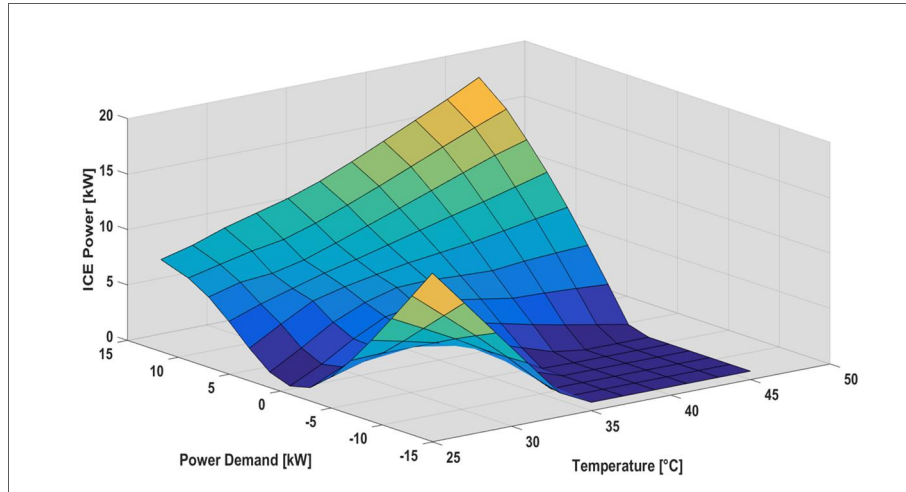


**Figure 98:** ICE power map during the “Cold Start” for an HEV vehicle

Equation 20, using the powertrain efficiencies presented in paragraph 3.3.5, computes the power adsorbed or released during the “Cold Start” event.



$$P_{Batt} = P_{Wheel} / \eta_{Fd} \cdot \eta_{Avg} - P_{ICE} \cdot \eta_{Gb} / \eta_{Avg}$$

**Equation 20:** Battery power computation during the “Cold Start”

### 3.3.8 Engine speed modelling

The engine speed modelling requests the knowledge of various mechanical parameters such as the transmission and the final drive ratios. Moreover, the revolution speed of an ICE is influenced by the thermal status, because at low temperatures the engine rotates at higher speeds due to the mixture enrichment necessary to quicken the engine warm-up. All these information are unknown, so the code should model the engine using the available data and discerning between the “Cold Start” and “Hot Start”.

As explained in paragraph 3.3.7, the code classifies as “Cold Start” all the measurements made in the first 100 seconds and it models the engine speed as a function of three parameters: vehicle speed, motive power and coolant temperature, as reported in Equation 21:

$$\omega_{Cold}(t) = X_{1,Cold} \cdot P_{Wheel}(t) + X_{2,Cold} \cdot v_{Vehicle}(t) + X_{3,Cold} \cdot \theta(t) + X_4$$

**Equation 21:** Modelling of engine speed during the “Cold Start”

Where  $\omega_{Cold}$  is the engine speed during the “Cold Start” event,  $P_{Wheel}$  is the motive power,  $v_{Vehicle}$  is the vehicle speed and  $\theta$  is the coolant temperature. The coefficients  $X_{1,Cold} \dots X_{4,Cold}$  are calibrated using the experimental acquisitions along the WLTC cycle, as shown in Figure 99. This methodology is applied for HEVs and PHEVs.

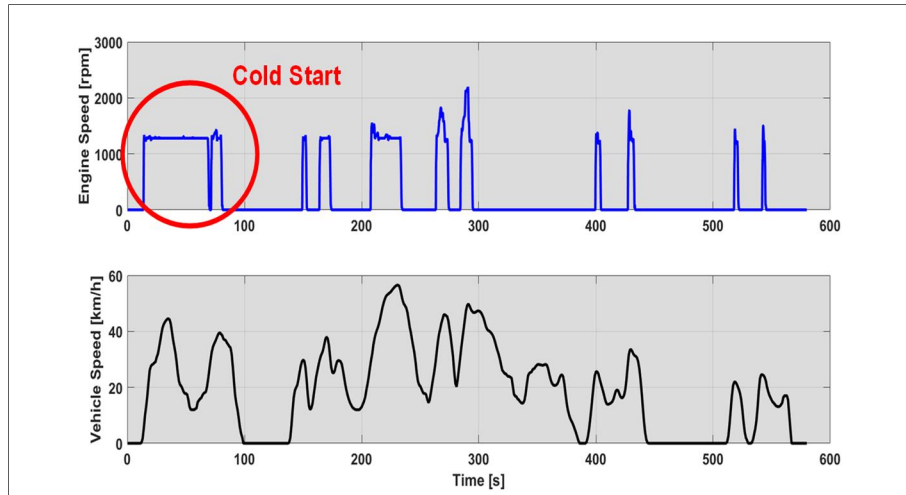


**Figure 99:** Engine speed calibration range for an HEV vehicle

The revolution speed during the “Hot Start” uses the same approach but in this case, the modelling approach does not consider the effect of coolant temperature, as reported in Equation 22.

$$\omega_{Hot}(t) = X_{1,Hot} \cdot P_{Wheel}(t) + X_{2,Hot} \cdot v_{Vehicle}(t) + X_{3,Hot}$$

**Equation 22:** Modelling of engine speed during the “Hot Start”

The coefficients  $X_{1,Hot} \dots X_{4,Hot}$  are calibrated using the experimental engine speed profile along the WLTC cycle.

### 3.3.9 Battery parameters

The simulation of a hybrid powertrain requests the correct modelling of the battery, because its behavior affects the ICE enabling, as seen in Chapter 2. Therefore, the simulation of the battery current along the NEDC cycle can be done using a circuit-based modelling, which represents the battery behavior as an equivalent electrical circuit, needing a limited number of data and a lower computation time than the chemical model at the expense of the result accuracy [39].

The equivalent circuit implemented in the model is illustrated in Figure 100.

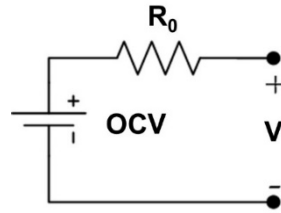


**Figure 100:** Equivalent circuit model of the battery

Where  $OCV$  is the voltage at the battery terminals when no load is applied,  $R_0$  is the internal resistance representative of the Ohm losses inside the battery and  $V$  is the terminal voltage between the battery terminals, correlated between them through the Ohm’s law, shown in Equation 23.

$$V = OCV - R_0 \cdot I$$

**Equation 23:** Ohm’s law

The OCV and the internal resistance vary depending on the load demand, on the temperature and battery SOC. In this case, they are supposed to be constant due to the narrow number of information available.

The detection is done using the measurements of current and voltage along the WLTC cycle, optimizing these two parameters to minimize the error function reported in Equation 24:

$$EF = \sum_{k=1}^N (V_{meas,k} - V_{sim,k})^2$$

Equation 24: Error function

Where  $V_{meas}$  is the measured voltage along the WLTC cycle,  $V_{sim}$  is the simulated voltage,  $EF$  is the quadratic error and  $N$  is the number of sample available from the test [40]. The optimization uses the Nelder-Mead method, implemented inside the function “*fminsearch*” available in the Matlab library. An example of the results obtained from the optimization process is reported in Figure 101, where the blue line represents the experimental voltage and the red one the simulated. The OCV and the internal resistance will be used to compute the battery current along the NEDC in order to evaluate the SOC swing.

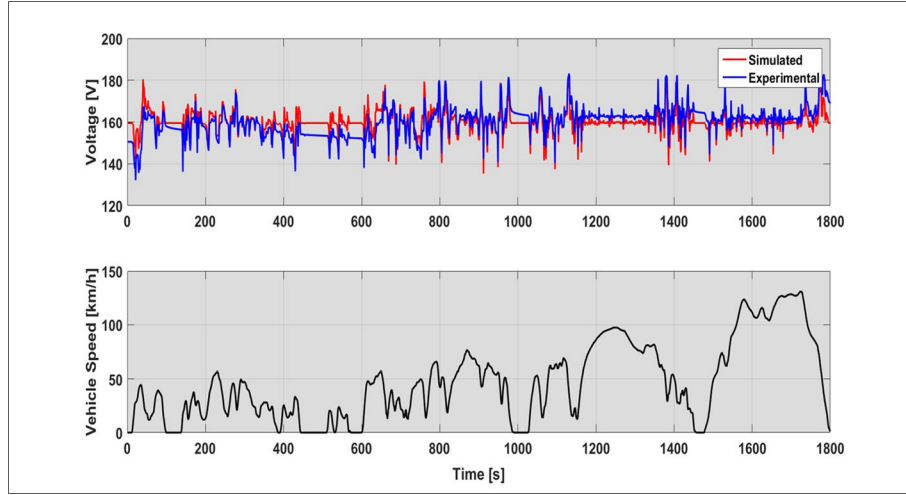


Figure 101: Example of battery parameters optimization along the WLTC cycle for an HEV

### 3.3.10 CO<sub>2</sub> virtual maps

The computation of CO<sub>2</sub> emissions along the NEDC passes through the definition of virtual maps from the experimental measurements. The vehicle operating area of WLTC includes the NEDC one, so the instantaneous measurements are used to build a map representative of the engine fuel rate along the European cycle. Whereas the engine calibration is unique independently from the battery SOC, all the acquisition necessary for the CO<sub>2</sub> TA value are gathered to increase the data population, improving the quality of map fitting.

The map generation, as like the engine speed model, requests the discerning between the “Cold Start” and “Hot Start” due to the different engine calibration. Therefore, the code classifies the engine operating points as “Cold” when the

coolant temperature is below the cat-heating temperature, which is generally reached along the WLTC after 100 seconds. Instead, it categorizes as “Hot” all the other acquisitions. For both cases, each engine operating point, described by the engine speed and torque, is gathered with the correspondent CO<sub>2</sub> value, as illustrated in Figure 102 and Figure 103.

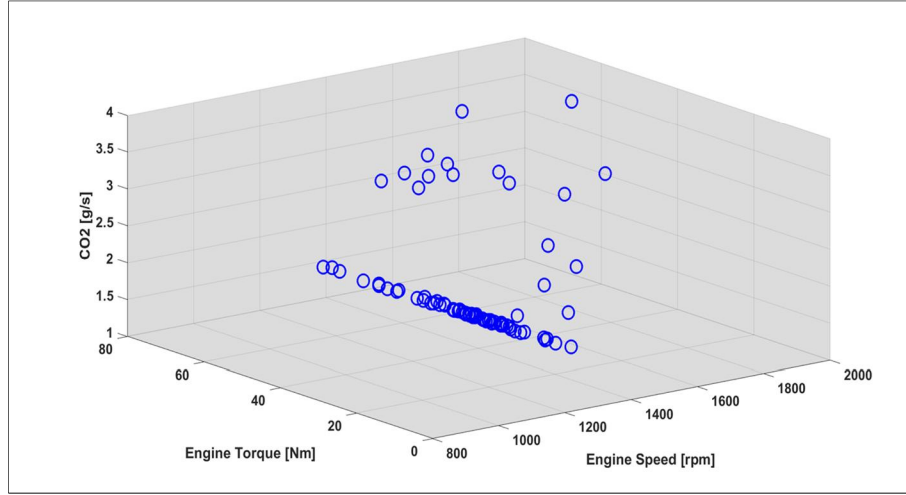


**Figure 102:** “Cold Start” CO<sub>2</sub> emissions as function engine speed and torque for an HEV

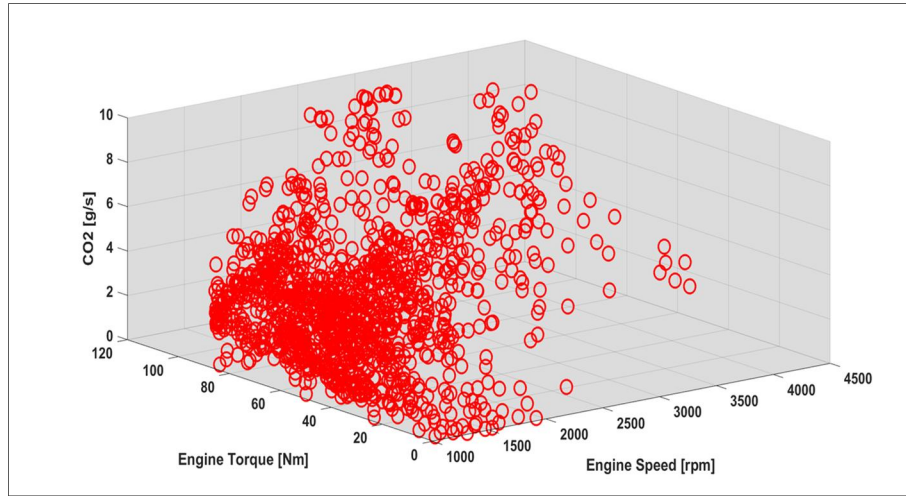


**Figure 103:** “Hot Start” CO<sub>2</sub> emissions as function engine speed and torque for an HEV

The fitting is done applying the least square method using the functions reported in Equation 25 and Equation 26 [41].

$$CO_{2,i,Cold} = C_1 + C_2 \cdot \omega_{i,Cold} + C_3 \cdot T_{i,Cold} + C_4 \cdot \omega_{i,Cold}^2 + C_5 \cdot T_{i,Cold}^2$$

**Equation 25:** CO<sub>2</sub> emissions function during the “Cold Start”

$$CO_{2i,Hot} = D_1 + D_2 \cdot \omega_{i,Hot} + D_3 \cdot T_{i,Hot}$$

**Equation 26:** CO<sub>2</sub> emissions function during the “Hot Start”

The resulting maps, which will be used interpolating the simulated engine speed and torque along the NEDC obtaining the resulting instantaneous value, are illustrated in Figure 104 and Figure 105.

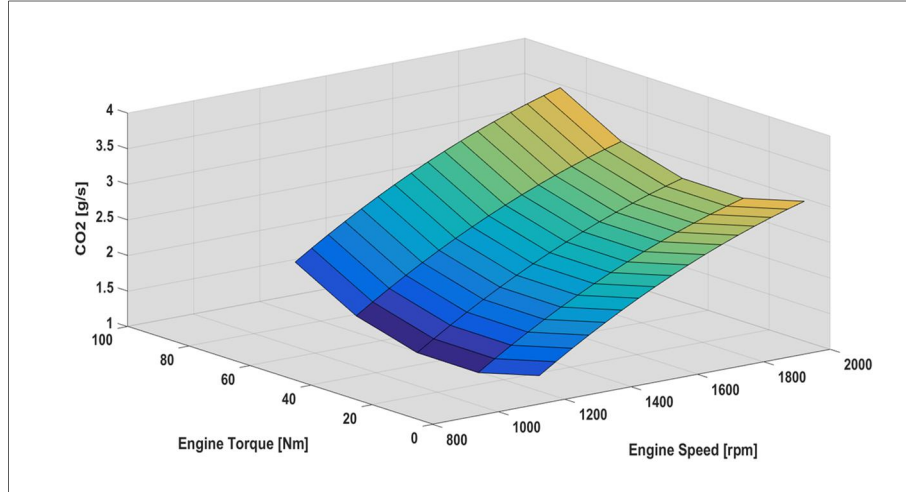


**Figure 104:** Example of “Cold” map for an HEV

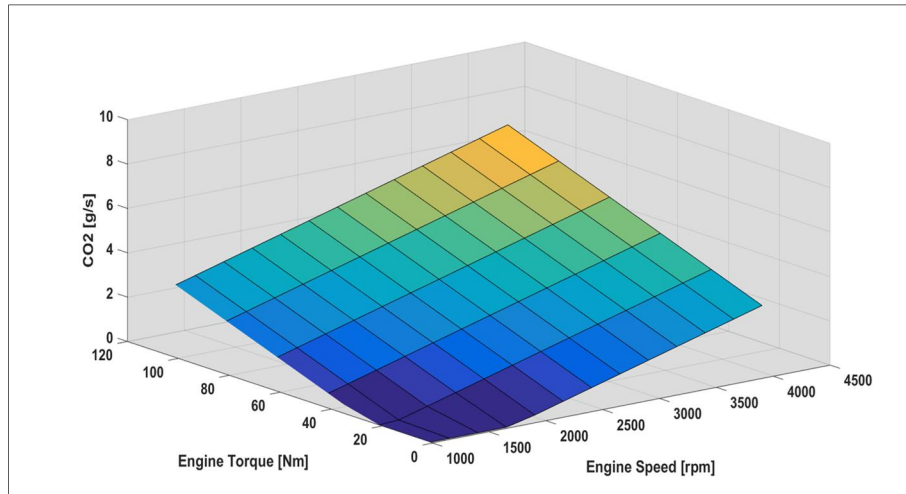


**Figure 105:** Example of “Hot” map for an HEV

## Chapter 4

# Meta-Model validation

### 4.1 Introduction

This chapter will present the meta-model validation based on the measurements illustrated in Chapter 2 for the Yaris Hybrid and the Golf GTE. The modelling of a hybrid architecture passes through the correct simulation of different operating parameters such as the engine enabling, the battery SOC, the coolant temperature and the engine speed. Each of them has an important weight on the CO<sub>2</sub> TA value.

In the first part, the validation of the Yaris Hybrid will be presented considering the two different initial levels of battery SOC, as presented in Chapter 2. The focus is the correct detection of the K-Factor and the simulation of the instantaneous CO<sub>2</sub> emissions, which together provides the TA value.

In the second part, the predictive capabilities of the Meta-Model will be proved the Golf GTE, considering both the CD and the CS tests. The keystone is represented by the correct detection of the distance travelled in electric drive conditions and on the simulation of the instantaneous CO<sub>2</sub> emissions during the CS test along the NEDC cycle.

### 4.2 The Yaris Hybrid test case

The validation of the Meta-Model, as presented in Chapter 2 and Chapter 3, requests the simulation of at least two NEDC cycles considering different initial values of battery SOC, which are necessary for the estimation of the K-Factor. The first part of this paragraph will present the main achievements obtained considering the battery fully charged at the beginning of the cycle, than the second one will

introduce the discharged battery case. Finally, the comparison between the simulated and experimental CO<sub>2</sub> and K-Factor will be shown.

#### 4.2.1 High SOC case

This section will present the validation of the Meta-Model considering the high voltage battery fully charged at the beginning of the NEDC cycle together with the “Cold Start” effect.

The estimation of the CO<sub>2</sub> emissions from a HEV passes through the detection of the battery SOC trend and of the ICE On/Off strategy. Figure 106 shows the engine enabling, the battery power and the SOC profiles along the urban phase of the NEDC cycle, comparing the experimental and the simulated cases, depicted respectively by the green and red lines.

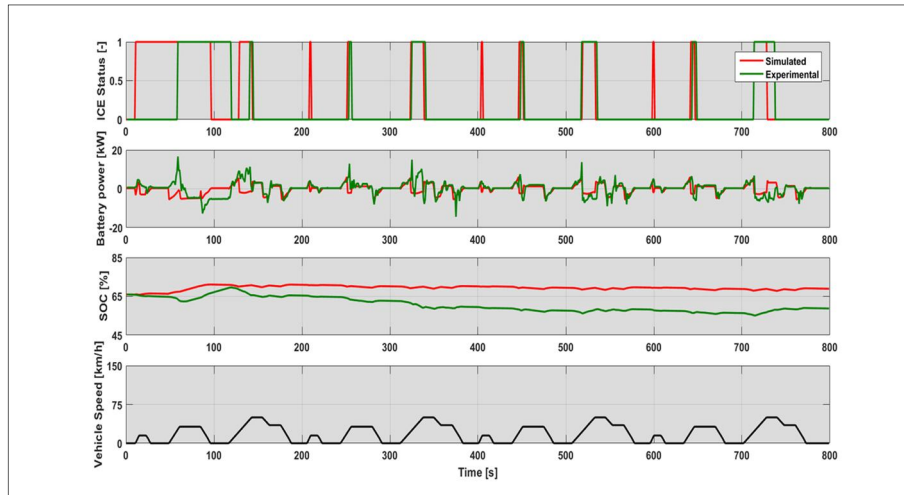


**Figure 106:** Yaris Hybrid validation - Powertrain behavior along the ECE cycle for the High SOC case

The Meta-Model reproduces fairly well the EMS along the Urban Driving Cycle (UDC or ECE), matching the experimental engine ignitions. Nevertheless, the simulation generates three fake ignitions with a time duration smaller than 3 seconds at 200, 400 and 600 seconds. Another important aspect is the simulation of the “Cold Start”, which shows how the code moves up the engine ignition respect to the reference case, affecting the CO<sub>2</sub> emissions and the integral of the battery current.

Figure 107 illustrates the EMS simulation along the Extra Urban Driving cycle (EUDC). In this case, the Meta-Model simulates correctly the EMS behavior, reproducing the proper engine actuation and the enabling of Smart Charge event, as evident from the SOC trend, which increases during this cycle portion. The final difference between the simulated and experimental battery SOC is around 5%, demonstrating the capabilities of the model to detect with good accuracy the

powertrain behavior and the battery operating parameters such as the OCV and the internal resistance, which are fundamental for the correct prediction of the current, needed for the K-Factor computation.

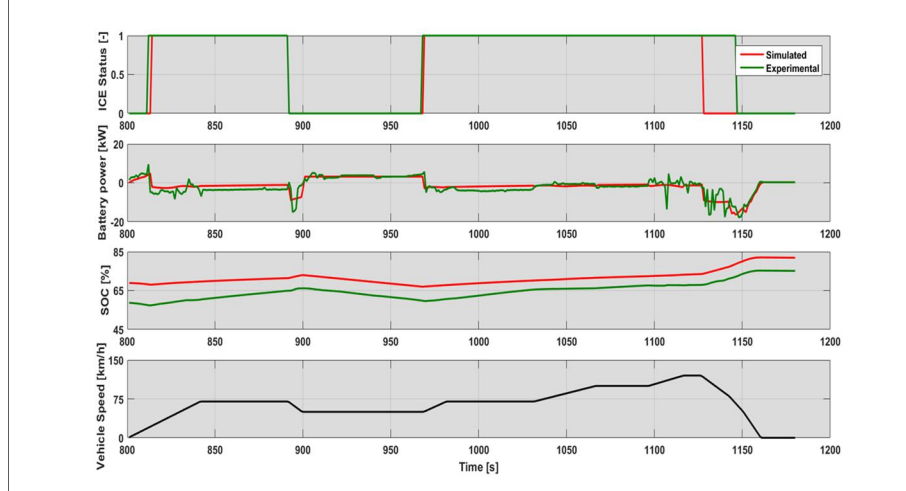


**Figure 107:** Yaris Hybrid validation - Powertrain behavior along the EUDC cycle for the High SOC case

In parallel with the EMS simulation, the code should simulate the engine thermal behavior, because, as explained in Chapter 2 and 3, it influences the engine enabling along the cycle, in particular at the beginning where the ECU actuates specific strategies to quicken the after-treatment warm-up. The comparison between the two profiles is reported in Figure 108, which highlights the same inaccuracy problems remarked in Figure 106. In particular, it is evident the move up of the engine ignition at the beginning of the cycle compared to the experimental case. However, the Meta-Model is able to simulate after all correctly the temperature trend on the NEDC, showing a maximum deviation of 7°C between the reference and the simulated.

Together with the EMS behavior and coolant temperature, the Meta-Model should reproduce with a good accuracy the engine speed, which is fundamental both for the coolant temperature simulation, as illustrated in Chapter 3, and for the computation of instantaneous CO<sub>2</sub> emissions. The comparison between the experimental and simulated revolution profiles is reported in Figure 109. The engine speed profile reflects the issues highlighted for the EMS detection and for the coolant temperature, since it stresses the problems of fake ignitions and of the “Cold Start” strategy advancing. Nevertheless, the developed model is able to simulate correctly the expected engine speed profile for the eCVT transmissions.



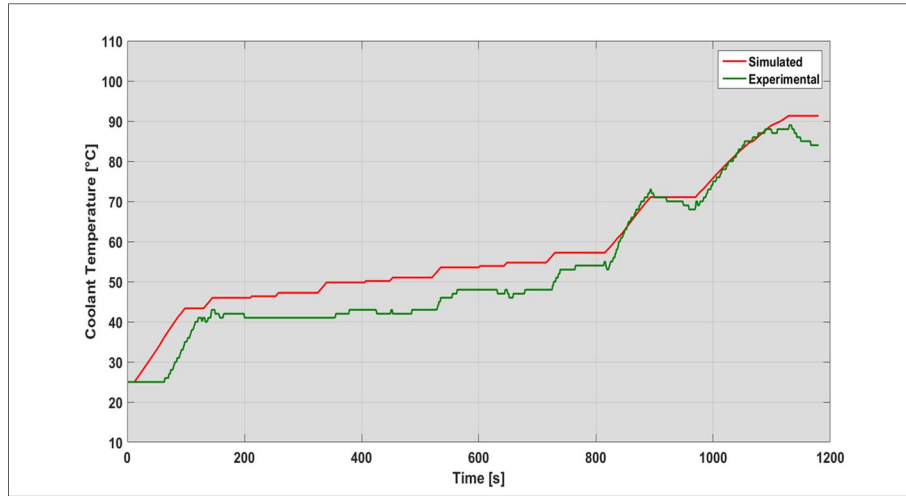


**Figure 108:** Yaris Hybrid validation - Coolant temperature profile along the NEDC cycle for the High SOC case

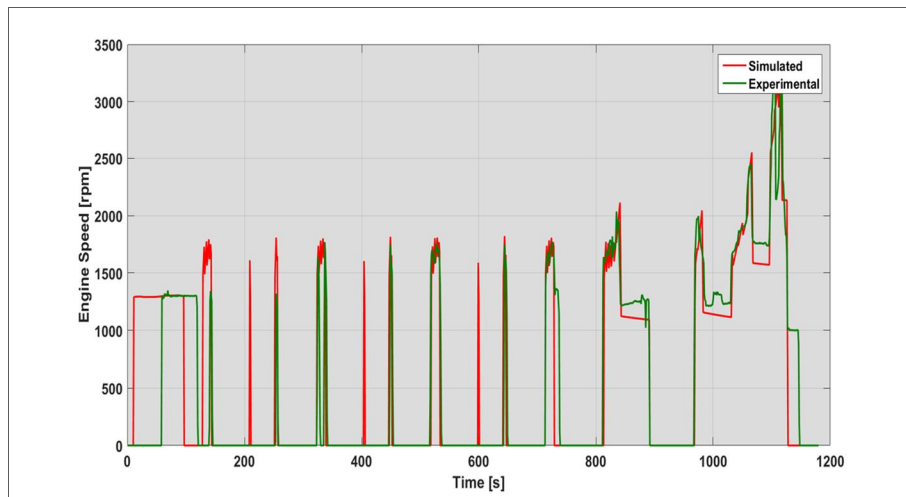


**Figure 109:** Yaris Hybrid validation - Engine speed profile along the NEDC cycle for the High SOC case

The combination of EMS, coolant temperature and engine speed simulations produces the instantaneous and cumulated CO<sub>2</sub> profiles reported respectively in Figure 110 and Figure 111. Figure 110 makes in evidence all the issues highlighted for the EMS simulation. In addition to these aspects, the evaluation of instantaneous emissions is careless at the steady state portions at 70 km/h, observing a significant underestimation of the instantaneous emissions. Figure 111 underlines the overestimation of the CO<sub>2</sub> emissions along the urban driving cycle, due to the “Cold Start” simulation and of the presence of some fake ignitions. The final error on

cumulated CO<sub>2</sub> emissions is around 2.7 % corresponding to a difference of 2.17 g/km.

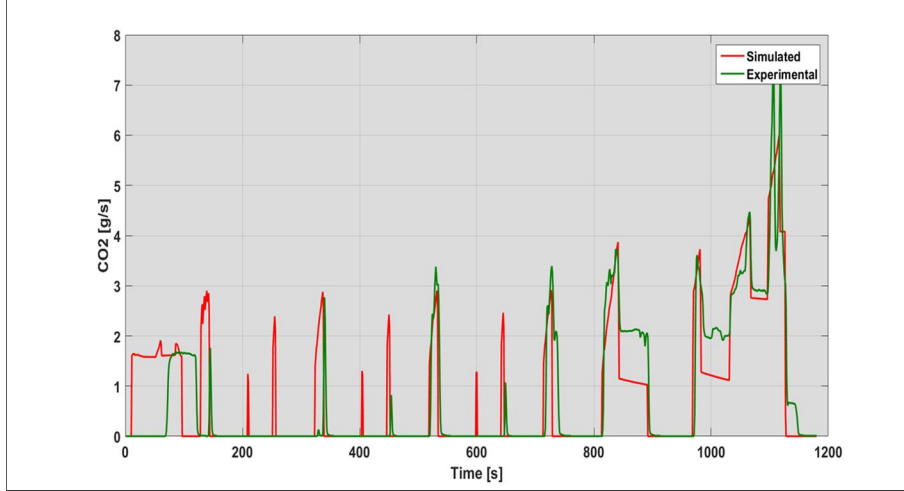


**Figure 110:** Yaris Hybrid validation - Instantaneous CO<sub>2</sub> emission profile along the NEDC cycle for the High SOC case

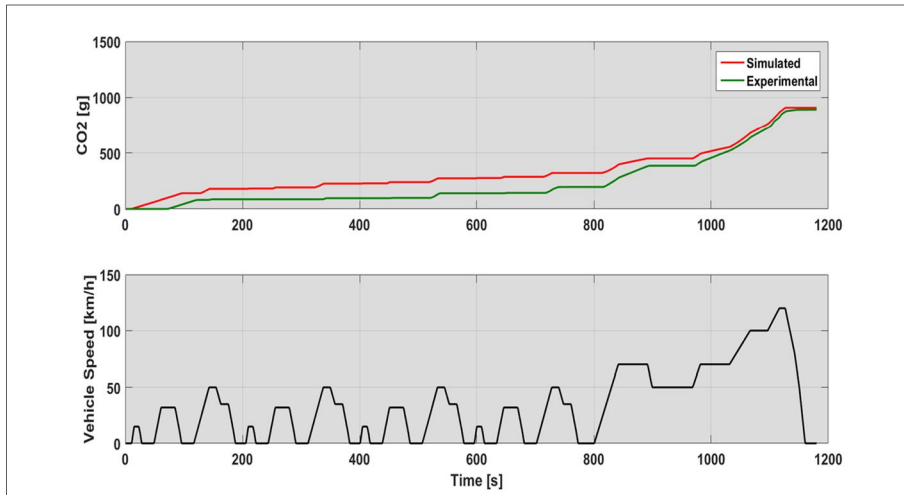


**Figure 111:** Yaris Hybrid validation - Cumulated CO<sub>2</sub> emissions along the NEDC cycle for the High SOC case

#### 4.2.2 Low SOC case

This paragraph will illustrate the principal results considering the high voltage battery completely discharged at the beginning of the cycle.

The validation protocol is the same adopted for the previous case, focusing on the evaluation of the correct engine enabling, on the simulation of battery power and consequently on the evolution of the SOC trend, as shown in Figure 112 and

Figure 113. Along the urban cycle, the Meta-Model is able to reproduce correctly the EMS strategy, matching correctly the engine ignitions and consequently the SOC trend. Similarly to the high SOC case, there is the presence of three fake ignition, characterized by a negligible duration at 200, 400 and 600 seconds. The simulation of the “Cold Start” in this case happens in the correct interval of time. In the end, the simulated EMS actuates always the Smart Charge event as confirmed by the battery power profile and by the SOC trend, demonstrating the correct strategy detection made along the WLTC cycle. Whereas, along the EUDC cycle there are no significant differences between the experimental and simulated EMS behavior, confirming always the actuation of the Smart Charge event, as highlighted by the SOC trend.

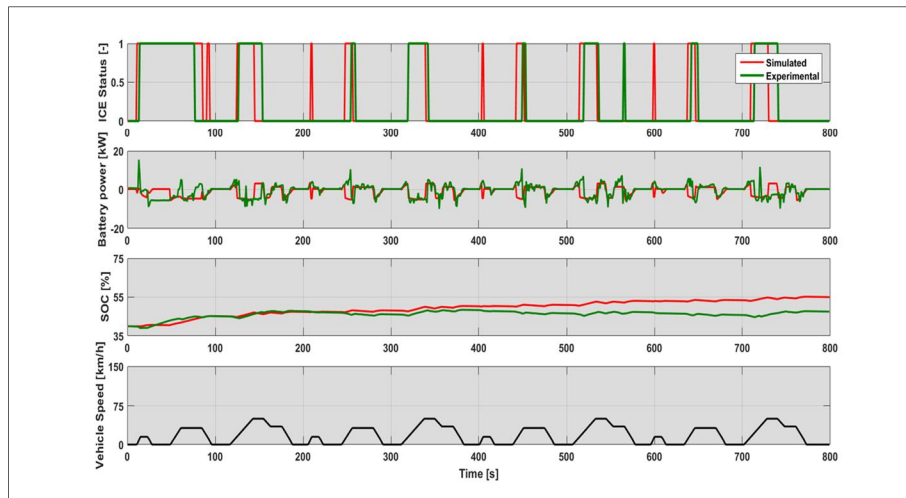


**Figure 112:** Yaris Hybrid validation - Powertrain behavior along the ECE cycle for the Low SOC case

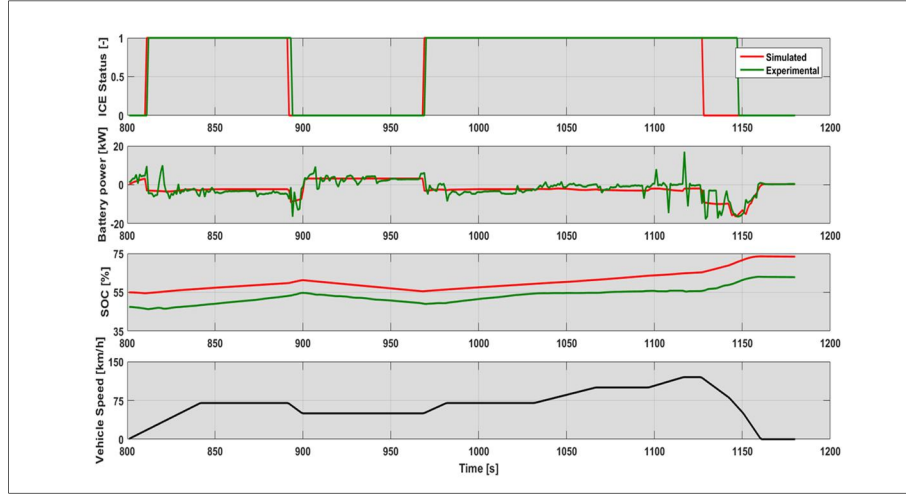


**Figure 113:** Yaris Hybrid validation - HEV validation: powertrain behavior along the EUDC cycle for the Low SOC case

The comparison between the simulated and experimental coolant temperature profiles is reported in Figure 114, showing the good predictive capabilities of the Meta-Model with a maximum deviation of 7°C compared to the experimental case. The divergence along the cycle does not represent a big issue, because the crucial part is represented by the warm-up phase, which influences the EMS and the engine calibration switching. Therefore, focusing on the first 100 seconds it is evident the good accuracy of the model to simulate the engine warm-up and its duration.

Finally, Figure 115 illustrates the engine speed profile along the NEDC cycle, confirming the good accuracy of the model.

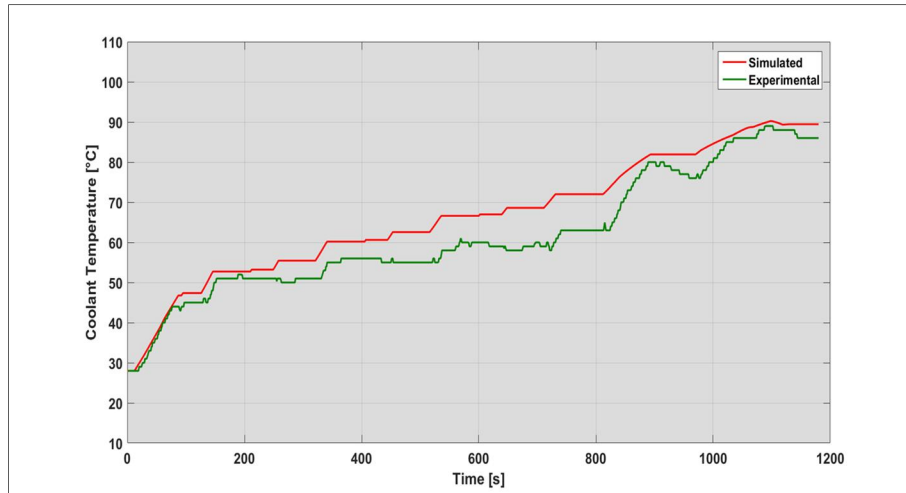


**Figure 114:** Yaris Hybrid validation - Coolant temperature profile along the NEDC cycle for the Low SOC case

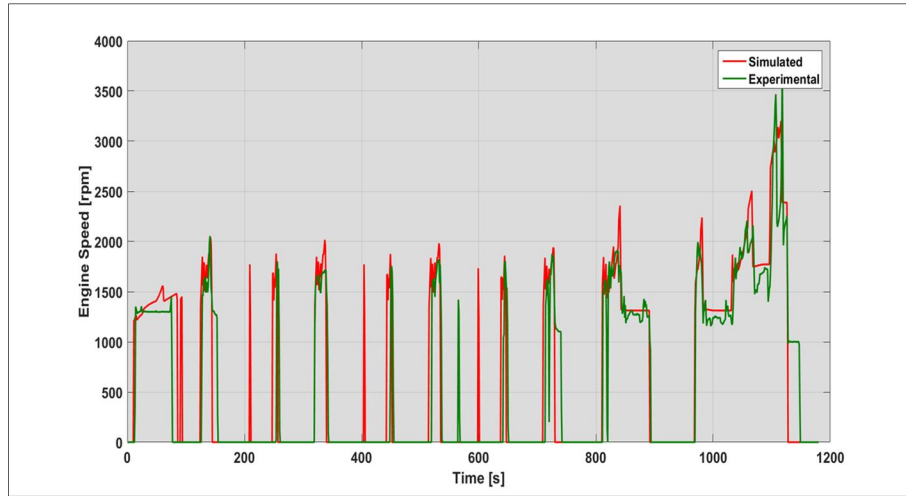


**Figure 115:** Yaris Hybrid validation - Engine speed profile along the NEDC cycle for the Low SOC case

The instantaneous and the cumulated CO<sub>2</sub> profiles are reported respectively in Figure 116 and Figure 117, highlighting the underestimation of 0.5 g/s during the steady state portions at 70 km/h during the extra-urban driving portion, likely the High SOC case. However, the accuracy during the urban driving cycle especially at the “Cold Start” is satisfactory, considering the limited number of available data for the simulation. The cumulated CO<sub>2</sub> profiles confirms the good accuracy of the simulation, showing a slight overestimation during the urban phase, leading to an error of 4.7% or 4 g/km on the final value.

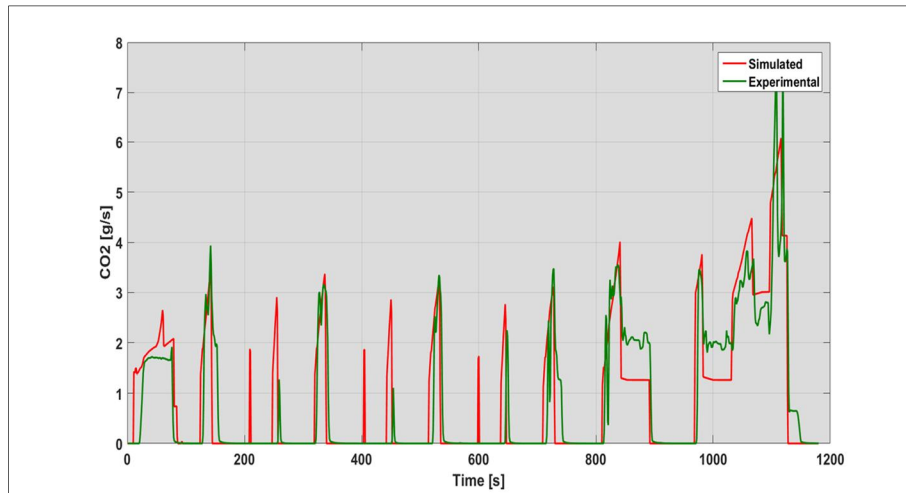


**Figure 116:** Yaris Hybrid validation - Instantaneous CO<sub>2</sub> emission profile along the NEDC cycle for the Low SOC case

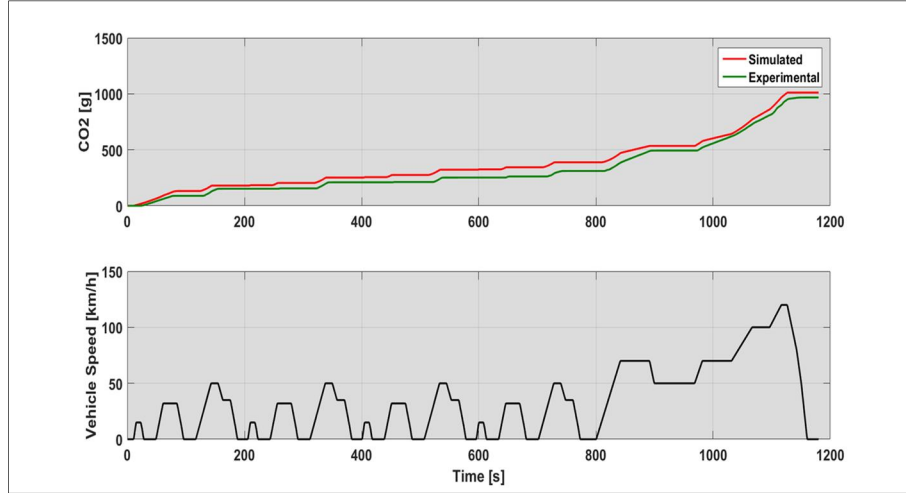


**Figure 117:** Yaris Hybrid validation - Cumulated CO<sub>2</sub> emissions along the NEDC cycle for the Low SOC case

### 4.2.3 CO<sub>2</sub> Type approval value for the Yaris Hybrid

As explained in Chapter 2, the evaluation of the TA CO<sub>2</sub> requests the correction of the single test emissions value in order to take into account the fuel penalty due to the battery recharge through the ICE. The Meta-Model produces per each NEDC simulation a cumulated CO<sub>2</sub> value and an integrated value of battery current, representative of the battery energy balance. The validation of the code focuses on the comparison between the experimental and simulated K-Factor and TA CO<sub>2</sub>.

Figure 118 shows the comparison between the experimental and simulated curves for the Toyota Yaris Hybrid case. The red dashed line represents the simulated curve, obtained by interpolating the model results (represented by the star markers, than the green represents the experimental one). It is evident that the integral of simulated currents are divergent respect to the experimental values. This results is due to the longer charging of the battery made by the simulated vehicle compared to the reference case, which lead to a higher CO<sub>2</sub> emissions. However, the Meta-Model is able to match the EMS behavior on the NEDC since the two straight lines are parallel, as demonstrated by the comparison of K-Factors presented in Table 14.

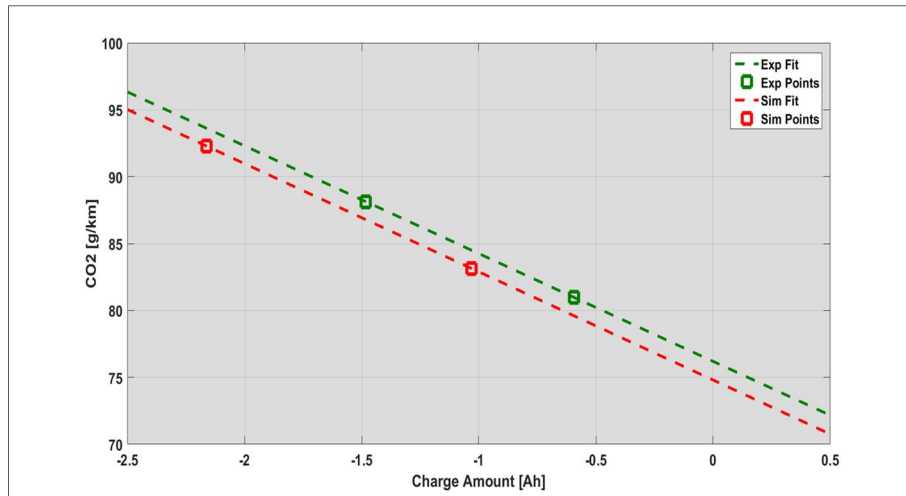


**Figure 118:** Yaris Hybrid validation – K-Factor

**Table 14:** Yaris Hybrid validation – Comparison between the experimental and simulated K-Factor

	Simulated	Experimental
<b>K Factor [g/(km•Ah)]</b>	-8.09	-8.06

The error between the experimental and simulated K-Factor is around 3%, which can be considered as a satisfactory achievement, since the limited number of available informations.

The comparison between the experimental and simulated TA CO<sub>2</sub> values is reported in Figure 119 and summarized in Table 15, showing an underestimation of -1.8% corresponding to a difference of 1.4 g/km.

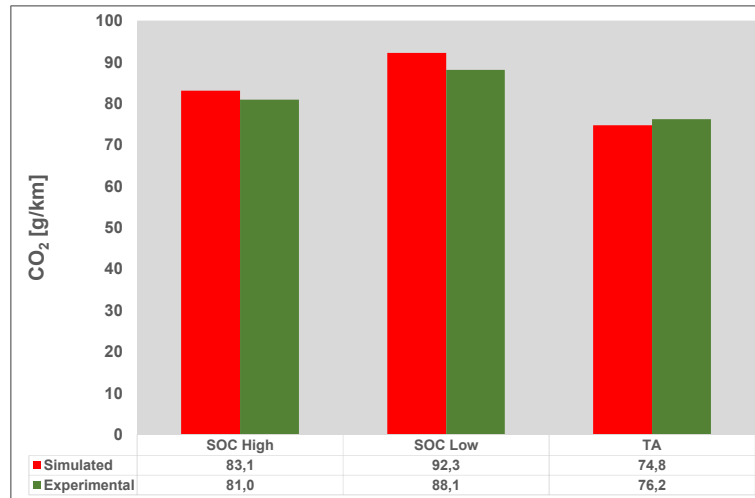


**Figure 119:** Yaris Hybrid validation - Comparison between the experimental and simulated CO<sub>2</sub> emissions along the NEDC

**Table 15:** Yaris Hybrid – Comparison between the experimental and simulated CO<sub>2</sub> TA values

	Simulated	Experimental
CO <sub>2</sub> [g/km]	74.8	76.2

### 4.3 The Golf GTE test case

The evaluation of the TA CO<sub>2</sub> requests for PHEVs two different tests performed respectively in CD and CS, as explained in Chapter 2 and 3. Therefore, the Meta-Model should be able to simulate the EMS behavior along the NEDC cycle for the two opposite conditions in order to compute correctly the CO<sub>2</sub> emissions for both cases and the distance travelled in electric mode. The first part will illustrate the model validation during the CD test, then the second part will present the CS case, considering as test case the Golf GTE presented in Chapter 2.

#### 4.3.1 The charge depleting case

Like the HEVs case, the model validation is focused on the correct detection of the engine enabling strategy and on the correct computation of the battery SOC trend. However, in this case the impact of “Cold Start” and consequently the simulation of coolant temperature during the CD simulation are neglected, since the vehicle as demonstrated in Chapter 2 travels for most of the time in electric mode along the NEDC. Figure 120 shows the comparison between the simulated EMS versus the experimental, represented respectively in red and green, along the first



of the four NEDC repetitions, focusing on the engine On/Off detection, battery power and SOC profile.

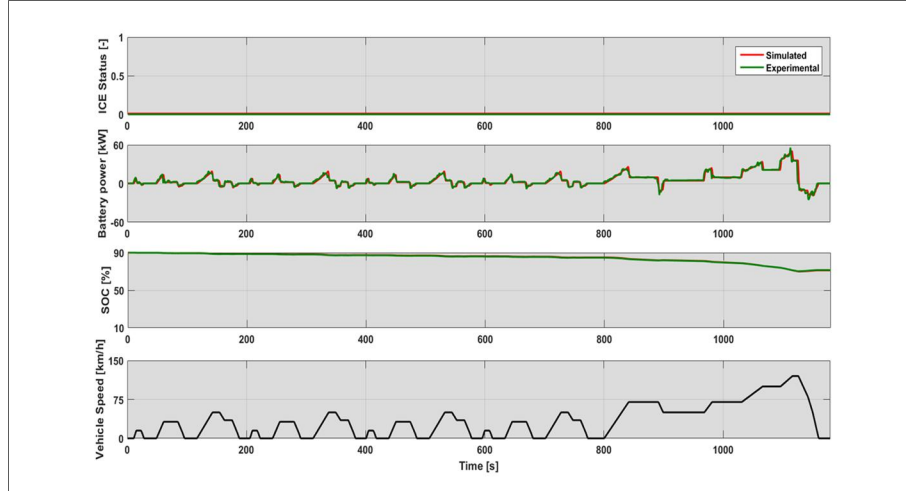


**Figure 120:** Golf GTE validation - Powertrain behavior along the first NEDC cycle during the CD test

Figure 120 highlights the good predictive capabilities of the Meta-Model, pointing out the capability to predict correctly the engine actuation and the evolution of battery SOC. The correct simulation of battery SOC trend is due off course on the proper detection of EMS behavior but also on the correct modelling of the powertrain efficiencies during the electric drive and the regenerative braking, as confirmed by the battery power profile. Figure 121 and Figure 122 represent the powertrain behavior along the second and third repetition, confirming the outcomes presented for the first NEDC.

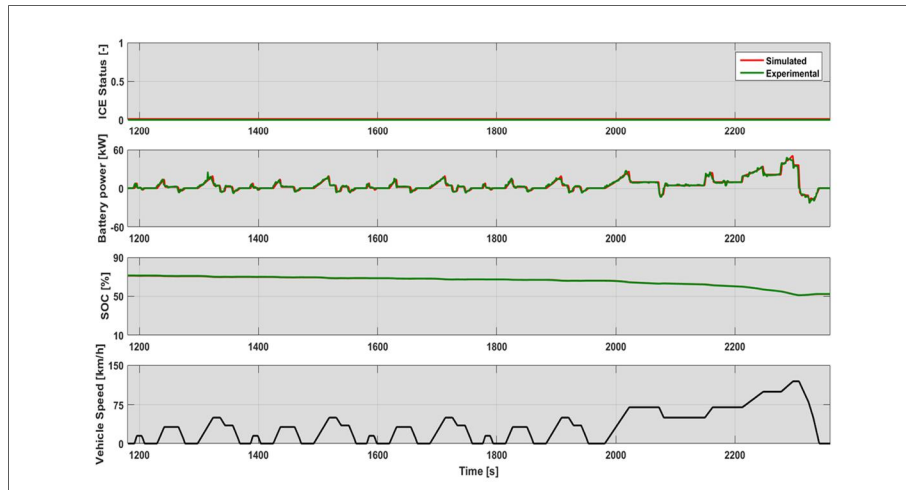


**Figure 121:** Golf GTE validation - Powertrain behavior along the second NEDC cycle during the CD test

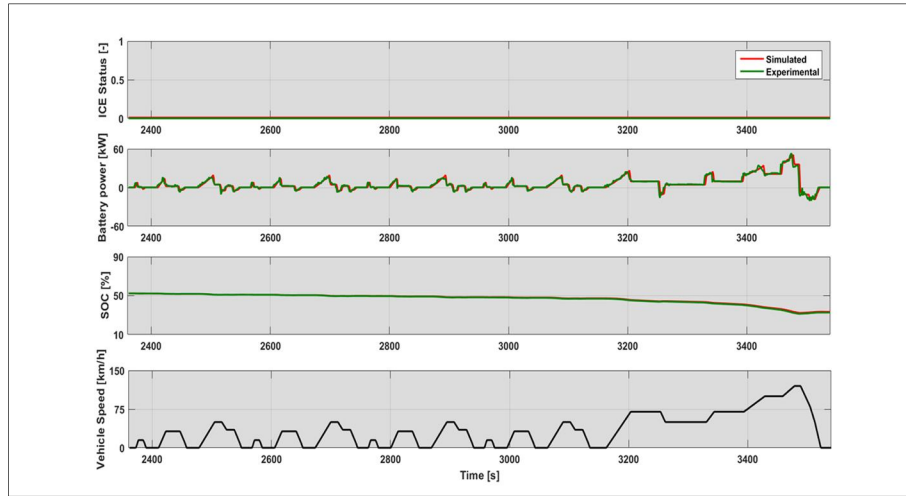


**Figure 122:** Golf GTE validation - Powertrain behavior along the third NEDC cycle during the CD test

At the end of fourth NEDC, the engine is turned on since the battery reaches the admissible SOC limit, as shown in Chapter 2. As depicted in Figure 123, the model is able to detect correctly the ignition event with an advance of 15 seconds, with a negligible impact on the estimation of electric distance.

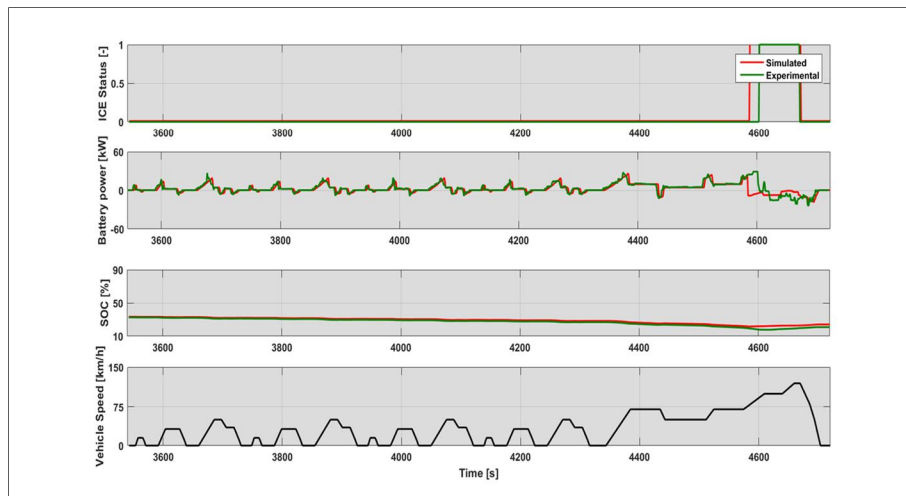


**Figure 123:** Golf GTE validation - Powertrain behavior along the fourth NEDC cycle during the CD test

The comparison between the simulated and experimental engine speed profile is reported in Figure 124, confirming the good predictive capabilities of the model also for DCT transmissions.

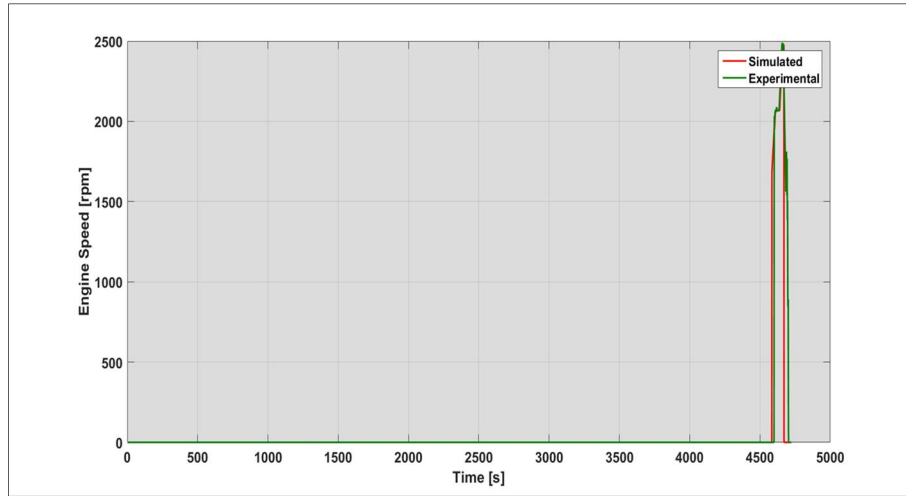


**Figure 124:** Golf GTE validation - Engine speed profile along the four NEDC cycle repetitions during the CD

Finally, Figure 125 illustrates the comparison between the instantaneous CO<sub>2</sub> emissions during the CD test, proving the good quality of virtual maps, engine torque and speed simulation. The error on cumulated value corresponds to an overestimation of 0.1 g/km equal to a difference of 1%.

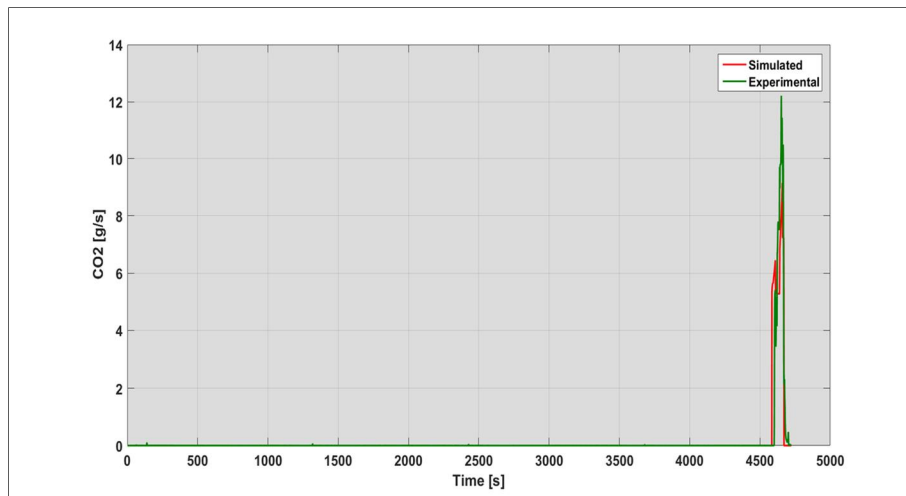


**Figure 125:** Golf GTE validation - Instantaneous CO<sub>2</sub> emission profile along the four NEDC cycle during the CD test

The last part is focused on the electric distance evaluation, presented in Table 16, according to the European procedure presented in Chapter 2, confirming the accuracy of the model. The error between the simulated and experimental EMS is around -2.2% due to the early engine ignition occurring during the last EUDC.

**Table 16:** Golf GTE validation - Comparison between the experimental and simulated electric distance

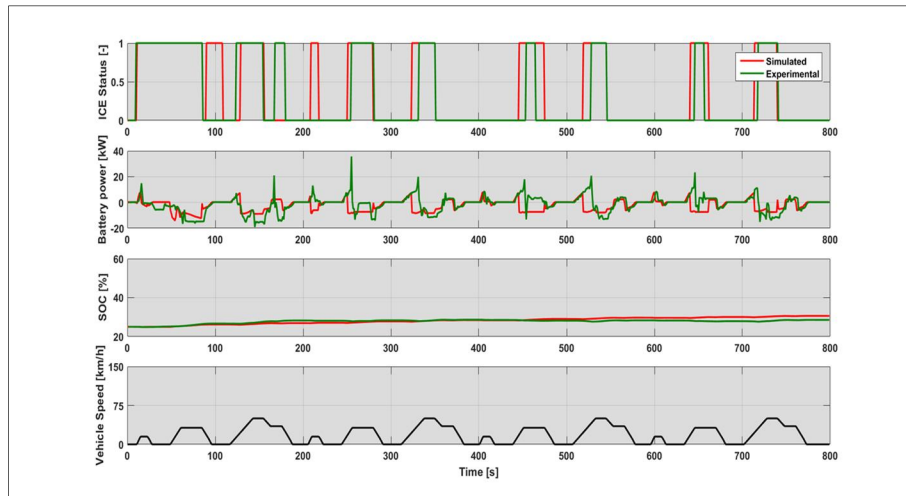
	<b>Simulated</b>	<b>Experimental</b>
<b>Dovc [km]</b>	40.8	41.7

### 4.3.2 The charge sustaining case

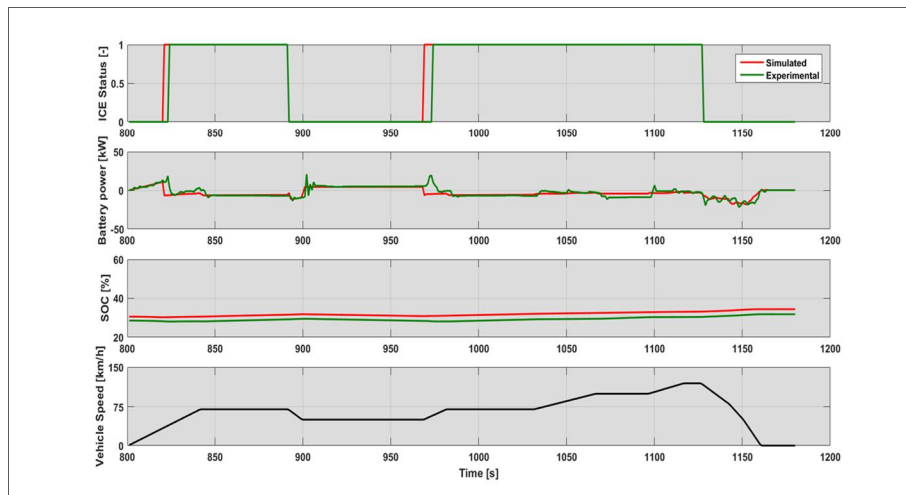
This section presents the validation of the CS test, which requests the battery depleted at the beginning of the cycle, taking into account the effect of “Cold Start” and the selection of the “most fuel consuming mode”, as requested by the TA procedure. The methodology adopted is identical to the HEV one.

Figure 126 and Figure 127 represent the engine enabling, the battery power and SOC respectively along the ECE and EUDC cycles. The Meta-Model is able to reproduce almost correctly the EMS behavior along the urban portion with some inaccuracy at the beginning of the cycle during the “Cold Start” and with the presence of a “fake” ignition at 200 seconds. The imprecision in the simulation of the “Cold Start” at 100 seconds is mainly due to an underestimation of coolant temperature of 5°C compared to the reference case, leading to a prolonged engine warm-up event. In general, it is possible to observe that the simulated engine ignitions are advanced of few seconds compared to the reference case. Anyway, the simulated SOC profile converges with the experimental one, showing a divergence at the end of urban phase of 1.5 %, confirming the correct actuation of the Load Point Moving event when the ICE is on and the right power adsorption from the high voltage battery. Concerning the EUDC cycle, it is possible to observe an earlier engine ignition compared to the experimental case and the correct actuation of the Load Point Moving, confirmed by the growing trend of the SOC profile.

The comparison between the experimental and simulated coolant temperature profiles is depicted in Figure 128. The simulated temperature profile is able to follow the trend of the experimental case, showing a maximum divergence of 10°C due to the difficulty of simulate the temperature drops caused by the engine turning off. As remarked for the HEV validation, the divergence is not a critical issue, because the simulation should be accurate during the cat-heating event, where the engine calibration differs.



**Figure 126:** Golf GTE validation - Powertrain behavior along the ECE cycle during the CS test



**Figure 127:** Golf GTE validation - Powertrain behavior along the EUDC cycle during the CS test

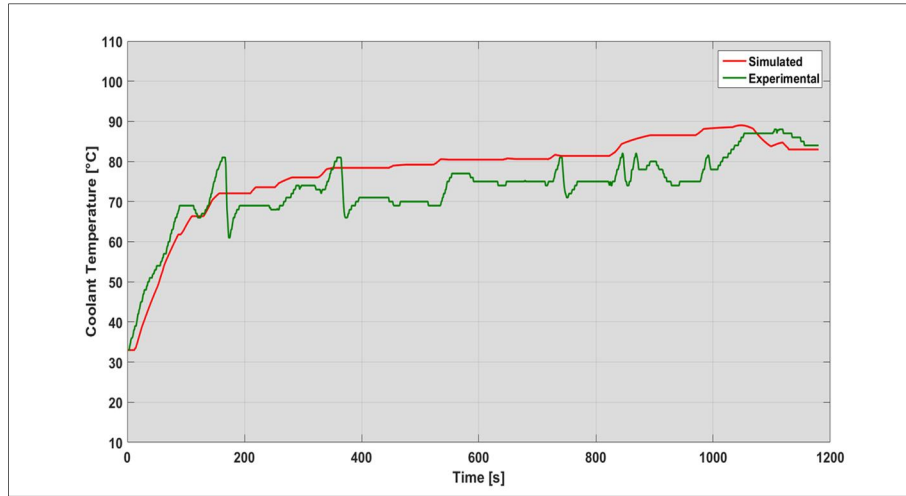


**Figure 128:** Golf GTE validation - Coolant temperature profile along the NEDC cycle during the CS test

Finally, the engine speed profile, the instantaneous and cumulated CO<sub>2</sub> emissions are shown respectively in Figure 129, Figure 130 and Figure 131, stressing the imprecisions presented in the EMS analysis. The error on the cumulated emissions is around -0.7% corresponding to underrate of 1.2 g/km.

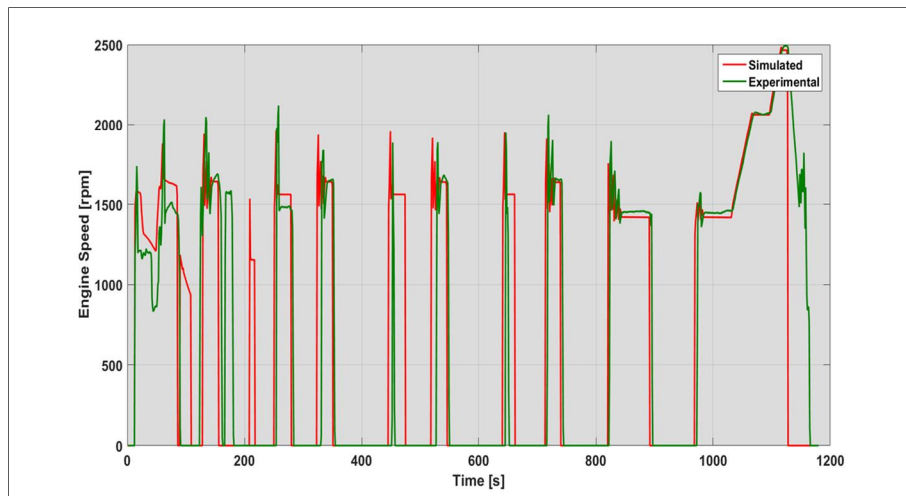


**Figure 129:** Golf GTE validation - Engine speed profile along the four NEDC cycle repetitions during the CS test

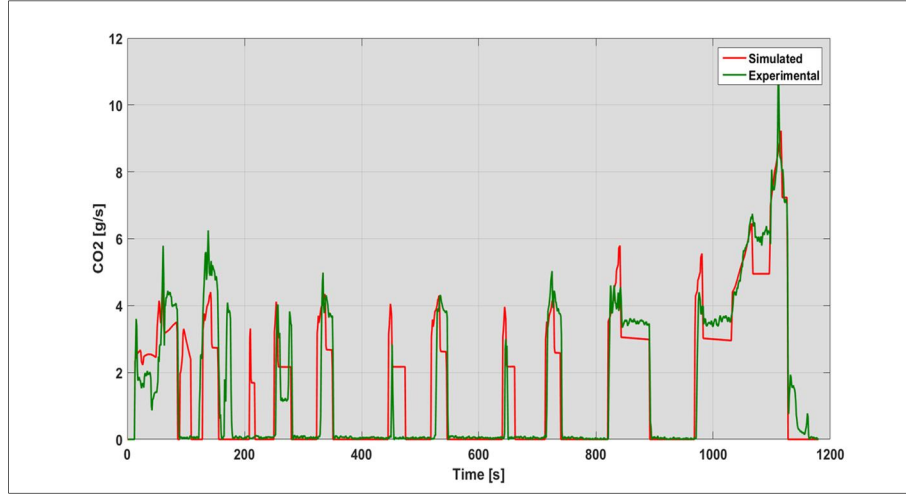


**Figure 130:** Golf GTE validation - Instantaneous CO<sub>2</sub> emission profile along the four NEDC cycle during the CS test

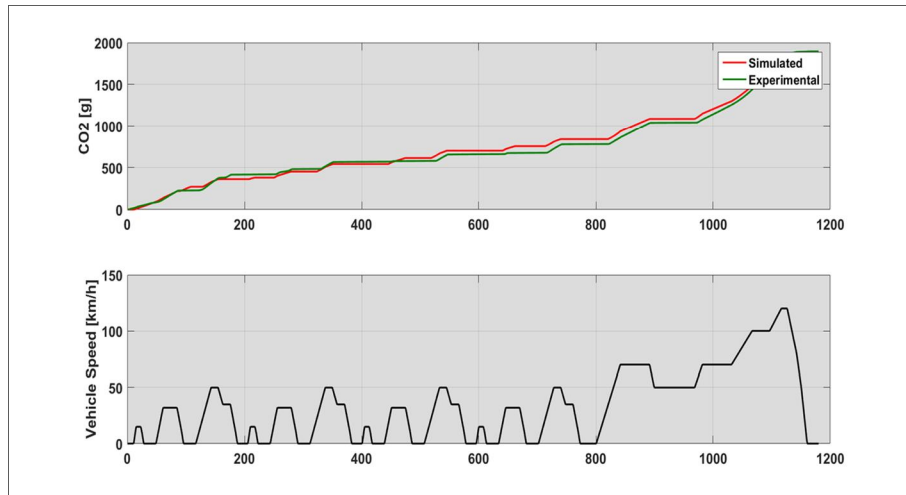


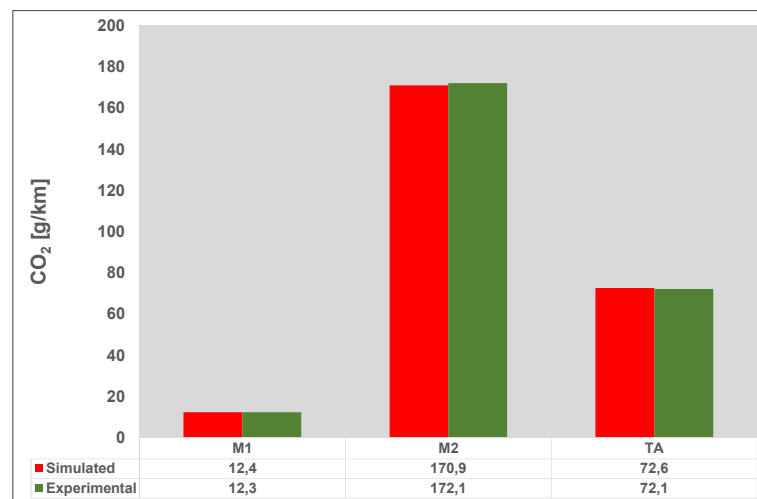
**Figure 131:** Golf GTE validation - Cumulated CO<sub>2</sub> emissions along the NEDC cycle during the CS test

### 4.3.3 CO<sub>2</sub> Type approval value for the Golf GTE

According to the European TA procedure, the computation of CO<sub>2</sub> emissions from PHEVs requests the evaluation of the cumulated values and of the distance travelled in electric drive. The formulation weighs the CD and CS emissions respectively with the electric distance and the average distance between two battery recharges, assumed equal to 25 km as described in Chapter 2. The results are summarized in Table 17 and Figure 132, where  $M_1$  refers to the CD emissions and  $M_2$  to the CS ones. The Meta-Model overestimates the TA CO<sub>2</sub> of 0.5 g/km, corresponding to an error of 0.6%.

**Table 17:** Golf GTE validation - Comparison between the experimental and simulated CO<sub>2</sub> TA values

	Simulated	Experimental
CO <sub>2</sub> [g/km]	72.6	72.1

**Figure 132:** Golf GTE validation - Comparison between the experimental and simulated CO<sub>2</sub> emissions along the NEDC



## Conclusions

The object of this work was the development of a tool applied to hybrid vehicles to correlate the CO<sub>2</sub> emissions measured according to the WLTP procedure, which will enter in force from September 2017, with the NEDC values, since the European 2020 CO<sub>2</sub> fleet target is based on the actual type approval procedure. The correlation function should be able to identify the energy management system of a large portfolio of hybrid architectures along the WLTC and reproduce it correctly throughout the NEDC, using a small amount of information available from the type approval test such as the battery current/voltage, the engine speed, the coolant temperature and the CO<sub>2</sub> measurement.

The starting point was the analysis of the hybrid portfolio technologies and architectures available on the European market, selecting the most representative vehicle models to set-up the experimental test campaign, necessary for the development of the model and its validation. The initial stage involved two vehicles:

- The Toyota Yaris Hybrid, which is an Euro 6 B-Segment HEV, is equipped with an eCVT architecture;
- The Volkswagen Golf GTE, which is a Euro 6 C-Segment PHEV, is combined with FAS architecture.

The test campaign, carried out along the WLTC and NEDC cycles, followed the procedure described in the Regulation 83, which is actually used by the European authorities for the certification of passenger cars. The decision to use the same procedure for both cycles lies on the necessity to find the similarities and eventually the divergence in the energy management behavior. The goal is the hybrid control logic identification through the correlation of vehicle measurements, such as battery SOC, vehicle speed, acceleration, etc., to define a simple and reliable methodology able to identify and model the principal operating conditions of an hybrid powertrain: the electric drive, the regenerative braking, the Smart Charge (or Load Point Moving) and the E-Boost.

The Yaris Hybrid was tested considering two different energy levels of the battery at the beginning of the cycle to compute the K-Factor, used by the type approval procedure to correct the CO<sub>2</sub> emissions according to a neutral energy balance of the battery. The analysis of the energy management shows a close relationship between the vehicle speed, the motive power and the acceleration, highlighting the use of electric drive in the low/medium speed and accelerations area, typical of the urban driving. The battery SOC is crucial in HEVs, especially when the battery is low at the beginning of the cycle, forcing the recharge through the Load Point Moving until the reaching of a normal operating condition of the battery around 55% of SOC.

An important outcome of this analysis is the effect of the new test procedure on CO<sub>2</sub> emissions. The WLTP procedure generates an increase of the cycle energy demand of 40% compared to the NEDC, leading to a 10% reduction of electric drive and consequently producing an increase of 23% of CO<sub>2</sub> emissions, calculated according the type approval procedure.

The EMS behavior of the Golf GTE was assessed in charge depleting and sustaining conditions, according to the requirements of Regulation 83. The charge depleting test was performed setting the E-Mode, which is characterized by an intensive use of the electric drive, while the charge sustaining using the GTE mode since it represents “the most fuel consuming mode” combined with the battery fully depleted at the beginning of the cycle. The E-Mode enables the electric driving on a wide range of speeds, accelerations and powers according to the physical limits of the electric powertrain and battery SOC. Instead, the GTE together with low battery SOC limits severely the electric driving to low speeds and accelerations area, promoting the aggressive battery recharge through the Smart Charge.

As the Yaris Hybrid case, the increasing of the cycle energy demand leads to a reduction of the electric drive, corresponding to a reduction of the “zero emission” distance of 20% from WLTC to NEDC, affecting the type approval CO<sub>2</sub> value. The weighing of charge depleting and sustaining emissions together with the electric range produces an increase of 70% in the type approval CO<sub>2</sub> emissions.

The outcomes from the experimental campaign were used for the development of the correlation tool for hybrid vehicles, which should reproduce the logic of the energy management system along the NEDC cycle, but should also reflect the requirements of Regulation 83 for the computation of CO<sub>2</sub> emissions for both HEVs and PHEVs. Therefore, the model should simulate in case of HEVs at least two NEDC cycles for the correct computation of the K-Factor, while for PHEVs the charge depleting and sustaining tests, sharing a unique modelling approach of the energy management logic. The model should detect from WLTC measurements the engine enabling logic, the efficiencies of the powertrain during the electric drive and the regenerative brake, the engine warm-up strategy during the “Cold Start” and the enabling of the Smart Charge/E-Boost.

The tool validation was carried out using the experimental tests on the Yaris Hybrid and the Golf GTE, focusing on the correct detection of the engine enabling, of the SOC swing, of the “Cold Start” strategy and of CO<sub>2</sub> emissions. The results achieved show the good predictive capabilities of the Meta-Model, which is able to simulate the engine strategy, the SOC evolution and the instantaneous CO<sub>2</sub> emissions with acceptable accuracy, considering the lack of information and the unified procedure used for both HEVs and PHEVs.

The error on CO<sub>2</sub> estimation according to the TA procedure was around 1.4 g/km for the Yaris Hybrid and of 0.5 g/km for the Golf GTE, fulfilling the target error of  $\pm 3$  g/km.

## References

1. Bujnicki, J., Dykstras, P., Fortunato, E., Heuer, R.-D., Villani, C., and Wegener, H.C., “Closing The Gap between light-duty vehicle real-world CO<sub>2</sub> emissions and laboratory testing,” ISBN 978-92-79-63184-9, 2016, doi:10.2777/762451.
2. Eurostat, “Sustainable Development,” 1–7, [http://ec.europa.eu/eurostat/statistics-explained/index.php/Sustainable\\_development\\_-\\_transport](http://ec.europa.eu/eurostat/statistics-explained/index.php/Sustainable_development_-_transport), 2015.
3. Fontaras, G. and Samaras, Z., “On the way to 130 g CO<sub>2</sub>/km-Estimating the future characteristics of the average European passenger car,” *Energy Policy* 38(4):1826–1833, 2010, doi:10.1016/j.enpol.2009.11.059.
4. Fontaras, G. and Samaras, Z., “A quantitative analysis of the European Automakers’ voluntary commitment to reduce CO<sub>2</sub> emissions from new passenger cars based on independent experimental data,” *Energy Policy* 35(4):2239–2248, 2007, doi:10.1016/j.enpol.2006.07.012.
5. European Union, Regulation (EC) No 443/2009 Of The European Parliament and of the Council of 23 April 2009 setting emission performance standards for new passenger cars as part of the Community’s integrated approach to reduce CO<sub>2</sub> emissions from light-duty vehicles, *Eur-Lex. Eur. eu/Notice. Do L140(05.06.2009):pp1-15*, 2009.
6. ICCT, “January 2014 EU CO<sub>2</sub> Emission Standards for Passenger Cars and Light-Commercial Vehicles,” 2014.
7. Mock, P., German, J., Bandivadekar, A., and Riemersma, I., “Discrepancies between type-approval and ‘real-world’ fuel-consumption and CO<sub>2</sub> values,” 2012.
8. Mock, P.; Tietge, U.; Franco, V.; German, J.; Bandivadekar, A.; Ligterink, N.; Lambrecht, U.; Kühlwein, J.; Riemersma, I., “From laboratory to road - A 2014 update of official and ‘real-world’ fuel consumption and CO<sub>2</sub>

- values for passenger cars in Europe,” 2014.
9. Tutuianu, M., Bonnel, P., Ciuffo, B., Haniu, T., Ichikawa, N., Marotta, A., Pavlovic, J., and Steven, H., “Development of the World-wide harmonized Light duty Test Cycle (WLTC) and a possible pathway for its introduction in the European legislation,” *Transp. Res. Part D Transp. Environ.* 40:61–75, 2015, doi:<http://dx.doi.org/10.1016/j.trd.2015.07.011>.
  10. Mock, P., Kühlwein, J., Tietge, U., Franco, V., Bandivadekar, A., and German, J., “The WLTP: How a new test procedure for cars will affect fuel consumption values in the EU,” 2014, doi:[10.1016/j.enpol.2013.12.013i](https://doi.org/10.1016/j.enpol.2013.12.013i).
  11. United Nations, Addendum 15 : Global technical regulation No . 15 - Worldwide harmonized Light vehicles Test Procedure, *Glob. Regist.* ECE/TRANS/:1–234, 2014.
  12. Tsokolis, D., Dimaratoros, A., Samaras, Z., Tsiakmakis, S., Fontaras, G., and Ciuffo, B., “Quantification of the effect of WLTP introduction on passenger cars CO<sub>2</sub> emissions,” *J. Earth Sci. Geotech. Eng.* 1:191–214, 2017.
  13. Tsokolis, D., Tsiakmakis, S., Dimaratos, A., Fontaras, G., Pistikopoulos, P., Ciuffo, B., and Samaras, Z., “Fuel consumption and CO<sub>2</sub> emissions of passenger cars over the New Worldwide Harmonized Test Protocol,” *Appl. Energy* 179:1152–1165, 2016, doi:[10.1016/j.apenergy.2016.07.091](https://doi.org/10.1016/j.apenergy.2016.07.091).
  14. Dimaratos, A., Tsokolis, D., Fontaras, G., Tsiakmakis, S., Ciuffo, B., and Samaras, Z., “Comparative Evaluation of the Effect of Various Technologies on Light-duty Vehicle CO<sub>2</sub> Emissions over NEDC and WLTP,” *Transp. Res. Procedia* 14:3169–3178, 2016, doi:[10.1016/j.trpro.2016.05.257](https://doi.org/10.1016/j.trpro.2016.05.257).
  15. Gamma-Technologies, GT-Suite User Manual, 2015.
  16. Morel, T., Keribar, R., and Leonard, A., “Virtual Engine/Powertrain/Vehicle” Simulation Tool Solves Complex Interacting System Issues,” *SAE Tech. Pap.*, 2003, doi:[10.4271/2003-01-0372](https://doi.org/10.4271/2003-01-0372).
  17. Millo, F., Rolando, L., and Andreatta, M., “Numerical Simulation for Vehicle Powertrain Development,” *Numer. Anal. - Theory Appl.* 519–540, 2011, doi:[10.1016/j.camwa.2011.04.011](https://doi.org/10.1016/j.camwa.2011.04.011).
  18. Millo, F., Caputo, S., Cubito, C., Calamiello, A., Mercuri, D., and Rimondi, M., “Numerical Simulation of the Warm-Up of a Passenger Car Diesel Engine Equipped with an Advanced Cooling System,” *SAE Tech. Pap.* 2016–April, 2016, doi:[10.4271/2016-01-0555](https://doi.org/10.4271/2016-01-0555).
  19. Stapf, P., Weinrich, M., Weller, R., and Siegert, R., Challenges in Thermal Management, 2014.
  20. European Union, Draft: setting out a methodology for determining the

- correlation parameters necessary for reflecting the change in the regulatory test procedure and amending Regulation (EU) No 1014/2010.
21. Arcidiacono, V., Tsiakmakis, S., Fontaras, G., Ciuffo, B., Valverde, V., Pavlovic, J., Kommos, D., and Anagnostopoulos, K., "CO2MPAS: Vehicle simulator predicting NEDC CO<sub>2</sub> emissions from WLTP," <https://co2mpas.io/>, 2017.
  22. Ciuffo, B., "Joint Research Centre - European Energy Efficiency Platform (EP3)," <http://e3p-beta.jrc.nl/articles/co2mpas>, 2017.
  23. European Union, Draft: setting out a methodology for determining the correlation parameters necessary for reflecting the change in regulatory test procedure, 2016.
  24. UNECE, "Regulation No. 83: Uniform provisions concerning the approval of vehicles with regard to the emission of pollutants according to engine fuel requirements," 2011.
  25. Toyota, "Toyota Hybrid System (THS II)," Tokyo, 2003.
  26. Volkswagen AG, Service Training, 2014.
  27. Millo, F., Engine Emissions Control - Lesson notes of Automotive Engineering course, 2012.
  28. Fontaras, G., Pistikopoulos, P., and Samaras, Z., "Experimental evaluation of hybrid vehicle fuel economy and pollutant emissions over real-world simulation driving cycles," *Atmos. Environ.* 42(18):4023–4035, 2008, doi:10.1016/j.atmosenv.2008.01.053.
  29. UNECE, Regulation No. 101 Uniform provisions concerning the approval of passenger cars powered by an internal combustion engine only, or powered by a hybrid electric power train with regard to the measurement of the emission of carbon dioxide and fuel consumption, 2013.
  30. Electric Vehicle News.
  31. Cubito, C., Rolando, L., Millo, F., Ciuffo, B., Serra, S., Trentadue, G., and Otura, Marcos Garcia Fontaras, G., "Energy Management Analysis under Different Operating Modes for a Euro-6 Plug-in Hybrid Passenger Car," *SAE Tech. Pap.*, 2017.
  32. Biasini, R., Onori, S., and Rizzoni, G., "A Near-optimal Rule-Based Energy Management Strategy for Medium Duty Hybrid Truck," *Int. J. Powertrains* 2(2/3):232–261, 2013, doi:10.1504/IJPT.2013.054151.
  33. Serrao, L., Onori, S., and Rizzoni, G., "A Comparative Analysis of Energy Management Strategies for Hybrid Electric Vehicles," *J. Dyn. Syst. Meas. Control* 133(3):31012, 2011, doi:10.1115/1.4003267.
  34. Rimaux, S., "WLTP-NEDC Hybrid correlation factor," 2015.

35. Volkswagen AG, Basic of Electric Drives in Automobiles - Design and Function, 2011.
36. Millo, F., Cubito, C., Rolando, L., Pautasso, E., and Servetto, E., "Design and development of an hybrid light commercial vehicle," *Energy* 1–10, 2016, doi:<http://dx.doi.org/10.1016/j.energy.2016.04.084>.
37. D'Errico, J., "Surface Fitting using gridfit," <https://it.mathworks.com/matlabcentral/fileexchange/8998-surface-fitting-using-gridfit?requestedDomain=www.mathworks.com>, 2008.
38. Vassallo, A., Cipolla, G., Mallamo, F., Paladini, V., Millo, F., and Mafrici, G., "Transient Correction of Diesel Engine Steady-State Emissions and Fuel Consumption Maps for Vehicle Performance Simulation," *Aachener Kolloquium Fahrzeug Und Mot.*, 2007.
39. Onori, S., Simulation and Control of Hybrid Vehicles, 2015.
40. Canova, M., Introduction to Electrochemical Energy Conversion and Storage Systems for Automotive Applications, 2015.
41. Cubito, C., "Sviluppo di metodologie per la previsione di emissioni di inquinanti e consumo di combustibile da motori Diesel automobilistici," Politecnico di Torino, 2013.